



National Library  
of Canada

Bibliothèque nationale  
du Canada

CANADIAN THESES  
ON MICROFICHE

THÈSES CANADIENNES  
SUR MICROFICHE

NAME OF AUTHOR/NOM DE L'AUTEUR Bruce James FORREST

TITLE OF THESIS/TITRE DE LA THÈSE MAGNETIC RESONANCE STUDIES OF MIXED MEMBRANE SYSTEMS.

UNIVERSITY/UNIVERSITÉ SIMON FRASER UNIVERSITY

DEGREE FOR WHICH THESIS WAS PRESENTED/  
GRADE POUR LEQUEL CETTE THÈSE FUT PRÉSENTÉE DOCTOR OF PHILOSOPHY

YEAR THIS DEGREE CONFERRED/ANNÉE D'OBTENTION DE CE GRADE 1978

NAME OF SUPERVISOR/NOM DU DIRECTEUR DE THÈSE Dr. R.J. Cushley

Permission is hereby granted to the NATIONAL LIBRARY OF  
CANADA to microfilm this thesis and to lend or sell copies  
of the film.

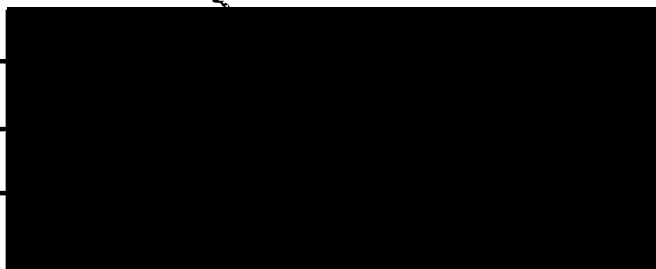
The author reserves other publication rights, and neither the  
thesis nor extensive extracts from it may be printed or other-  
wise reproduced without the author's written permission.

L'autorisation est, par la présente, accordée à la BIBLIOTHÈ-  
QUE NATIONALE DU CANADA de microfilmer cette thèse et  
de prêter ou de vendre des exemplaires du film.

L'auteur se réserve les autres droits de publication; ni la  
thèse ni de longs extraits de celle-ci ne doivent être imprimés  
ou autrement reproduits sans l'autorisation écrite de l'auteur.

DATED/DATÉ December 8, 1977 SIGNED/SIGNÉ \_\_\_\_\_

PERMANENT ADDRESS/RÉSIDENCE FIXE \_\_\_\_\_





National Library of Canada

Cataloguing Branch  
Canadian Theses Division

Ottawa, Canada  
K1A 0N4

Bibliothèque nationale du Canada

Direction du catalogage  
Division des thèses canadiennes

## NOTICE

The quality of this microfiche is heavily dependent upon the quality of the original thesis submitted for microfilming. Every effort has been made to ensure the highest quality of reproduction possible.

If pages are missing, contact the university which granted the degree.

Some pages may have indistinct print especially if the original pages were typed with a poor typewriter ribbon or if the university sent us a poor photocopy.

Previously copyrighted materials (journal articles, published tests, etc.) are not filmed.

Reproduction in full or in part of this film is governed by the Canadian Copyright Act, R.S.C. 1970, c. C-30. Please read the authorization forms which accompany this thesis.

**THIS DISSERTATION  
HAS BEEN MICROFILMED  
EXACTLY AS RECEIVED**

## AVIS

La qualité de cette microfiche dépend grandement de la qualité de la thèse soumise au microfilmage. Nous avons tout fait pour assurer une qualité supérieure de reproduction.

S'il manque des pages, veuillez communiquer avec l'université qui a conféré le grade.

La qualité d'impression de certaines pages peut laisser à désirer, surtout si les pages originales ont été dactylographiées à l'aide d'un ruban usé ou si l'université nous a fait parvenir une photocopie de mauvaise qualité.

Les documents qui font déjà l'objet d'un droit d'auteur (articles de revue, examens publiés, etc.) ne sont pas microfilmés.

La reproduction, même partielle, de ce microfilm est soumise à la Loi canadienne sur le droit d'auteur, SRC 1970, c. C-30. Veuillez prendre connaissance des formules d'autorisation qui accompagnent cette thèse.

**LA THÈSE A ÉTÉ  
MICROFILMÉE TELLE QUE  
NOUS L'AVONS REÇUE**

MAGNETIC RESONANCE STUDIES

OF

MIXED MEMBRANE SYSTEMS

by

Bruce James Forrest

B.Sc., University of Western Ontario 1971

M.Sc., Bishop's University 1973

A THESIS SUBMITTED IN PARTIAL FULFILLMENT

OF THE REQUIREMENTS FOR THE DEGREE OF

DOCTOR OF PHILOSOPHY

in the Department

of

Chemistry

© Bruce James Forrest 1977

Simon Fraser University

December 1977.

All rights reserved. This thesis may not be reproduced in whole or in part, by photocopy or other means, without permission of the author.

## APPROVAL

Name: Bruce James Forrest

Degree: Doctor of Philosophy

Title of Thesis: Magnetic Resonance Studies of Mixed Membrane Systems

Examining Committee:

Chairman: Dr. F.W.B. Einstein

Dr. R.J. Cushley  
Senior Supervisor

Dr. S. Aronoff

~~Dr. E.J. Wells~~

Dr. A.J. Davison

Dr. I.C.P. Smith  
External Examiner  
Division of Biological Sciences  
National Research Council of Canada  
Ottawa

Date Approved: Dec. 5, 1977

PARTIAL COPYRIGHT LICENSE

I hereby grant to Simon Fraser University the right to lend my thesis, project or extended essay (the title of which is shown below) to users of the Simon Fraser University Library, and to make partial or single copies only for such users or in response to a request from the library of any other university, or other educational institution, on its own behalf or for one of its users. I further agree that permission for multiple copying of this work for scholarly purposes may be granted by me or the Dean of Graduate Studies. It is understood that copying or publication of this work for financial gain shall not be allowed without my written permission.

Title of Thesis/Project/Extended Essay

MAGNETIC RESONANCE STUDIES OF MIXED MEMBRANE SYSTEMS.

---

---

---

---

Author:

(signature)

Bruce James FORREST

(name)

December 8, 1977

(date)

## ABSTRACT

The isoprenoids, phytol, Vitamin E, and phytanic acid have been incorporated into lecithin model membranes, and the effects of this incorporation upon the structure and permeability of the mixed bilayer systems have been studied by nuclear magnetic resonance (NMR) spectroscopy. The fluidity of the membrane as evidenced by  $^{13}\text{C}$   $T_1$  relaxation times increases in the order phytol < Vitamin E < phytanic acid. Kinetic analysis of paramagnetic praseodymium infusion into lecithin vesicles containing the various phytol compounds has been performed using  $^{31}\text{P}$ -NMR. Relative rates of  $\text{Pr}^{3+}$  leakage through the mixed lecithin-phytol compound bilayer compared with pure lecithin (relative rate = 1.00) were: phytol = 7.8, Vitamin E = 47.7, and phytanic acid = 2897. By use of Arrhenius plots, the activation energy for  $\text{Pr}^{3+}$  diffusion through the lecithin-phytol bilayer (3:1 mole ratio lecithin:phytol) was found to be  $20.3 \pm 0.2$  kcal, and similarly, reorientation processes for the lecithin fatty acid chains as monitored by  $^{13}\text{C}$   $T_1$  relaxation times were found to have activation energies of approximately 3-5 kcal/mole.

The effects of the incorporation of phytol, Vitamin E, and phytanic acid are explained in terms of the disruption of normal lipid-lipid packing due to the difficulty in accommodating these branched chain compounds. The position occupied by phytol in the

mixed membrane has been determined by means of an intermolecular linear electric field effect upon the phytol olefinic carbons, which originates from the polar phospholipid headgroup. Upon incorporation into egg yolk lecithin vesicles, a  $^{13}\text{C}$  electric field chemical shift of the phytol olefinic carbons, C2 and C3, of 0.97 ppm was found. This characteristic upfield- downfield chemical shift difference due to the electric field with origin at the membrane surface places the midpoint of the phytol double bond approximately 4.7 Å below the plane of the lecithin headgroup. This is a rare example of an intermolecular linear electric field effect. The position occupied by phytol in the bilayer has been verified by producing changes in phospholipid, temperature, and the presence of ions in the bulk aqueous phase.

The effects of the incorporation of cholesteryl esters into model membrane systems have been investigated using electron spin resonance spectroscopy (ESR), as well as NMR. ESR studies of oriented phospholipid multilayers containing nitroxide labeled cholesteryl esters, and the rate of ascorbate reduction of these labels indicate that the ester is present in a "horseshoe" type configuration with the ester linkage near the hydrophilic region. The addition of 10 mole% cholesterol to lecithin multilayers has been shown to alter the accessibility of the cholesteryl ester spin probes to ascorbate. In addition, the presence of the saturated ester cholesteryl palmitate, over the concentration range of 0-19 mole%, has been shown to exert

differential effects upon the rate of reduction of the cholesterol analogue, 3-doxycholestane, present in lecithin multilayers. Thus, the mutual interactions of phospholipid, cholesterol, and cholesteryl esters are important contributors to the properties of the mixed membrane.

Permeability studies using the paramagnetic lanthanide,  $\text{Pr}^{3+}$ , showed that changes in the rate of ion permeation of cholesteryl ester-lecithin bilayers are a function of the nature of the fatty acyl tail of the ester as well as the amount of ester present. It was found that the incorporation of 5 mole% cholesteryl palmitate increased the rate of the inward diffusion of  $\text{Pr}^{3+}$  by approximately ten-fold.

Also, it was found possible, through the use of the saturated phospholipid, dipalmitoyl lecithin, to monitor directly cholesteryl ester present in a multilamellar model membrane system using natural abundance  $^{13}\text{C}$  NMR.

Finally, membranes prepared from reconstituted human aortas give rise to natural abundance  $^{31}\text{P}$  and  $^{13}\text{C}$  NMR spectra, and therefore should prove useful for further studies on biological membranes.



To my wife, Jane

## ACKNOWLEDGEMENTS

The author wishes to express his sincere thanks to Dr. R.J. Cushley for his genuine interest and guidance during the course of this investigation. Recognition is also due Dr. S. Aronoff and Dr. E.J. Wells for their time spent as members of the supervisory committee.

The author also wishes to thank Dr. A.C. Oehlschlager for the gift of two of the nitroxide spin labels used in this study.

The author is indebted to the other members of the Chemistry Department at Simon Fraser University, and especially to the other members of the research group for many interesting discussions.

The financial support of the National Research Council of Canada and the British Columbia Heart Foundation through research grants to Dr. R.J. Cushley, and the support of Simon Fraser University are gratefully acknowledged.

## TABLE OF CONTENTS

Title Page  
 Examining Committee Approval  
 Abstract  
 Dedication  
 Acknowledgements  
 Table of Contents  
 List of Tables  
 List of Figures

CHAPTER	PAGE
1. INTRODUCTION	1
A. Model Membranes	1
B. Vitamin E, Phytol, and Phytanic Acid	7
C. Cholesteryl Esters	11
D. Statement of the Problem	13
2. EXPERIMENTAL	14
A. Materials	14
B. Sample Preparation	15
1. Vesicles	15
2. Phytol Dispersions	17
3. Phospholipid multilamellar liposomes	18
4. Oriented lipid multilayers	18
5. Aorta membrane	19
C. Nuclear Magnetic Resonance Spectra	20
1. $^{13}\text{C}$ NMR	20
2. $^{31}\text{P}$ NMR	22
D. Electron Spin Resonance Spectra	23
1. General	23
2. Ascorbate permeation	23

3. THEORETICAL CONSIDERATIONS	25
A. Spin-Lattice Relaxation	26
1. General	26
2. Dipole-dipole relaxation	30
3. Measurement of spin-lattice relaxation times	33
B. Linear Electric Field Effects in NMR	37
C. ESR of Nitroxide Spin Labels	44
4. RESULTS AND DISCUSSION, PART I: VITAMIN E, PHYTOL, AND PHYTANIC ACID	52
A. Activation Energies for $^{13}\text{C}$ $T_1$ Processes	52
B. $^{13}\text{C}$ NMR of Egg Yolk Lecithin-Phytol Bilayers	56
C. $^{13}\text{C}$ NMR of Dipalmitoyl Lecithin-Phytol Bilayers	72
D. Intermolecular Field Effects	74
E. $^{13}\text{C}$ NMR of EYL-Vitamin E and EYL-Phytanic Acid Bilayers	81
F. Phytol Compounds and Membrane Packing	91
G. Permeability Studies by $^{31}\text{P}$ NMR	95
H. $^{31}\text{P}$ NMR Permeability Studies of EYL-Cholesteryl Ester Vesicles	111
I. Mechanism of Vesicle Permeability	119
5. RESULTS AND DISCUSSION, PART II: CHOLESTERYL ESTERS AND ATHEROSCLEROSIS	128
A. ESR of Oriented Lipid Multilayers	128
1. Orientation of cholesteryl esters in phospholipid multilayers	128
2. Effect of cholesterol	152
3. Effect of cholesteryl palmitate on cholestane	155

B. Incorporation of Cholesteryl Esters into EYL Vesicles	158
C. <sup>13</sup> C NMR of Lecithin-Cholesteryl Ester Dispersions	162
D. Aorta Membrane	176
1. <sup>31</sup> P NMR	176
2. <sup>13</sup> C NMR	181
6. CONCLUSION	187
A. Vitamin E, Phytol, and Phytanic Acid	187
B. Cholesteryl Esters	191
7. FUTURE DIRECTIONS	197
BIBLIOGRAPHY	199

## LIST OF TABLES

TABLE		PAGE
I	Longitudinal bond polarizabilities.	43
II	Selected $^{13}\text{C}$ $T_1$ relaxation times for 20% w/v egg yolk lecithin vesicles	53
III	Fatty acid composition of egg yolk lecithin	55
IV	Activation energies for selected $^{13}\text{C}$ resonances	58
V	Lecithin $^{13}\text{C}$ chemical shifts for egg yolk lecithin and egg yolk lecithin-phytol 1:1 mixed vesicles.	59
VI	$^{13}\text{C}$ chemical shifts for phytol.	60
VII	Lecithin $^{13}\text{C}$ relaxation times for egg yolk lecithin and egg yolk lecithin-phytol 1:1 mixed vesicles	65
VIII	$^{13}\text{C}$ $T_1$ relaxation times for phytol.	68
IX	$^{13}\text{C}$ $T_1$ relaxation times for dipalmitoyl lecithin and dipalmitoyl lecithin-phytol mixed vesicles at $52^\circ\text{C}$ .	73
X	$^{13}\text{C}$ chemical shifts for 10% w/v EYL vesicles and for vesicles containing 25 mole% Vitamin E or phytanic acid at $11^\circ\text{C}$ .	83
XI	$^{13}\text{C}$ $T_1$ relaxation times for lecithin and lecithin- Vitamin E and lecithin-phytanic acid bilayers.	84
XII	$^{13}\text{C}$ $T_1$ relaxation times for 20% w/v EYL vesicles and 20% EYL vesicles containing a 10:1 mole ratio lecithin:Vitamin E at $52^\circ\text{C}$ .	90
XIII	$^{13}\text{C}$ $T_1$ relaxation times for 10% w/v EYL vesicles and 10% w/v EYL vesicles containing 25 mole% incorporated palmitic acid at $11^\circ\text{C}$ .	94

XIV	Leak rates for lecithin and lecithin-phytyl compound vesicles at 33°C.	102
XV	Permeation rates of $\text{Pr}^{3+}$ into EYL vesicles containing 25 mole% phytol at various temperatures	106
XVI	Permeation rates of $\text{Pr}^{3+}$ into EYL vesicles containing various concentrations of incorporated Vitamin E at 33°C. (relative to EYL = 1.00).	109
XVII	NMR signal intensity of inward facing $^{31}\text{P}$ nuclei.	121
XVIII	Spectral parameters of spin labels I-V in lecithin multilayers at 23°C.	131
XIX	First half lives of reaction with ascorbate of spin probes in lecithin multilayers at 23°C.	146
XX	$^{13}\text{C}$ $T_1$ relaxation times of lecithin carbons for 40% w/v EYL dispersions in 0.3 M sucrose, and for 40% w/v EYL dispersions containing 25 mole % cholesteryl palmitate.	164
XXI	$^{13}\text{C}$ NMR assignments for cholesteryl linoleate carbons in 40% w/v dispersions of DPL containing 25 mole% cholesteryl linoleate at 52°C.	170
XXII	$^{13}\text{C}$ $T_1$ relaxation times for cholesteryl linoleate carbons in 40% w/v EYL dispersions containing 25 mole% cholesteryl linoleate.	173
XXIII	$^{13}\text{C}$ chemical shifts of sonicated aorta, 37°C.	185

## LIST OF FIGURES

FIGURE		PAGE
1.	The structure of lecithin.	2
2.	The structures of Vitamin E, phytol, and phytanic acid.	9
3.	Structure of various nitroxide spin probes.	16
4.	The homospoil pulse sequence.	36
5.	Orientation of a dipole moment with respect to molecular axes.	40
6.	$^{13}\text{C}$ NMR spectrum of 20% w/v egg yolk lecithin vesicles.	54
7.	Arrhenius plots of $T_1$ vs the inverse of absolute temperature for $^{13}\text{C}$ resonances of egg yolk lecithin vesicles.	57
8.	Proton noise decoupled $^{13}\text{C}$ NMR spectra for the region 5 ppm to 45 ppm at 52°C.	63
9.	Space filling molecular models illustrating the proposed structure of the lecithin-phytol bilayer.	80
10.	Proton noise decoupled $^{13}\text{C}$ NMR spectra of lecithin-Vitamin E and lecithin-phytanic acid vesicles, 11°C.	82
11.	The relative $^{13}\text{C}$ $T_1$ relaxation times for fatty acid carbons of lecithin and mixed lecithin-phytyl compound vesicles in $\text{D}_2\text{O}$ at 11°C.	85
12.	$^{31}\text{P}$ NMR spectra of 10% w/v egg yolk lecithin vesicles at 33°C.	97



13.  $^{31}\text{P}$  NMR spectra of 10% w/v egg yolk lecithin vesicles containing 25 mole% phytol or 25 mole% Vitamin E at the indicated times after addition of 0.005 M  $\text{Pr}^{3+}$ . 100
14. Percent total of "inside"  $^{31}\text{P}$  NMR signal relative to its initial value vs time for various lecithin-phytyl compound mixed vesicles. 101
15. Arrhenius plot of vesicle leak rate vs the inverse of absolute temperature for 10% w/v egg yolk lecithin vesicles containing 25 mole% phytol. 107
16. Effect of Vitamin E concentration on the permeability of 10% w/v egg yolk lecithin vesicles at 33°C. 110
17. Relative intensity of "inside"  $^{31}\text{P}$  NMR signal (initial value = 100%) vs time for pure and mixed vesicles containing cholesterol or cholesteryl palmitate. 112
18.  $^{31}\text{P}$  NMR spectra at 33°C of egg yolk lecithin-cholesteryl palmitate vesicles. 114
19. Effect of cholesteryl palmitate concentration on the permeability of egg yolk lecithin vesicles at 33°C. 117
20. Structure of various nitroxide spin probes. 129
21. Positional dependence of the order parameter in a lipid bilayer as detected by fatty acid spin probes. 132
22. Interactions between cholesteryl-5-doxy palmitate, cholesterol and egg yolk lecithin at 23°C. 135

23. Interactions between cholesteryl-16-doxylstearate, cholesterol and egg yolk lecithin at 23°C. 136
24. Interactions between 3-doxylcholestane, cholesteryl palmitate and egg yolk lecithin at 23°C. 137
25. Ascorbate induced ESR signal decay vs time 139
26. Effect of initial ascorbate concentration on the first half life of ascorbate reduction. 142
27. Possible orientations of cholesteryl esters incorporated into lipid bilayers. 149
28. Orientation and relative depths of various spin probes in lecithin multilayers. 153
29. Gel filtration of 10% w/v egg yolk lecithin vesicles containing 5 mole% cholesteryl palmitate. 161
30.  $^{13}\text{C}$  NMR spectra at 37°C of egg yolk lecithin and egg yolk lecithin-cholesteryl palmitate dispersions. 163
31.  $^{13}\text{C}$  NMR spectrum of a 40% w/v dispersion of egg yolk lecithin containing 25 mole% cholesteryl linoleate at 37°C. 166
32.  $^{13}\text{C}$  NMR spectra at 37°C of dipalmitoyl lecithin and dipalmitoyl lecithin-cholesteryl linoleate dispersions. 167
33.  $^{13}\text{C}$  NMR spectra at 52°C of dipalmitoyl lecithin and dipalmitoyl lecithin-cholesteryl linoleate dispersions. 169
34.  $^{31}\text{P}$  NMR spectrum of unsonicated aorta membrane. 37°C. 177
35.  $^{31}\text{P}$  NMR spectrum of sonicated aorta membrane. 37°C. 179
36.  $^{13}\text{C}$  NMR spectrum of sonicated aorta. 37°C. 182

## CHAPTER 1

### INTRODUCTION

#### A. Model Membranes

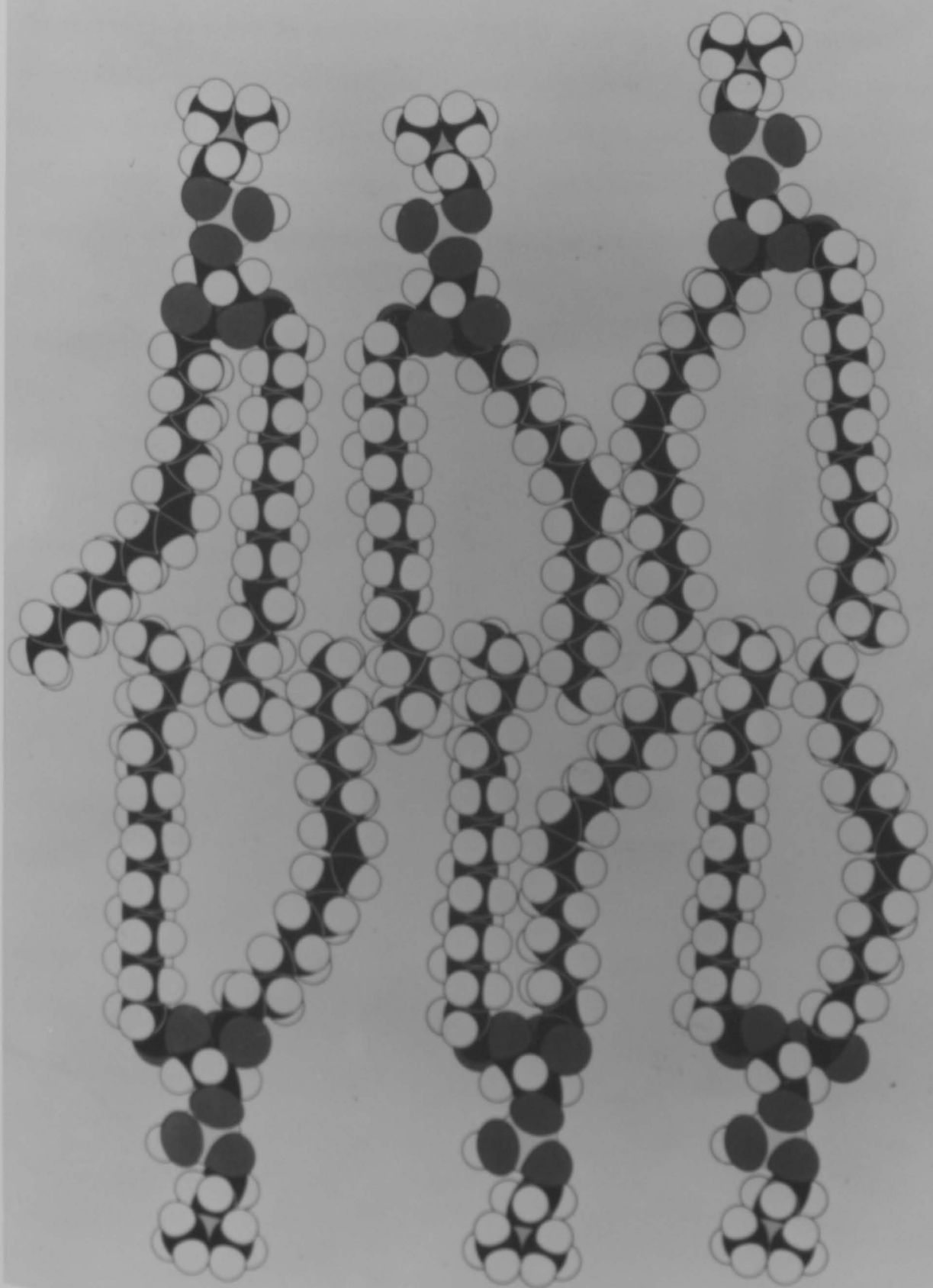
Membranes are basic structural units of living systems, forming the boundaries of cells, and their interior organelles, and providing a framework for many metabolic and physiological processes (1).

Increased interest in biological membranes in recent years has been spurred by the development of easily prepared phospholipid models, the most commonly used systems being multilamellar liposomes, single walled vesicles, monolayers, and oriented multilayers. Only with detailed information concerning simple models will it be possible to elucidate the complex interactions of membrane constituents.

When a phospholipid such as lecithin (Figure 1) is shaken in the presence of an aqueous phase, the lipid spontaneously forms large multilamellar liposomes ( $>2000\text{\AA}$  in diameter), which are composed of concentric bilayers (2). The treatment of these lipid dispersions with ultrasonic radiation leads to the formation of closed vesicles with an average diameter of approximately  $250\text{\AA}$  (3,4). These sealed vesicles consist of a single continuous bilayer which encloses a volume of aqueous solution.

2a

Figure 1. The structure of lecithin. Taken from reference '206.



A space-filling model of a section of a highly fluid phospholipid bilayer membrane.

The properties of phospholipid vesicle systems have been extensively studied by nuclear magnetic resonance (NMR) spectroscopy since above the phospholipid gel-liquid crystalline phase transition temperature,  $T_m$ , these systems give rise to high resolution spectra, narrow linewidths being obtained due to rapid tumbling of the small vesicles, and rapid lateral diffusion of the phospholipids in the plane of the bilayer (5,6). Carbon-13 NMR investigations have been especially elucidating. Despite the low natural abundance of  $^{13}\text{C}$  (1.1%), the development of pulse Fourier transform NMR has made possible the use of the nonperturbing  $^{13}\text{C}$  nucleus as a membrane probe. In addition, the large chemical shift window allows the resolution of many individual carbon atoms of membrane lipids, allowing the simultaneous observation of different areas of the membrane.

$^{13}\text{C}$  spin lattice relaxation times,  $T_1$ , of carbons with directly bonded hydrogens in large molecules are dominated by intramolecular dipole-dipole interactions, and thus these relaxation times reflect reorientation of the carbon-hydrogen internuclear vector, i.e. segmental motion about individual carbon-carbon bonds. Therefore an indication of the relative "fluidity" of the bilayer may be obtained from  $^{13}\text{C}$   $T_1$  relaxation measurements.

A large number of studies have utilized  $^{13}\text{C}$  NMR in the investigation of both model and biological membranes (7-25). These

investigations have shown the existence of a fluidity gradient along the fatty acid chains of lecithin bilayers, motional freedom increasing as the chain termini are approached. The effect of the presence of unsaturation in the fatty acid chains has been shown to increase motional freedom throughout the bilayer, whereas the intercalation of cholesterol in the membrane causes a reduction in the  $^{13}\text{C}$   $T_1$  relaxation times, and concomitant line broadening.

Below the phospholipid gel-liquid crystalline phase transition temperature,  $T_m$ , the  $^{13}\text{C}$  resonances are severely broadened due to static dipolar interactions. This broadening may be so severe as to broaden the signal into the background noise. Therefore factors such as the transition temperature, degree of unsaturation, and the amount of cholesterol present influence the type of  $^{13}\text{C}$  spectra which are determined for biological membranes. Spectra have been obtained for a variety of natural membranes, including erythrocytes (8), rabbit muscle sarcoplasmic reticulum (10), rat liver mitochondrial membranes (12), and  $^{13}\text{C}$  labelled E. coli (9). Thus, it is clear that many membrane systems, both model, and natural, lend themselves well to  $^{13}\text{C}$  NMR investigations.

Aided by the high natural abundance of  $^{31}\text{P}$  (100%), vesicle systems have also been investigated by phosphorus-31 NMR. Many of these studies have made use of paramagnetic lanthanide shift reagents (26-29). The addition of paramagnetic ions to preformed lecithin

vesicles causes a large chemical shift for outward facing  $^{31}\text{P}$  nuclei, thereby allowing the independent observation of both "inside" and "outside"  $^{31}\text{P}$ . Thus, as the paramagnetic lanthanide crosses the bilayer and is able to shift "inside"  $^{31}\text{P}$  nuclei, changes in the  $^{31}\text{P}$  spectra will reflect the membrane permeability.

$^{31}\text{P}$  NMR has also been utilized to study the motion and orientation of the phospholipid headgroups, and to monitor the lipid gel-liquid crystalline phase transition (30-35). Recently,  $^{31}\text{P}$  NMR has also been used to study lateral diffusion of phospholipids in the plane of the bilayer (36).

A second model membrane system is that of lipid monolayers which have been extensively studied in order to gain information regarding the surface potential and surface dipole moments of pure and mixed membrane systems (37-50). When an amphiphilic molecule is spread at an air-water interface, monolayers are formed with the polar portion of the molecule extending into the aqueous phase, and the nonpolar portions (the fatty acid chains of lecithin) extending away from the aqueous phase.

In addition, monolayer force-area measurements provide information concerning the packing of lipid molecules. It has been shown that mixed monolayers of cholesterol and lecithin do not follow the additivity rule i.e. the area per molecule of



cholesterol-lecithin mixed monolayers is different from that expected on the basis of their individual area requirements since above the phospholipid gel-liquid crystalline phase transition temperature, cholesterol is able to fit into cavities between adjacent lecithin molecules, while below this temperature, much denser lipid-lipid packing exists. A phospholipid with fully saturated fatty acid chains will exist in the low energy all trans (straight chain) conformation which results in a maximization of packing density. Since interlipid cavities are no longer available for occupation by cholesterol, below the  $T_m$ , the intercalation of cholesterol involves a pushing apart of lecithin molecules, leading to decreased monolayer packing. Therefore, cholesterol is said to place the membrane in an "intermediate fluid" condition. This behaviour is also manifested in the severe broadening of the lecithin phase transition by intercalated cholesterol.

A third type of model membrane system is that of oriented lipid multilayers. Such models have been most often studied by electron spin resonance (ESR) spectroscopy using nitroxide labelled membrane components as reporter groups (51-72). The spectra obtained are sensitive both to the orientation and the mobility of these spin labels, and the angular dependence of the hyperfine splittings has been utilized to discern orientation angles i.e. the angles which the nitroxide  $2p\pi$  orbital makes with the membrane surface.

7

Use has also been made of the fact that nitroxide spin labels are readily reduced by sodium ascorbate to the corresponding hydroxylamine with concomitant loss of ESR signal intensity. The rate of signal decay may therefore be used as a spectroscopic ruler to determine the depth at which various spin probes lie within oriented multilayers and to monitor the permeability of these membrane models (73).

A fourth type of model system, multilamellar liposomes, has also yielded valuable information via magnetic resonance techniques. Insight into the motion and orientation of the lecithin phosphate group has been obtained from  $^{31}\text{P}$  NMR (74-79), while the  $^2\text{H}$  NMR spectra of these phospholipid dispersions have proved to be of great utility for the measurement of order parameters of deuterium labelled lipids (80-86).

From the foregoing, it is clear that magnetic resonance techniques are powerful tools for the investigation of both the structure and motions of membranes.

#### B. Vitamin E, Phytol, and Phytanic Acid

There has been much interest concerning the physiological role played by Vitamin E. While it is well known that Vitamin E functions as an antioxidant in vitro, protecting unsaturated lipids from free radical attack (87), it has also recently been shown that  $\alpha$ -tocopherol

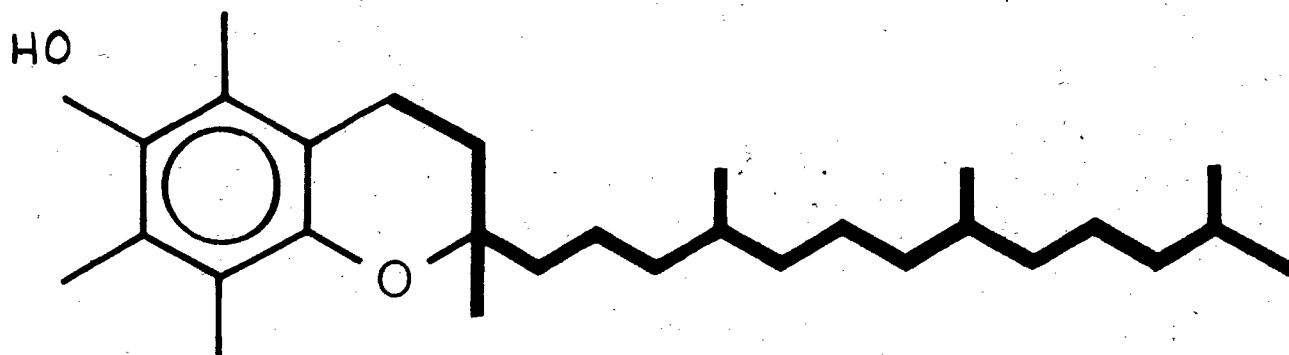
is a very efficient quencher of  $^1O_2$ , and as such may perform a protective role in vivo (88-90). Singlet molecular oxygen reacts with membrane constituents (e.g. unsaturated fatty acids and cholesterol) to form haemolytic hydroperoxide products. Therefore the inactivation of  $^1O_2$  by  $\alpha$ -tocopherol has been proposed to increase cell viability.

There also exist a number of observations which suggest that Vitamin E may play a structural role in membranes. Vitamin E has been implicated as a dietary factor in the prevention of atherosclerosis (91). It has been claimed that cholesterol diets which are supplemented with  $\alpha$ -tocopherol are less atherogenic in rabbits than cholesterol diets alone. Since this therapeutic effect was observed without concomitant lowering of the level of lipid peroxides present in the tissue, it is possible that the observed effect are structural in origin.

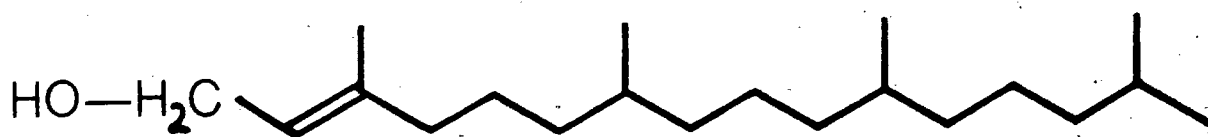
Vitamin E ( $\alpha$ -tocopherol; D-2.5.7.8-tetramethyl-2-(4.8.12-trimethyltridecyl)-6-chromanol), as well as the isoprenoids phytol and phytanic acid (Figure 2) have also been found to be effective in the treatment of nutritional muscular dystrophy in chicks (92). Lucy and Dingle have demonstrated that the rapid haemolysis of rabbit erythrocytes by added retinol is inhibited in vitro by  $\alpha$ -tocopherol as well as other branched chain compounds, namely 6-O-acetyl- $\alpha$ -tocopherol, squalene, ubiquinone-30, vitamin K<sub>1</sub>, and phytol, while N-N'-phenylenediamine, and hydroquinone are completely ineffective.

9a

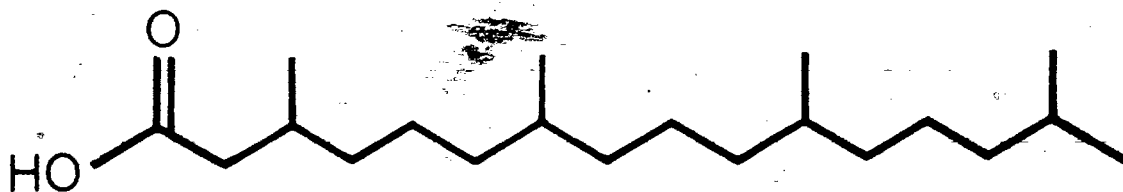
Figure 2. The structures of Vitamin E, phytol, and phytanic acid.



VITAMIN E



PHYTOL



PHYTANIC ACID

However, higher concentrations of Vitamin E and phytol were also found to cause extensive haemolysis (93).

It has also been shown that cytochrome-c reductase which has been inactivated by its extraction from porcine liver is re-activated not only by Vitamin E, but also by 6-O-acetyl- $\alpha$ -tocopherol, phytanic acid, and phytol (94). It appears that these effects are not due to the  $\alpha$ -tocopherol ring system which provides the antioxidant activity, but rather that these effects are due to the branched nature of the phytol side chain.

Moreover, the matter does not rest there. Methylmalonic aciduria results in the excretion of large amounts of methylmalonic acid in the urine of children. It has been proposed that a deficiency of B<sub>12</sub> coenzyme leads to the buildup of methylmalonyl CoA which in turn leads to the biosynthesis of branched chain fatty acids which are not normally produced, causing the harmful neurological effects (95).

The accumulation of branched chain compounds has also been found to be a factor in the progression of Refsum's disease. Patients afflicted with this disorder are not able to  $\alpha$ -oxidize and decarboxylate phytanic or similar branched chain fatty acids, and an accumulation of branched acids results. This buildup has been cited as a causative factor in the degeneration (demyelination) of the nervous system, which eventually leads to death (96).

The question remains: how may such effects be rationalized on a molecular level? Unlike cholesterol which is known to intercalate between the phospholipid fatty acid chains, thereby affecting membrane fluidity and permeability, very little is known of the orientation of Vitamin E in membranes, although the main effects of Vitamin E deficiency seem to be reflected in the lipid moiety (97).

### C. Cholesterol Esters

The effects of cholesterol on model membrane systems has been widely investigated by a variety of techniques. Substantially less is known of the effects of cholesterol esters. This is rather surprising since cholesterol esters have been implicated in the progressive development of atherosclerosis (98).

Since the presence of cholesterol is known to decrease the permeability of membranes (99), and since the amount of cholesterol present in the human aorta is known to increase with age, it is somewhat perplexing that the permeability to lactate, glucose, and iodide of sclerotic human aorta is higher than that of normal tissue (100,101). This apparent anomaly may be clarified by an examination of the cholesterol ester-free cholesterol ratio during the progression of the disease. For disease free type 0 tissue, this ratio is 5.6/8.0, while for type III tissue which is characterized by fatty streaks, fibrous plaques, and lesions, this ratio is 33.8/19.3 (102).

(The numbers in these ratios represent the percentage which the particular components comprise of the total lipid present.) As can be seen from the ratios, the increment in cholesterol ester content is much greater than the increase in free cholesterol, i.e. a 6 fold increase from 5.6% to 33.8% as opposed to only a two fold increase in free cholesterol from 8.0% to 19.3%.

The suggestion has been made that even before morphological changes appear, certain areas of the aortic intima are predisposed to the development of atherosclerotic lesions (98). Such areas have been associated with little change in lipid content, save for a small increase in the amount of cholesterol ester. More importantly, these areas have also been associated with increased permeability (98). Other evidence comes from the fact that increased cholesterol ester formation occurs at a very early stage of atherosclerosis. For example, the synthesis of cholesterol esters is increased by four to six times in only slightly diseased arteries of squirrel monkeys (103).

Whether increased permeability is simply an intrinsic property of the developing lesions, or whether there exists a causal relationship between permeability and atherogenesis is unclear. However, the possibility that cholesterol esters might exert an influence opposite to that of cholesterol on membrane properties is intriguing in itself. If, in fact, cholesterol esters increase membrane permeability, a loss



may occur from the aortic intima of certain materials necessary for metabolic control, resulting in an even greater lipid over-accumulation (101). Thus, the elucidation of the effects of cholesterol esters on membrane structure and permeability may shed light on the progressive development of atherosclerosis.

#### D. Statement of the Problem

The aims of this investigation are twofold; first to study the effects of the incorporation of the isoprenoids Vitamin E, phytol, and phytanic acid on the structure and properties of model membrane systems, and secondly, to study the effects of cholesterol esters on lecithin model membranes, and to extend these findings to a natural system, namely human aortic tissue, since the results of such studies may have possible implications for atherosclerosis.

In spite of the obvious physiological importance of Vitamin E, phytol, phytanic acid, and cholesterol esters, very little was known of their effects on a molecular level, not even whether or not they could be successfully incorporated into simple model membrane systems, let alone the effects of their presence on membrane properties. Therefore, it was decided to investigate the nature of mixed membrane systems containing Vitamin E, phytol, phytanic acid, and cholesterol esters, using magnetic resonance techniques.

## CHAPTER 2

## EXPERIMENTAL

## A. Materials

Egg yolk lecithin (EYL) was extracted from fresh yolks by the method of Singleton et al (104). Thin layer chromatographic analysis (0.25 mm Silica Gel G. developed with  $\text{CHCl}_3:\text{MeOH}:\text{H}_2\text{O} = 65:35:4$ ) showed a single spot when sprayed with 50%  $\text{H}_2\text{SO}_4$  and heated, or when exposed to  $\text{I}_2$  vapour. The fatty acid composition of EYL was determined by means of GLC analysis of the corresponding methyl esters using the methylating agent, methElute (methanolic trimethylanilinium hydroxide, 0.2M). Approximately 1 mg of purified EYL was added to 0.5 ml methElute and a 1 ul aliquot injected onto a 6 ft x 4 mm Silar 10C column. Settings were as follows: column temperature =  $180^\circ\text{C}$ , detector temperature =  $250^\circ\text{C}$ , injector temperature =  $250^\circ\text{C}$ . Peaks were identified by comparison with known standards.

3-Doxylcholestane(4',4'-dimethylspiro[5- $\alpha$ -cholestane-3,2'-oxazolidin]-3'-yloxy), I, and 5-doxylpalmitic acid (2-(10-carboxydecyl)-2-butyl-4,4-dimethyl-3-oxazolidinyloxy), II, were the generous gifts of Dr. A.C. Oehlschlager, Chemistry Dept., Simon Fraser University, while 16-doxylstearic acid (2-(14-carboxytetradecyl)-2-ethyl-4,4-dimethyl-3-oxazolidinyloxy), III, was purchased from Syva, Palo Alto.

California. The corresponding cholesteryl esters of 5-doxy palmitic acid and 16-doxy stearic acid, IV and V, respectively, were prepared in this laboratory by Dr. A.K. Grover by the method of Boss et al (105), as was cholesteryl-1-<sup>14</sup>C-palmitate. The structures of I-V are shown in Figure 3.

Other chemicals were purchased from the following sources: phytol - Nutritional Biochemical Corporation, or Aldrich Chemical Co.; Vitamin E (dl- $\alpha$ -tocopherol), dipalmitoyl lecithin (99%) (DPL), cardiolipin, phosphatidic acid (95%), cholesteryl palmitate (99%), cholesteryl linoleate (99%), and L-ascorbic acid, sodium salt - Sigma Chemical Co.; disodium ethylenediaminetetraacetate (EDTA), and cholesterol - Fisher Scientific Co.; praseodymium nitrate (99.9%) - Alfa Inorganics; phytanic acid (99.7%) - Analabs; deuterium oxide (99.7%) - Merck, Sharp and Dohme; palmitic acid - J.T. Baker Chemical Co.; methElute (methanolic trimethylanilinium hydroxide, 0.2M) - Aldrich Chemical Co.; 1-<sup>14</sup>C-palmitic acid - New England Nuclear.

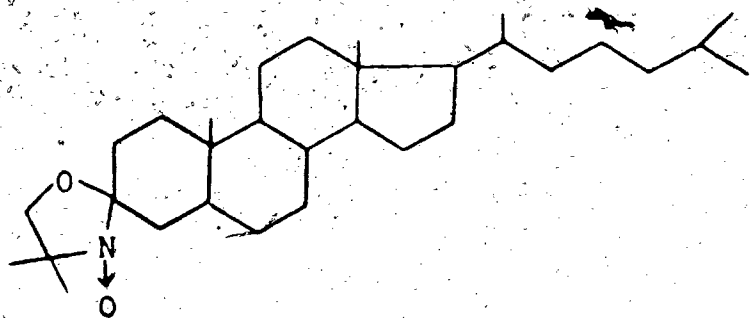
## B. Sample Preparation

### 1. Vesicles

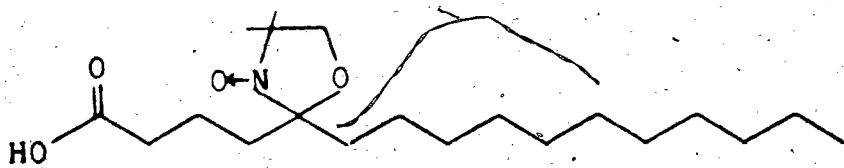
Lecithin dispersions (EYL or DPL, 10-20% w/v) were prepared by shaking the dry phospholipid with a suitable volume of an aqueous phase (3-4 ml of D<sub>2</sub>O in the case of <sup>13</sup>C spectra, and 0.05M Tris pH=7.22, 0.05M in KCl, in the case of <sup>31</sup>P spectra). The dispersions

Figure 3. The structure of various nitroxide spin probes.

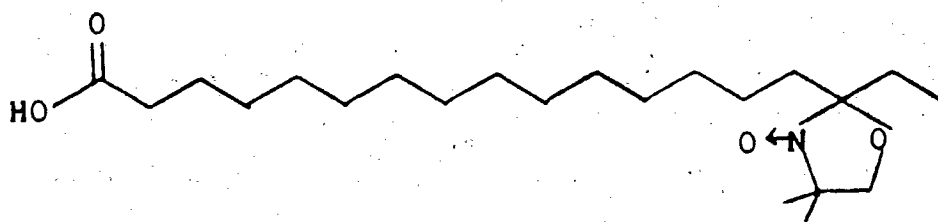
I, 3-doxylcholestane; II, 5-doxylpalmitate;  
III, 16-doxylstearate; IV. the cholesteryl  
ester of II; V. the cholesteryl ester of III.



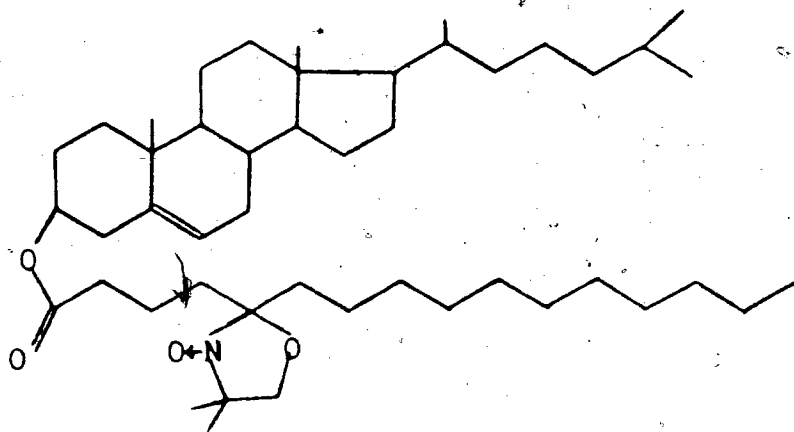
I



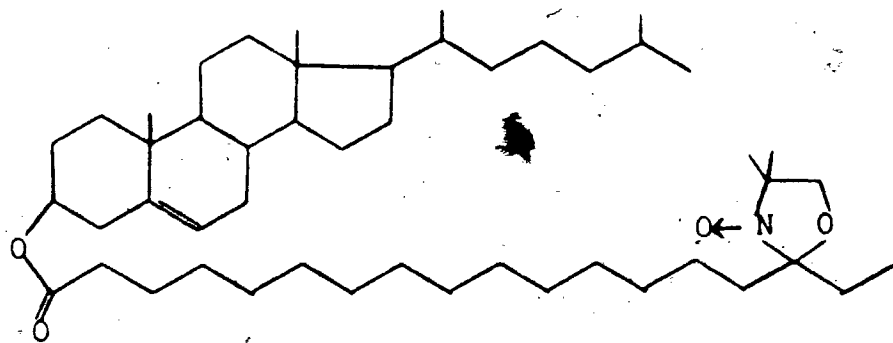
II



III



IV



V

were then sonicated under nitrogen on a Biosonik III probe type sonicator above the phospholipid gel-liquid crystalline phase transition temperature until translucence. Sonication time was approximately 10 minutes, except in the case of EYL:phytol, 1:1 mole ratio, mixed vesicles which required more prolonged sonication (20 min-2 hr). The temperature was maintained at approximately 10°C in the case of EYL preparations and at approximately 50°C in the case of DPL preparations by means of water flowing through a jacket surrounding the sample. The vesicle preparations were then centrifuged or passed through a 0.45  $\mu$  Millipore filter to remove titanium debris or any larger liposomes, and subsequently transferred under nitrogen to 12 mm NMR tubes. The spectra were determined immediately. Subsequent TLC analysis of the samples showed little (<5%) decomposition of the samples during the intervening time period.

Mixed vesicle preparations were prepared in a similar manner by first co-dissolving the components in chloroform, followed by solvent removal, and exhaustive pumping to obtain the dry lipid mixture.

## 2. Phytol dispersions

Phytol was dispersed in D<sub>2</sub>O (10% w/v) with the addition of 2-20 mole % sodium dodecylsulfate (SDS) and mechanical shaking. The dispersions were then sonicated and subsequently treated in the manner described in Section 2.B.1.

### 3. Phospholipid multilamellar liposomes

Lecithin multilamellar liposomes 40% w/v in either D<sub>2</sub>O or 10% sucrose in D<sub>2</sub>O were prepared by mechanical shaking of the dry lipid with a suitable volume of the aqueous phase. These dispersions were stabilized by approximately six heat-freeze-thaw cycles. Homogeneous mixed dispersions of lecithin:cholesteryl ester = 3:1 mole ratio were prepared in a similar manner. The dry lipid mixture was prepared as described in Section 2.B.1. by first co-dissolving both components in chloroform.

All attempts to disperse cholesteryl ester alone in an aqueous phase were unsuccessful, even in the presence of large quantities of detergents such as SDS or Tween 20 even above the melting point of the ester.

### 4. Oriented lipid multilayers

Oriented lipid multilayers used in ESR spectral determinations were prepared by slowly passing wet nitrogen through a quartz aqueous ESR cell which contained approximately 0.10 ml of chloroform solution containing the multilayer components. This solution was prepared from stock solutions of  $5 \times 10^{-2}$  M lipid, and  $1 \times 10^{-3}$  M spin label. The total lipid:spin label mole ratio was 100:1 unless otherwise specified.

The lipid multilayers were then placed in the dark under vacuum for at least three hours to remove residual chloroform, and subsequently hydrated with 0.05M Tris pH = 7.40. Each sample was used for at least two spectral determinations, one with the magnetic field parallel, and another with the magnetic field perpendicular to the normal to the multilayer surface.

#### 5. Aorta membrane

The aorta, type II, of a 55 year old female was obtained from Vancouver General Hospital. The frozen aorta was thawed overnight at 5°C in 0.01M borate, pH=7.5, which was 0.25M in sucrose. A small amount of connective tissue was removed and the entire aorta cut into strips approximately 1 cm x 0.5 cm. The tissue was then homogenized under nitrogen in a Waring blender in the borate buffer for approximately 2 minutes, and subsequently centrifuged at 1000 x g for 10 minutes. The pellet was then rehomogenized, and the combined supernatants centrifuged at 100,000 x g for 90 minutes. This pellet was then suspended under nitrogen in a 12 mm NMR tube in 2 ml of 0.05M Tris, pH=7.2, which was 0.05M in KCl.  $^{31}\text{P}$  NMR spectra were determined immediately.

The thick membrane suspension was then sonicated under nitrogen at 11°C for approximately 10 minutes. The consistency of the sample was altered by this treatment to that of a cloudy non-viscous liquid.  $^{31}\text{P}$  spectra were then redetermined.



The sample was subsequently dialysed against three changes of 2000 ml of distilled water while nitrogen was continually bubbled through the bulk solution. Following the dialysis, the sample was resonicated and transferred under nitrogen to a 12 mm NMR tube, and  $^{13}\text{C}$  spectra determined.

### C. Nuclear Magnetic Resonance Spectra

All NMR spectra were determined on a Varian XL-100-15 NMR spectrometer operating in the pulse Fourier transform mode.

#### 1. $^{13}\text{C}$ NMR

$^{13}\text{C}$  NMR spectra were determined at 25.2 MHz using an internal  $^1\text{H}$  field-frequency lock with an 8K dataset. Chemical shifts were measured relative to external tetramethylsilane (TMS) or hexamethyldisilane (HMDS) present in a co-axially mounted capillary. All reported chemical shifts were converted to the TMS scale by the relationship

$$\delta_{\text{TMS}} = \delta_{\text{HMDS}} - 2.34\text{ppm}$$

II-1

In the initial stages of this investigation,  $^{13}\text{C}$   $T_1$  relaxation times for 20% w/v lecithin vesicles and for lecithin-phytol mixed vesicles were measured by the inversion recovery method of Vold et al (106) which employs a  $(\pi-\tau-(\pi/2)-T)$  pulse sequence where  $\tau$  is

the delay time between the  $180^\circ$  and  $90^\circ$  pulses. This pulse sequence was repeated after a time  $T$  which was at least five times the largest  $T_1$  value to be measured. Although the time required for a set of inversion-recovery spectra is up to 48 hours, the samples remained homogeneous and subsequent TLC analysis showed little lipid decomposition. In addition, there were no major differences in proton noise decoupled  $^{13}\text{C}$  spectra obtained before and after the inversion-recovery experiments.

During the later stages of this investigation, it became possible to employ the timesaving homogeneity spoiling technique of McDonald and Leigh (107). This pulse sequence, which is discussed in detail in Section 3.A.2. was used to determine the  $^{13}\text{C}$   $T_1$  relaxation times for the lecithin-Vitamin E, and lecithin-phytanic acid vesicle systems, and for the lecithin-cholesteryl ester dispersions.  $T_1$ 's for several carbons which were indicated to be less than 0.3 sec were checked by the inversion-recovery method and were found to be in agreement with the homospoil determinations to within experimental error.

The percentage error for each measurement was approximately 6-7%; occasionally duplicate experiments showed a variance of up to 10%. Therefore the confidence limit is set at  $\pm 10\%$  and if the variance exceeded the % error, the variance is reported.

## 2. <sup>31</sup>P NMR

<sup>31</sup>P NMR spectra were determined at 40.5 MHz using an external <sup>19</sup>F field-frequency lock and a 2K dataset with external H<sub>3</sub>PO<sub>4</sub> (85%) as a reference.

For permeability measurements of pure EYL and mixed vesicle systems to Pr<sup>3+</sup>, samples were prepared as described in Section 4.B.1. Initial spectra were determined and a 150 ul portion of 0.1M Pr(NO<sub>3</sub>)<sub>3</sub> · 5H<sub>2</sub>O in the aforementioned buffer solution was then added. The use of 3 ml of vesicle preparation resulted in a Pr<sup>3+</sup> concentration of 0.005M. Subsequent spectra were determined at intervals, and the rate of disappearance of the sharp upfield <sup>31</sup>P resonance was monitored. Subsequent to the disappearance of this peak, 300 ul of 0.2M EDTA which complexes with Pr<sup>3+</sup> was routinely added, and the spectra redetermined.

Separate experiments were also performed in order to study the rate of EDTA permeation through pure EYL vesicles. EYL was dispersed in the previously mentioned buffer which has been made 0.005M in Pr<sup>3+</sup>. Subsequent sonication of this dispersion results in vesicles which possess lanthanide both inside and out. Initial spectra were determined followed by the addition of 300 ul of 0.2M EDTA, and the rate of increase of the area of the sharp upfield resonance was monitored.

## D. Electron Spin Resonance Spectra

### 1. General

All ESR spectra were determined at 23°C on a Varian E-4 EPR spectrometer operating in the X band at approximately 9.5 GHz. Oriented multilayer samples were prepared as described in Section 2.B.3. Typical spectrometer settings were: scan range = 100-400 G., receiver gain =  $5 \times 10^2$ , modulation amplitude = 0.5 G., time constant = 0.3 sec. scan time = 4 min. microwave power = 10-100mW.

### 2. Ascorbate permeation

For the study of the permeation of sodium ascorbate into the lipid multilayers, hydration was carried out by the addition of freshly prepared, thoroughly deoxygenated 0.01M sodium ascorbate which was 0.15M in NaCl. The pH of the ascorbate solution had been previously adjusted to  $6.8 \pm 0.1$  with NaOH or HCl. All spectra were determined with the magnetic field perpendicular to the multibilayer surface. In the case of EYL samples, there was observed an immediate change in the spectral shape upon ascorbate addition, indicating complete hydration of the lipid films. This was not found to be the case for DPL multilayers; however, prehydration of the films in 0.15M NaCl for approximately one hour, followed by rinsing and hydration with the ascorbate solution produced the desired result.

The kinetics of the spin label reduction were followed by recording the low field component of the ESR spectrum at intervals (15 sec-4 min), since this line does not overlap with that due to the ascorbate radical which is produced during the reaction. The rate of decay of the height of the low field component is proportional to the rate of ascorbate reduction of the incorporated spin probe, if there is no change in spectral shape during the course of the reaction and this, indeed, was found to be the case.

## CHAPTER 3

## THEORETICAL CONSIDERATIONS

This chapter will present in two major parts an outline of the existing theory which provides the basis for the experimental techniques used in this investigation. The first part deals briefly with nuclear magnetic relaxation processes and the pulse sequences used in the determination of spin-lattice relaxation times. Following this is a discussion of linear electric field effects on  $^{13}\text{C}$  chemical shifts of olefinic carbons. A more complete discussion of nuclear magnetic resonance can be found in works by Abragam (108), and by Slichter (109). For a detailed account of the applications of NMR to biological membranes, the reader is referred to a recent review by Lee, Birdsall, and Metcalfe (110).

The second part of this chapter deals with the basic principles of the electron spin resonance of nitroxide spin probes, outlining the type of information which may be gained through the use of this tool. A recent treatise (111) provides an excellent overview of progress in this area.

## A. Spin-Lattice Relaxation

### (1) General

Bloch et al (112,113) discovered that the motion of the macroscopic magnetization of nuclei in the presence of an applied static field could be described by a set of phenomenological differential equations. In a static field  $H_z = H_0$ , if the magnetization is disturbed from its equilibrium value by the application of a radiofrequency pulse applied at right angles to the applied field  $H_0$ , the components of the magnetization will decay to their equilibrium values according to the equations governing the rate of approach to equilibrium (108).

$$\frac{dM_z}{dt} = - \frac{(M_z - M_0)}{T_1} \quad \text{III-1}$$

$$\frac{dM_x}{dt} = - \frac{M_x}{T_2} \quad \text{III-2}$$

$$\frac{dM_y}{dt} = - \frac{M_y}{T_2} \quad \text{III-3}$$

where  $M_x$ ,  $M_y$ , and  $M_z$  are the components of the magnetization in the x, y, and z directions, and  $T_1$  and  $T_2$  are the longitudinal (spin lattice) and transverse (spin-spin) relaxation times respectively.

The return of the z component of the net magnetization along  $H_0$  (the z direction) is therefore characterized by a time  $T_1$ , the spin-lattice relaxation time. The nonradiative return to equilibrium arises from the interaction of the nuclei with oscillatory magnetic fields produced by molecular motion in the sample (110). If the rates of motion overlap with the Larmor precession frequency of the nucleus concerned, a transition may occur from the upper spin state to the lower spin state.

The equation of motion for the macroscopic magnetization vector  $\bar{M}$  in a magnetic field  $\bar{H}$  is given by (114)

$$\frac{d\bar{M}}{dt} = \gamma(\bar{M} \times \bar{H}) \quad \text{III-4}$$

where  $\gamma$  is the gyromagnetic ratio of the nucleus in question. The presence of an observation field  $H_1$  applied to right angles to the static field,  $H_0$ , may be thought of as a field rotating in the xy plane, about the z axis at an angular frequency,  $\omega$  (115). The components of the magnetic field are therefore (115)

$$H_x = H_1 \cos \omega t \quad \text{III-5}$$

$$H_y = -H_1 \sin \omega t \quad \text{III-6}$$

$$H_z = 0 \quad \text{III-7}$$

Expanding the cross product in equation III-4 and substituting from equations III-5, III-6 and III-7 yields (115)



$$\frac{dM_x}{dt} = \gamma M_y H_0 + \gamma M_z H_1 \sin \omega t \quad \text{III-8}$$

$$\frac{dM_y}{dt} = \gamma M_z H_1 \cos \omega t - \gamma M_x H_0 \quad \text{III-9}$$

$$\frac{dM_z}{dt} = -\gamma M_x H_1 \sin \omega t - \gamma M_y H_1 \cos \omega t \quad \text{III-10}$$

Since  $M_x$  and  $M_y$  relax back to an equilibrium value of zero, and  $M_z$  relaxes to an equilibrium value of  $M_0$ , therefore (115)

$$\frac{dM_x}{dt} = \gamma (M_y H_0 + M_z H_1 \sin \omega t) - (M_x/T_2) \quad \text{III-11}$$

$$\frac{dM_y}{dt} = \gamma (M_z H_1 \cos \omega t - M_x H_0) - (M_y/T_2) \quad \text{III-12}$$

$$\frac{dM_z}{dt} = -\gamma (M_x H_1 \sin \omega t + M_y H_1 \cos \omega t) - (M_z - M_0)/T_1 \quad \text{III-13}$$

Thus the equations III-1, III-2 and III-3 are seen to be damping terms for the rate of motion equations describing the NMR experiment.

In general, any mechanism by which fluctuating magnetic fields are produced at the nucleus is a possible mechanism of nuclear relaxation. These processes are (110):

1. magnetic dipole-dipole interactions
2. chemical shift anisotropy
3. scalar coupling
4. spin rotation
5. electric quadrupole for nuclei with  $I > 1/2$  where  $I$  is the nuclear spin quantum number.

For any random motional fluctuation,  $F(t)$ , an autocorrelation function may be defined which relates the value of  $F(t)$  at one time to its value after a time interval  $\tau$ , as (116)

$$G(\tau) = \overline{F^*(t+\tau) F(t)} \quad \text{III-14}$$

where the bar denotes an average overall time. If  $G(\tau)$  decays exponentially with a time constant  $\tau_c$ , the autocorrelation function takes the form (116)

$$G(\tau) = \overline{F^*(t) F(t)} \exp(-|\tau|/\tau_c) \quad \text{III-15}$$

Since the spectral density of  $F(t)$  is the Fourier transform of the autocorrelation function (116),

$$J(\omega) = \int_{-\infty}^{+\infty} G(\tau) e^{i\omega\tau} d\tau \quad \text{III-16}$$

or (116),

$$J(\omega) = \frac{2\tau_c}{1+\omega^2\tau_c^2} \overline{F^*(t) F(t)} \quad \text{III-17}$$

Thus, for a fluctuating nuclear dipole-dipole interaction, for example, the spectral density gives the energy available for producing nuclear relaxation at the frequency,  $\omega$  (110).

The dominant mechanism for spin-lattice relaxation of  $^{13}\text{C}$  nuclei with directly bonded protons in large molecules is through intramolecular  $^{13}\text{C}$ - $^1\text{H}$  dipole-dipole interactions (117-119). This has been verified by nuclear Overhauser enhancement studies. Therefore the discussion of  $^{13}\text{C}$   $T_1$  relaxation mechanisms will be limited to that induced by dipole-dipole interactions with directly bonded protons.

## 2. Dipole-dipole relaxation

The Hamiltonian for the interaction of two magnetic dipoles is given by (116)

$$H_{dd} = \sum_{i < j} \bar{I}(i) \bar{D}_{ij} \bar{I}(j) \quad \text{III-18}$$

where  $\bar{I}(i)$  and  $\bar{I}(j)$  are the spin vector operators of the two nuclei,

and  $\bar{D}_{ij}$  is the dipolar interaction tensor between the nuclei  $i$  and  $j$ .

In the case of intramolecular dipole-dipole relaxation, the components of  $D_{ij}$  are time dependent since molecular reorientations cause changes in the angle between the internuclear vector, and the applied magnetic field (110).

For a fully proton decoupled  $^{13}\text{C}$ -H system, the  $^{13}\text{C}$   $T_1$  relaxation time is given by (119)

$$1/T_1 = W_0 + 2W_1 + W_2 \quad \text{III-19}$$

where the  $W$ 's are the probabilities for the transitions by which relaxation occurs. These transition probabilities may be calculated by the method of Bloembergen, Purcell and Pound (120) to be (121)

$$W_0 = \frac{\tau_c}{8\hbar^2} \langle F_0^2 \rangle \frac{1}{1 + (\omega_c - \omega_H)^2 \tau_c^2} \quad \text{III-20}$$

$$W_1 = \frac{\tau_c}{2\hbar^2} \langle |F_1|^2 \rangle \frac{1}{1 + \omega_c^2 \tau_c^2} \quad \text{III-21}$$

$$W_2 = \frac{2\tau_c}{\hbar^2} \langle |F_2|^2 \rangle \frac{1}{1 + (\omega_c + \omega_H)^2 \tau_c^2} \quad \text{III-22}$$

where  $\omega_C$  and  $\omega_H$  are the Larmor frequencies in radians per second for carbon and hydrogen respectively, and where  $F_0$ ,  $F_1$  and  $F_2$  represent orientation functions for the fluctuating dipole-dipole interaction. If this motion is isotropic, the average value of the orientation functions are given by (121)

$$\langle F_0^2 \rangle = (4/5)K^2 \quad \text{III-23}$$

$$\langle |F_1|^2 \rangle = (3/10)K^2 \quad \text{III-24}$$

$$\langle |F_2|^2 \rangle = (3/10)K^2 \quad \text{III-25}$$

where

$$K = \hbar^2 \gamma_C \gamma_H / r^3 \quad \text{III-26}$$

and where  $\gamma_H$  and  $\gamma_C$  are the gyromagnetic ratios of  $^1\text{H}$  and  $^{13}\text{C}$  respectively, and  $r$  is the carbon-hydrogen internuclear distance.

Substitution of equation III-26 into equations III-23 to III-25 and subsequently into equations III-20 to III-22 yields

$$W_0 = \frac{\hbar^2 \gamma_C^2 \gamma_H^2 \tau_c}{10r^6} \left[ \frac{1}{1 + (\omega_C - \omega_H)^2 \tau_c^2} \right] \quad \text{III-27}$$

$$W_1 = \frac{3\hbar^2 \gamma_C^2 \gamma_H^2 \tau_c}{20r^6} \left[ \frac{1}{1 + \omega_C^2 \tau_c^2} \right] \quad \text{III-28}$$

$$W_2 = \frac{6\hbar^2 \gamma_C^2 \gamma_H^2 \tau_c}{10r^6} \left[ \frac{1}{1 + (\omega_C + \omega_H)^2 \tau_c^2} \right] \quad \text{III-29}$$

and substitution of equations III-27 to III-29 into equation III-19 yields

$$\frac{1}{T_1} = \frac{\hbar^2 \gamma_C^2 \gamma_H^2 \tau_c}{10r^6} \left[ \frac{1}{1 + (\omega_C - \omega_H)^2 \tau_c^2} + \frac{3}{1 + \omega_C^2 \tau_c^2} + \frac{1}{1 + (\omega_C + \omega_H)^2 \tau_c^2} \right] \quad \text{III-30}$$

In the case of phospholipid membrane systems, the correlation times decrease with increasing temperature (7,21), indicating that  $w^2\tau_c^2 \ll 1$ . Neglecting long range  $^{13}\text{C}-^1\text{H}$  interactions, and summing over all directly bonded protons yields the expression (118)

$$\frac{1}{T_1} = \frac{\hbar^2 \gamma_H^2 \gamma_C^2 N \tau_c}{r^6} \quad \text{III-31}$$

where N is the number of directly bonded protons. However, the preceding treatment assumes that the motional fluctuation of the  $^{13}\text{C}-^1\text{H}$  dipole is isotropic. Taking into account anisotropy of internal reorientation which is believed to be present in phospholipid bilayers requires the modification of the time average orientation functions of equations III-20 to III-22 (21, 118, 122). The resultant modification of equations III-20 to III-22 may be expressed in terms of an anisotropy parameter, A, as (5.147)

$$\frac{1}{T_1} = \frac{A \gamma_C^2 \gamma_H^2 \hbar^2 N \tau_c}{r^6} \quad \text{III-32}$$

where  $A = \langle (3/2) \cos^2\theta - (1/2) \rangle^2$  where  $\theta$  is the angle between the  $^{13}\text{C}-^1\text{H}$  vector and the axis of internal reorientation. Thus for rapid anisotropic motion, the  $^{13}\text{C}$  spin-lattice relaxation times for carbon nuclei in a phospholipid bilayer are given by (21)

$$\frac{1}{T_1} = \frac{1}{4} \langle 3 \cos^2\theta - 1 \rangle^2 \frac{\gamma_C^2 \gamma_H^2 \hbar^2 N \tau_c}{r^6} \quad \text{III-33}$$

Unfortunately, the contributions to the observed  $^{13}\text{C}$   $T_1$  relaxation times cannot be separated into their components due to rate

of motion ( $\tau_c$  dependence) and that due to anisotropy of the motion (angular dependence), as has been pointed out previously (84,86). It can readily be seen that in the isotropic limit, equation III-33 reduces to equation III-31, and thus  $T_1$  is a direct measure of rate of motion. In the case of anisotropy of the reorientation of the  $^{13}\text{C}$ - $^1\text{H}$  internuclear vector, an increase in  $^{13}\text{C}$   $T_1$  relaxation times for a phospholipid membrane system may be due to increased rate of segmental motion about individual carbon-carbon bonds, or due to increased disorder of the motion or both. Nevertheless,  $^{13}\text{C}$   $T_1$  relaxation times for phospholipid membrane systems are still a measure of relative motional freedom, or bilayer "fluidity", regardless of whether the effects are due to changes in the anisotropy of the motion, its rate, or both.

### 3. Measurement of spin-lattice relaxation times

Pulsed NMR methods are best understood if they are discussed in terms of the bulk magnetization of the sample, considered in the rotating frame. One method of measuring spin lattice relaxation times is the inversion-recovery method of Vold et al (106) which involves a  $(180^\circ, \tau, 90^\circ)$  pulse sequence.

Initially, the magnetization lies along the  $z'$  axis. A  $180^\circ$  pulse is applied which flips the magnetization to the  $-z'$  axis. The magnetization is then allowed to undergo longitudinal relaxation for a

time  $\tau$ . If  $\tau$  is very long compared with  $T_1$ , the magnetization will eventually relax from a value of  $-M_0$  through zero to its equilibrium value,  $+M_0$ . After a specified time,  $\tau$ , a  $90^\circ$  pulse is applied along the  $x'$  axis. The remaining magnetization is thereby rotated to the  $y'$  (or  $-y'$ ) axis, and the free induction decay is measured. Thus if  $\tau$  is very short compared with  $T_1$ , very little relaxation will occur during the time,  $\tau$ , and the result will be negative resonance signal. As the duration of  $\tau$  is increased, more relaxation occurs before the application of the  $90^\circ$  pulse. The result of a series of increasing  $\tau$  values will be a series of spectra with resonances whose intensity varies from a negative value, through zero, and finally approaches a maximum positive value at very long  $\tau$ . The pulse train of  $(180^\circ - \tau - 90^\circ - T)_n$  is repeated a specified  $n$  times until sufficient signal/noise is achieved. The quantity  $T$  in the pulse sequence is a time of at least  $5xT_1$ , during which the system is allowed to return to equilibrium.

The free induction decay is then Fourier transformed and the signal intensity is measured. Repeating this process for different values of  $\tau$  enables the determination of the spin-lattice relaxation time  $T_1$  since integration of equation III-1 with the condition  $M_z = -M_0$  at  $t=0$  yields (115)

$$M_z = M_0 (1 - 2 \exp^{-t/T_1}) \quad \text{III-34}$$

It follows that

$$\ln(A_\infty - A_\tau) = \ln 2A_\infty - (\tau/T_1) \quad \text{III-35}$$

where  $A_\infty$  is the spectral amplitude for  $\tau > 5T_1$ ,  $A_\tau$  is the spectral amplitude for a specified value of  $\tau$ , and  $\tau$  is the interval between the  $180^\circ$  and  $90^\circ$  pulses.  $T_1$  may be obtained from the slope of a plot of  $\ln(A_\infty - A_\tau)$  vs  $\tau$ .

$T_1$  may also be measured by the homogeneity spoiling technique of McDonald and Leigh (107) which is illustrated in Figure 4. An initial  $90^\circ$  pulse which shifts the net magnetization into the x'y' plane is followed by a field gradient pulse which is applied through the magnet's shim coils. This spoils the field homogeneity and causes a rapid dephasing of the magnetization in the x'y' plane, resulting in zero net magnetization. After a time interval  $\tau$ , during which the spins are allowed to relax, a second  $90^\circ$  pulse is applied, and the magnitude of the free induction sampled. The field gradient is then reapplied to eliminate any remaining magnetization in the x'y' plane, and the pulse sequence may be repeated immediately. The repeating sequence is thus (90-spoil- $\tau$ -90-sample-spoil) $_n$ . The variation of signal intensity with  $\tau$  follows the relationship (110).

$$A(\tau) = A_\infty [1 - \exp(-\tau/T_1)] \quad \text{III-36}$$

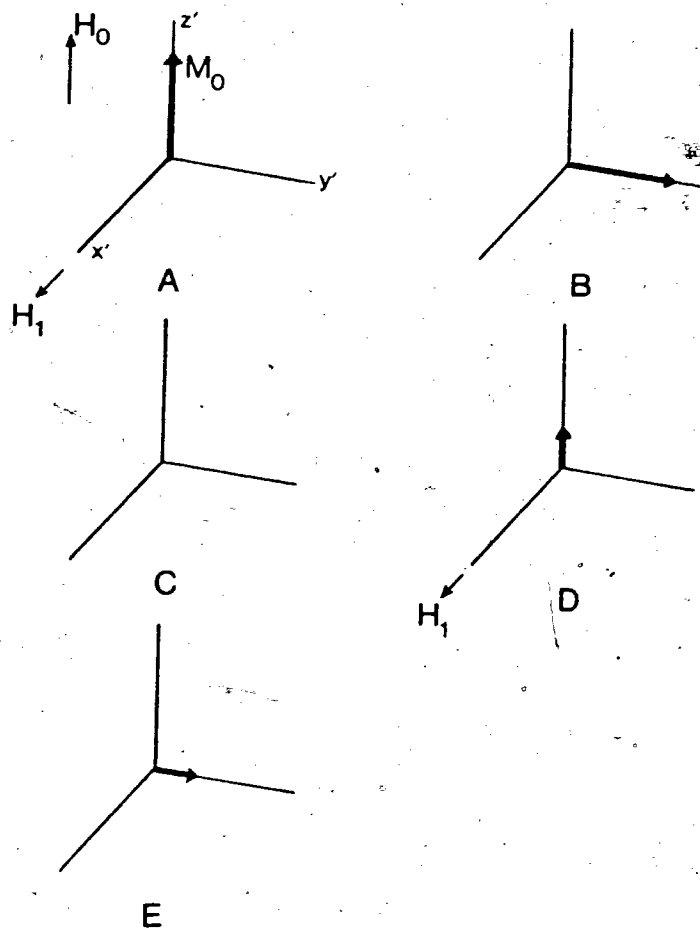
$T_1$  is again obtained from the slope of a plot of  $\ln(A_\infty - A_\tau)$  vs  $\tau$ .

This method of  $T_1$  determination results in a very great timesaving over that required for an inversion-recovery determination since it is not necessary to wait ( $5xT_1$ ) each time before the pulse sequence is repeated. Therefore it is especially useful for the



7

Figure 4. The homospoil pulse sequence. Taken from reference 110.



measurement of long relaxation times. However, for measurement of very short  $T_1$ 's, i.e.  $T_1 < 0.2$  sec, this sequence is of limited utility. This is because of the relatively long duration of the spoiling pulse, typically on the order of 0.05 sec. Thus, the available range of  $T$  values is limited to those greater than 0.05 sec. It should be pointed out that during the course of this investigation,  $T_1$ 's as low as 200 msec have been determined using the homospoil technique. These  $T_1$  values were found to agree with those values determined by the inversion recovery method to less than  $\pm 10\%$ .

One other criticism which has been raised against the use of the homospoil pulse sequence is that this method may be more sensitive to the accuracy of the  $90^\circ$  pulse. As well, the long spoiling pulse may have traumatic effects on the NMR field-frequency lock. This was not found to be a problem with the XL-100-15 system used in this investigation.

#### B. Linear Electric Field Effects in NMR

The substitution of a methylene group with a polar substituent, X, may cause large changes in the chemical shifts of nearby protons (123). The chemical shift change brought about by this substitution may be defined as

$$\Delta\delta = \Delta\delta_{el} + \Delta\delta_w + \Delta\delta_{magn} + \Delta\delta_{solv} \quad \text{III-37}$$

where  $\Delta\delta_{el}$  is due to the difference in the electric dipole moment upon substitution,  $\Delta\delta_w$  is the difference due to altered Van der Waals interactions,  $\Delta\delta_{magn}$  is the contribution due to different anisotropies

of the magnetic susceptibilities of the C-X and C-H bonds. while  $\Delta\delta_{\text{solv}}$  reflects that portion of  $\Delta\delta$  which is due to differences in the interaction with solvent molecules due to the introduction of a polar substituent (123).

It is the term  $\Delta\delta_{\text{el}}$  which is of interest in this investigation since it describes the change in chemical shift which may be caused by the introduction of an electric field which may originate at a molecular dipole, point charge or other inter- or intramolecular source (124). One such other source is the surface dipole moment of a phospholipid membrane system, and it is to a system with such a source that a linear electric field treatment will be applied (see section 4.D).

Buckingham (125) has shown that if a molecule is placed in the presence of a uniform electric field, E, the effect on the nuclear screening constant of the atom in question may be expressed as a power series in E, and therefore  $\Delta\delta_{\text{el}}$  may also be expressed in this form as

$$\Delta\delta_{\text{el}} = AE + BE^2 \quad \text{III-38}$$

where A and B are constants which describe the particular system.

The electric field strength squared originating from a polar group with dipole moment  $\mu$  is given by (123)

$$E^2 = \mu^2 (3 \cos^2\phi_1 + 1)/R^6 \quad \text{III-39}$$

where  $\phi_1$  is the angle between the origin of the dipole moment vector, and the proton whose chemical shift is being considered. Since the second order term falls off rapidly with increasing distance, the final term in equation III-38 may be neglected, and the change in chemical shift due to an electric field caused by a dipole moment may be expressed in terms of this dipole as (123)

$$\Delta\delta_{el} = AE = \mu c/R^3 \quad \text{III-40}$$

where  $c$  encompasses the modification of the value of the electric field at the atom in question due to the orientation of the dipole moment with respect to the proton (or carbon) whose chemical shift is being calculated. The inclusion of this geometrical factor gives (123)

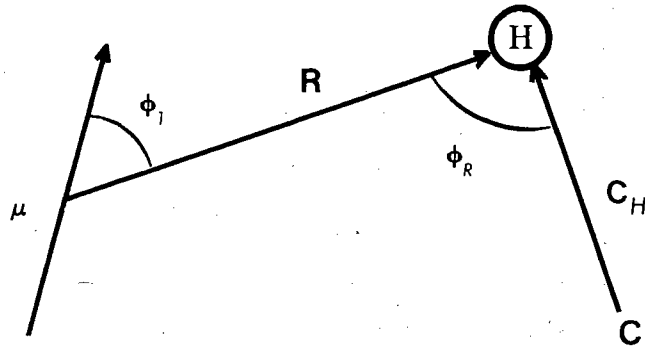
$$E_1 = \mu(3 \cos \phi_1 \cos \phi_R - \cos \phi_u)/R^3 \quad \text{III-41}$$

where the angles  $\phi_1$  and  $\phi_R$  are defined by Figure 5, and  $\phi_u$  is the angle between the dipole moment vector and the C-H bond direction. In other words,  $E_1$  is now the component of the electric field along the carbon-proton bond. Thus, it is clear that the chemical shift change due to the presence of an electric field is highly dependent not only on the distance from the electric field, but also on the orientation of the molecular bond with respect to it. Therefore, electric field effects are very useful tools for the elucidation of molecular geometry.

Since a constant electric field polarizes a carbon-hydrogen (or carbon-carbon) bond, and induces a dipole moment  $\mu$ , the magnitude of the induced dipole is related not only to the charge density of the atom in question, but also to the polarizability of carbon-hydrogen

40a

Figure 5. Orientation of a dipole moment with respect to  
molecular axes. Definition of the angles of Equation III-41



(or carbon-carbon) bond by (126)

$$\mu = e\delta_q l = b_{11}E_1 \quad \text{III-42}$$

where  $e$  is the electronic charge,  $\delta_q$  is the induced charge density on the atom in question,  $l$  is the atomic bond length, and  $b_{11}$  is the bond polarizability along the bond axis. Therefore the change in electron density in the case of protons is given by (126)

$$\delta_q = (b_{11}/el) E_1 \quad \text{III-43}$$

and the resulting chemical shift difference by (127)

$$\Delta\delta_{el} = (\delta/e) \rho \quad \text{III-44}$$

where  $(\delta/e)$  is the induced shift per electron.

In the case of  $^{13}\text{C}$  chemical shifts, polarization of all bonds to the carbon atom in question must be considered and the resulting change in charge density is given by (127,128)

$$\delta_q = \sum (b_{11}E_1/el) \quad \text{III-45}$$

where the summation is over all bonds of the atom. Therefore, the final expression for changes in  $^{13}\text{C}$  chemical shifts due to the presence of an electric field is given by

$$\Delta\delta_{el} = (\delta/e) \sum (b_{11}E_1/el) \quad \text{III-46}$$

For example, the chemical shift non-equivalence for the olefinic carbons of a series of monounsaturated fatty acids has been shown to be due to a linear electric field effect which has its origin in the carboxyl headgroup (127). Thus, the field effect induced shift which is absent in the case of the parent hydrocarbons, is dependent upon



the distance of the double bond from the carboxyl moiety. For unsaturated carbons, the longitudinal bond polarizability is very large when compared to a C-C or C-H bond (129) as can be seen from Table I, and thus the sum in equation III-45 is reduced to a single term. In the case of monounsaturated fatty acids, the effect of the head group is to increase the electron density on the olefinic carbon atom nearer the headgroup, and to decrease the electron density on the olefinic carbon remote from the headgroup. Such changes in electron density predict characteristic equal and opposite  $^{13}\text{C}$  chemical shifts for the two olefinic carbons (127). The olefinic carbon nearest the headgroup is shifted upfield, while the carbon further away is shifted downfield. The effect of the electric field at the site of unsaturation is dependent both on the distance of the double bond from the source, and on its orientation with respect to the dipole since  $E_{\parallel}$  in equation III-42 is the component of the electric field resolved parallel to the olefinic linkage. In the case of monounsaturated amines, for example, in which the direction of the headgroup dipole moment is reversed, the effect on  $^{13}\text{C}$  chemical shifts is opposite to that observed for carboxylic acids; that is, the double bond is oppositely polarized, the carbon nearer the headgroup bearing a decreased charge, and as a result being shifted downfield (124).

The foregoing theory will be applied in Section 4D to describe the effects of incorporation of the unsaturated isoprenoid, phytol,

Table I

Longitudinal Bond Polarizabilities<sup>a</sup>

Bond	$b_{11} \times 10^{23} \text{ cm}^3$
C-H	0.064
C-C	0.099
C=C	0.280

<sup>a</sup> From reference 129

into a phospholipid bilayer on the  $^{13}\text{C}$  chemical shifts of the olefinic carbons. The increased chemical shift non-equivalence of the phytol olefinic carbons upon intercalation of phytol can be used to calculate the value of the electric field at the site of unsaturation with the aid of the equation III-46. Subsequently, assuming an orientation of the phytol molecule within the bilayer, equation III-41 may be used to calculate the distance of the olefinic carbons from the origin of the field, the membrane surface dipole moment, and hence the depth at which phytol sits in the membrane.

Very recently, Seidman and Maciel (128) have carried out molecular orbital calculations concerning the effect of the placement of an electric dipole near a molecular hydrocarbon framework upon the  $^{13}\text{C}$  chemical shifts. The results of this theoretical quantum mechanical treatment, which were explained in terms of a simple bond polarization model, are in agreement with the prediction of the previous classical treatment (125). Only small effects were present in the case of a saturated molecular framework, consistent with the low polarizability of C-C and C-H bonds relative to an olefinic linkage, while larger effects, in agreement with previous experimental reports (124,127), were found for unsaturated hydrocarbon frameworks.

### C. ESR of Nitroxide Spin Labels

The spin Hamiltonian for a nitroxide free radical is given by  
(130)

$$\mathcal{H} = \beta_e \bar{H} \cdot \bar{g} \cdot \bar{S} + h \bar{S} \cdot \bar{T} \cdot \bar{I} - g_N \beta_N \bar{I} \cdot \bar{H} + \bar{S} \bar{D} \bar{S} + \bar{J} \cdot \bar{S}_1 \cdot \bar{S}_2 \quad \text{III-47}$$

where  $\beta_e$  is the electron Bohr magneton,  $H$  is the applied magnetic field,  $g$  is the  $g$ -value tensor for the electron and  $S$  is the spin operator for the electron,  $T$  is the electron nuclear hyperfine tensor,  $I$  is the spin operator for a coupled nuclear spin,  $g_N$  is the  $g$  factor for the nucleus,  $\beta_N$  is the nuclear Bohr magneton,  $D$  is the electron dipolar interaction tensor, and  $J$  is the exchange interaction between two electron spin operators  $S_1$  and  $S_2$ .

The first term is the electronic Zeeman interaction while the second term is the electron-nuclear hyperfine interaction. The third term in equation III-47 is the spin Hamiltonian for the nucleus which is negligible compared with the electronic Zeeman interaction while the final two terms are due to electron-electron interactions and are unimportant for dilute solutions of molecules which possess a single unpaired electron.

Thus the spin Hamiltonian for an isolated free radical is well approximated by (130)

$$\mathcal{H} = \beta_e \bar{H} \cdot \bar{g} \cdot \bar{S} + \bar{S} \cdot \bar{T} \cdot \bar{I} \quad \text{III-48}$$

For nitroxide spin labels, each of the electron Zeeman levels is split into three  $(2I+1)$  components due to coupling with the  $^{14}\text{N}$  nucleus ( $I=1$ ). The allowed transitions are those which satisfy the selection rules  $\Delta M_S = \pm 1$ , and  $\Delta M_I = 0$ .

Since both the g tensor and the hyperfine coupling tensor are anisotropic both the g value and the hyperfine splittings are dependent upon the orientation of the N-O  $2p\pi$  orbital with respect to the direction of the applied magnetic field (131). It has been determined from oriented crystal studies that the hyperfine coupling tensor is very nearly axially symmetric i.e.  $T_{xx} \sim T_{yy} \sim 6G$ , and  $T_{zz} \sim 32G$ , where the z axis is defined as being parallel to the nitrogen  $2p\pi$  orbital, and the x axis as being along the N-O bond direction, while the y axis completes a right hand co-ordinate system (60, 132).

Therefore the hyperfine splitting is described by the axially symmetric tensor  $\bar{T}$  (60)

$$\bar{T} = \begin{pmatrix} T_{xx} & 0 & 0 \\ 0 & T_{yy} & 0 \\ 0 & 0 & T_{zz} \end{pmatrix} \quad \text{II-49}$$

In dilute solutions of low viscosity where the nitroxide radicals are undergoing rapid isotropic tumbling, these principal hyperfine splittings are averaged out, and a three-line spectrum with the components separated by  $1/3 (T_{xx} + T_{yy} + T_{zz}) \sim 14.7G$  is observed. If however the reorientation of the label is slow on the ESR time scale, a superposition of orientations will be observed (131). Thus the ESR spectra are sensitive both to the orientation, and the rate of motion of the nitroxide.

It has been found that both spin labeled fatty acids, and cholestane, when incorporated into lecithin multilayers, undergo rapid anisotropic motion, rotating rapidly about their long molecular axes (133).

In discussing the orientation of these spin probes, it is more convenient to express the hyperfine splittings in terms of an alternate set of space fixed coordinates X, Y, Z, where Z is the direction of the applied magnetic field. The transformation may be accomplished with the use of the orthogonal transformation matrix, L. (131)

$$L = \begin{matrix} \cos \eta_1 & \cos \eta_2 & \cos \eta_3 \\ \cos \epsilon_1 & \cos \epsilon_2 & \cos \epsilon_3 \\ \cos \theta_1 & \cos \theta_2 & \cos \theta_3 \end{matrix} \quad \text{III-50}$$

where  $\cos \eta_1$ ,  $\cos \eta_2$ ,  $\cos \eta_3$  are the direction cosines between the nitroxide x, y, z axes and the space fixed X direction,  $\cos \epsilon_1$ ,  $\cos \epsilon_2$ ,  $\cos \epsilon_3$  are the direction cosines between the nitroxide x, y, z axes, and the Y direction, while  $\cos \theta_1$ ,  $\cos \theta_2$ , and  $\cos \theta_3$  are the directional cosines between the nitroxide x, y, z axes and the Z direction (direction of the magnetic field). This leads to the transformation (131)

$$T' = LTL^{-1} \quad \text{III-51}$$

where  $L^{-1}$  is the inverse of III-50.

The effective Hamiltonian  $\mathcal{H}'$  has the form (132)

$$\mathcal{H}' = \beta \bar{S} \cdot \bar{g} \cdot \bar{H} + h \bar{S} \cdot \bar{T} \cdot \bar{I}$$

III-52

and the energy is given by (132)

$$E = \beta g'_{zz} S_z H_z + h T'_{zz} S_z I_z \quad \text{III-53}$$

and in terms of the basic Hamiltonian by (132)

$$E = \beta (\overline{\cos^2 \theta_1} g_{xx} + \overline{\cos^2 \theta_2} g_{yy} + \overline{\cos^2 \theta_3} g_{zz}) S_z H_z \\ + h (\overline{\cos^2 \theta_1} T_{xx} + \overline{\cos^2 \theta_2} T_{yy} + \overline{\cos^2 \theta_3} T_{zz}) S_z I_z \quad \text{III-54}$$

where  $\overline{\cos^2 \theta_1}$ ,  $\overline{\cos^2 \theta_2}$ , and  $\overline{\cos^2 \theta_3}$  are the time averages of the direction cosines averaged over the rapid anisotropic molecular motion about the long axis of the fatty acid spin labels which is coincident with the nitroxide  $2p\pi$  orbital direction. The hyperfine splitting tensor upon transformation takes the form (60)

$$T' = \begin{pmatrix} T_{\perp} & 0 & 0 \\ 0 & T_{\perp} & 0 \\ 0 & 0 & T_{\parallel} \end{pmatrix} \quad \text{III-55}$$

where  $T_{\parallel} = T'_{zz}$ .

It follows from equations III-53 and III-54 that (132)

$$T_{\parallel} = \overline{\cos^2 \theta_1} T_{xx} + \overline{\cos^2 \theta_2} T_{yy} + \overline{\cos^2 \theta_3} T_{zz} \quad \text{III-56}$$

From the orthogonality of the direction cosines

$$\overline{\cos^2 \theta_1} + \overline{\cos^2 \theta_2} + \overline{\cos^2 \theta_3} = 1 \quad \text{III-57}$$

and since the trace of the T matrix is unchanged upon transformation (116)

it follows that

$$2T_{\perp} + T_{\parallel} = T_{xx} + T_{yy} + T_{zz} \quad \text{III-58}$$

Combining equations III-58 and III-56 yields

$$T_{\perp} = \frac{1}{2}T_{xx}(1-\cos^2\theta_1) + \frac{1}{2}T_{yy}(1-\cos^2\theta_2) + \frac{1}{2}T_{zz}(1-\cos^2\theta_3) \quad \text{III-59}$$

Since  $T_{xx} = T_{yy}$  for the nitroxide ring system (60)

$$T_{\perp} = \frac{1}{2}T_{xx}(1+\cos^2\theta_3) + \frac{1}{2}T_{zz}(1-\cos^2\theta_3) \quad \text{III-60}$$

and similarly from Equation III-56 (60)

$$T_{\parallel} = T_{xx}(1-\cos^2\theta_3) + T_{zz}(\cos^2\theta_3) \quad \text{III-61}$$

A useful experimental parameter is the quantity  $T_{\parallel} - T_{\perp}$  which is the difference in the hyperfine splitting observed when the applied magnetic field is parallel and perpendicular, respectively, to the bilayer normal. Combining equations III-60 and III-61 yields

$$T_{\parallel} - T_{\perp} = (T_{zz} - T_{xx}) \cdot \frac{1}{2}(3\cos^2\theta_3 - 1) \quad \text{III-62}$$

The quantity  $(3\cos^2\theta_3 - 1)$  has been termed to be an order parameter since it describes the time average deviation of  $z$  from the  $Z$ -axis, i.e. the time average deviation of the direction of the nitroxide  $2p\pi$  orbital from the direction of the applied magnetic field (132,134).

Thus the order parameter may be expressed as (60)

$$S = (T_{\parallel} - T_{\perp}) / (T_{zz} - T_{xx}) \quad \text{III-63}$$

or equivalently (125)

$$S = (T_{\parallel} - T_{\perp}) / (T_{zz} - \frac{1}{2}(T_{xx} + T_{yy})) \quad \text{III-64}$$

In the case of the cholestane spin probe, the nitroxide  $2p\pi$  orbital is very nearly orthogonal to the long molecular axis, and thus the equivalent expression for the order parameter is (135)

$$S = \frac{T_{\parallel} - T_{\perp}}{T_{yy} - (T_{xx} + T_{zz})} \quad \text{III-65}$$



Since the hyperfine splittings are slightly solvent dependent (61,132), the expressions for the order parameter must be slightly modified to give the final form of the order parameters for the fatty acid spin probes as (132)

$$S = \frac{T_{\parallel} - T_{\perp}}{T_{zz} - \frac{1}{2}(T_{xx} + T_{yy})} \cdot \frac{(T_{xx} + T_{yy} + T_{zz})}{T_{\parallel} + 2T_{\perp}} \quad \text{III-66}$$

and for the cholestane spin label as (132)

$$S = \frac{T_{\parallel} - T_{\perp}}{T_{yy} - \frac{1}{2}(T_{xx} + T_{zz})} \cdot \frac{(T_{xx} + T_{yy} + T_{zz})}{T_{\parallel} + 2T_{\perp}} \quad \text{III-67}$$

Equations III-66 and III-67 assume that the molecular long axis, and the normal to the bilayer surface are coincident. In other words there is no angle of tilt. The axis of rapid anisotropic motion is the bilayer normal. If the molecular long axis is tilted at an angle  $\delta$  from the normal to the membrane surface the order parameter calculated from equation III-66 or equation III-67 will be artificially lowered. Modification of equation III-66 to include a tilt angle,  $\delta$ , yields

$$S = \frac{T'_{\parallel} - T'_{\perp}}{T'_{zz} - (T'_{xx} + T'_{yy})} \cdot \frac{(T'_{xx} + T'_{yy} + T'_{zz})}{T'_{\parallel} + 2T'_{\perp}} \quad \text{III-68}$$

where

$$T'_{\parallel} = (T_{\parallel}^2 \cos^2 \delta + T_{\perp}^2 \sin^2 \delta)^{1/2} \quad \text{III-69}$$

and

$$T'_{\perp} = (T_{\parallel}^2 \sin^2 \delta + T_{\perp}^2 \cos^2 \delta)^{1/2} \quad \text{III-70}$$

When  $\delta=0$ , equation III-68 reduces to equation III-66 while if  $\delta=45^\circ$ , then  $T'_{\parallel} = T'_{\perp}$ , leading to an order parameter of zero, while if  $45^\circ < \delta < 90^\circ$ , the result is a negative order parameter. Thus, the

observation of a negative order parameter may be indicative that the axis about which rapid rotation occurs is oriented at an angle  $>45^\circ$  from the bilayer normal.

It is to the ESR spectra of spin probes I-V (see Figure 3) that the preceding treatment will be applied, initially assuming that the long molecular axes about which rapid rotation takes place is parallel to the bilayer normal. Admittedly, the assumption of rapid anisotropic motion may not be valid in the case of the cholesteryl ester labels, but without this simplification the observed spectra may only be interpreted with the aid of computer simulation.

## CHAPTER 4

RESULTS AND DISCUSSION FOR VITAMIN E,  
PHYTOL, AND PHYTANIC ACIDA. Activation Energies for  $^{13}\text{C}$   $T_1$  Processes

The spin lattice relaxation times for 20% w/v egg yolk lecithin (EYL) vesicles were determined at three temperatures, namely 11, 30, and 52°C. These values are reported in Table II, while a representative  $^{13}\text{C}$  NMR spectrum is depicted in Figure 6. Assignments were taken from those made by Batchelor et al (13), and by a comparison with the  $^{13}\text{C}$  chemical shifts for a series of fatty acids and their methyl esters (127). The fatty acid composition of EYL was determined by the manner described in Section 2A. The results shown in Table III are in good agreement with previous reports (40,136). The main fatty acids present are palmitic (16:0), stearic (18:0), oleic (18:1) and linoleic (18:2) acids, with the unsaturated species constituting approximately 40% of the total.

Since the re-orientational correlation time,  $\tau_c$ , is exponentially dependent on temperature for purely dipolar relaxation, the activation energies for re-orientational processes may be calculated from  $^{13}\text{C}$   $T_1$  relaxation times by

$$\tau_c = \tau_0 \exp(E_a/RT)$$

Table II

## Fatty Acid Composition of Egg Yolk Lecithin

Fatty Acid	Area %
Palmitic (16:0)	42.7
Palmitoleic (16:1)	1.6
Stearic (18:0)	16.9
Oleic (18:1)	27.7
Linoleic (18:2)	11.0

Figure 6.  $^{13}\text{C}$  NMR spectrum of 20% w/v egg yolk lecithin vesicles.

Lecithin Vesicles

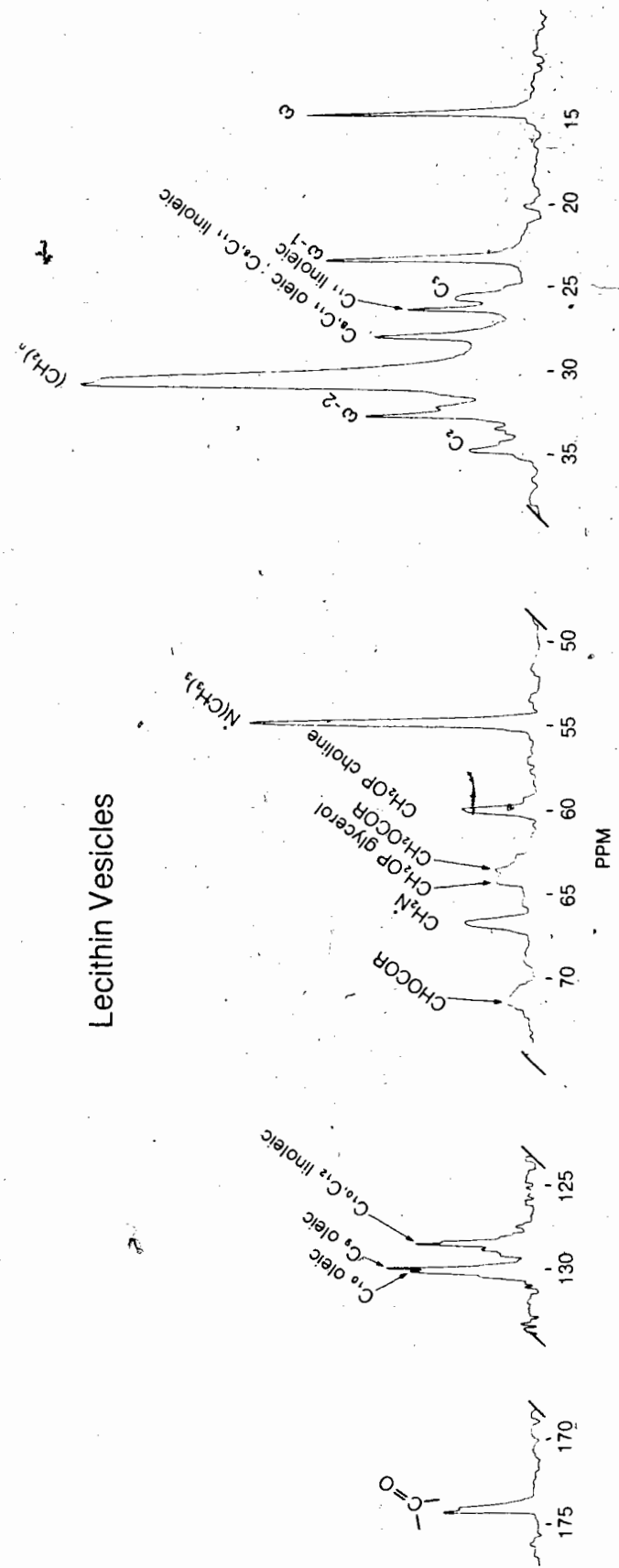


Table III

Selected  $^{13}\text{C}$   $T_1$  relaxation times for 20% w/v  
egg yolk lecithin vesicles.

Carbon	$T_1$ (sec)		
	11°C	30°C	52°C
C2	0.09	0.15	0.28
$(\text{CH}_2)_n$	0.23	0.38	0.59
$\text{CH}_3$	1.58	2.42	4.12
$\text{CH}_2\text{CH}_3$	0.73	1.15	2.25
$\text{CH}_2\text{CH}_2\text{CH}_3$	0.50	0.62	1.11
C11 linoleic	0.35	0.53	1.22
C8 and 11 oleic	0.28	0.43	0.76
C8 and 14 linoleic			

where  $E_a$  is the activation energy,  $R$  is the gas constant,  $T$  is the absolute temperature, and  $\tau_0$  is a constant of the system with units of time (137).

Activation energies for the thermal internal re-orientational processes have been calculated from the slopes of plots of  $T_1$  vs the inverse of absolute temperature (Arrhenius plots). These plots, shown in Figure 7 are linear, indicating that the  $^{13}\text{C}$ - $^1\text{H}$  dipole-dipole relaxation is the dominant mechanism which is operative. Selected values of the activation energies are presented in Table IV. These values are similar to literature values for the barriers to internal rotation in alkanes (138), and to values determined by Stoffel et al (21) using specifically  $^{13}\text{C}$  labeled lipids. An examination of these activation energies reveals a decrease in the activation energy for reorientation as the chain terminus is approached, consistent with the existence of a fluidity gradient along the hydrocarbon chains.

#### B. $^{13}\text{C}$ NMR of Egg Yolk Lecithin-Phytol Bilayers

Lecithin-phytol (1:1 mole ratio) mixed vesicles were prepared as described in Section 2B.1. Resonances were resolved not only for the lecithin carbons, but also for those of phytol. The chemical shifts for the lecithin carbons at 52 and 11°C are given in Table V for pure EYL vesicles (20% w/v in  $\text{D}_2\text{O}$ ) and for vesicles with incorporated phytol. Chemical shifts for the phytol carbons at 52 and 11°C are given in Table VI for neat phytol, phytol dispersed in



Figure 7. Arrhenius plots of  $T_1$  vs the inverse of absolute temperature for  $^{13}\text{C}$  resonances of the fatty acyl chains of egg yolk lecithin vesicles.

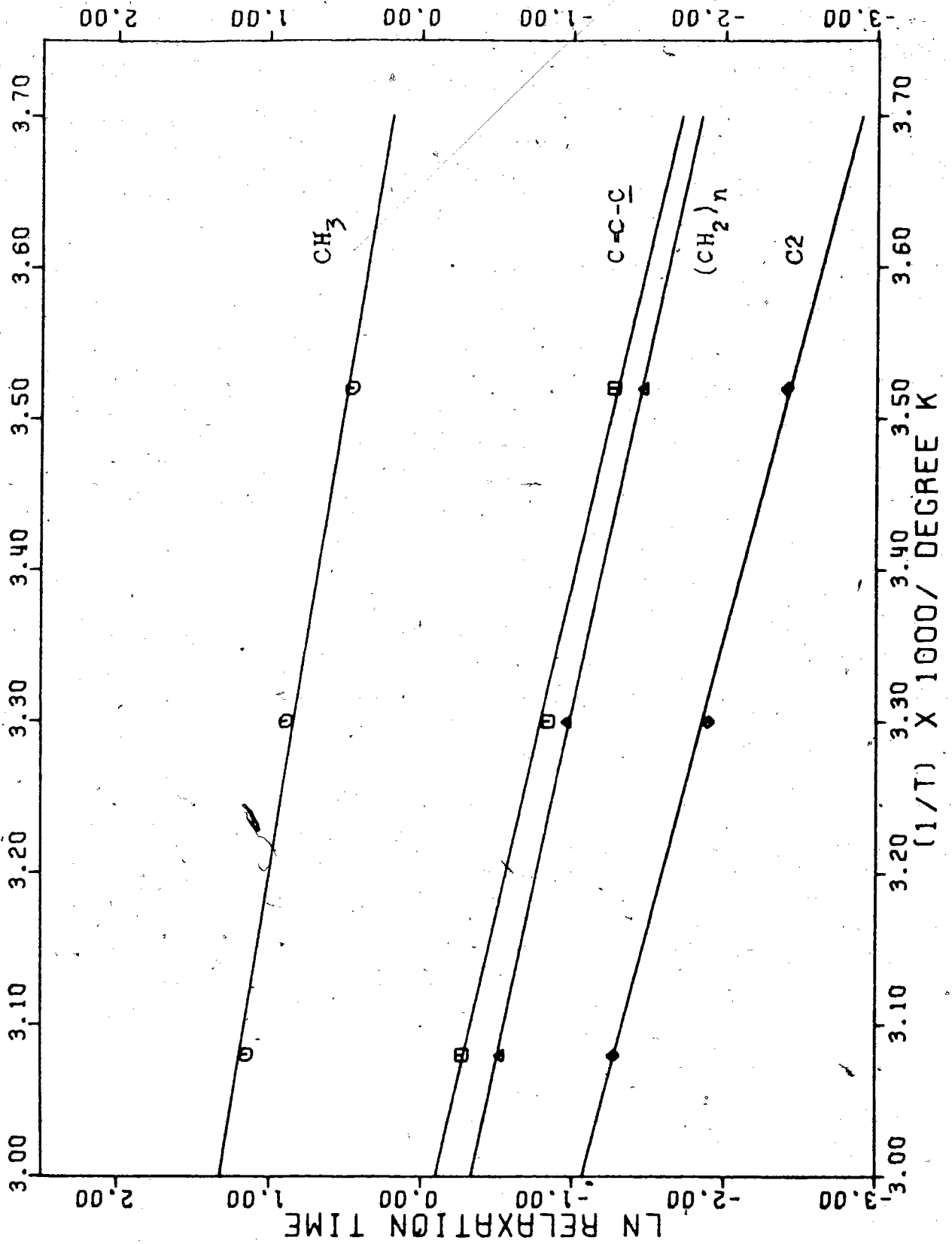


Table IV

Activation energies for selected  $^{13}\text{C}$  resonances

Carbon	$E_a$ (Kcal/mole)
$\text{CH}_3$	3.2
$\text{CH}_2\text{CH}_3$	3.8
$(\text{CH}_2)_n$	4.3
$\text{C}_2$	5.2
$\text{C}=\text{C}$	4.6
$\text{C}=\text{C}-\text{C}^*$	4.6

Table V

Lecithin  $^{13}\text{C}$  chemical shifts for egg yolk lecithin and  
lecithin - phytol 1:1 mixed vesicles

Carbon	Chemical shift* at 52°C		Chemical shift at 11°C	
	Lecithin	Lecithin + phytol	Lecithin	Lecithin + phytol
Choline $\text{N}^+(\text{CH}_3)_3$	54.87	54.78	54.30	54.24
$\text{N}^+\text{CH}_2$	66.96	66.80	66.36	65.98
$\text{CH}_2\text{OP}$	60.08	60.00	59.79	59.79
Chain				
C1	174.04	173.87	173.90	173.50
C2	34.73	34.66	34.33	34.40
C3	25.62	#	25.46	#
$(\text{CH}_2)_n$	30.39	{ 29.91	30.27	{ 30.03
		{ 30.39		{ 30.30
$\text{CH}_3$	14.47	14.46	14.36	14.33
$\text{CH}_2\text{CH}_3$	23.24	23.15†	23.16	22.90†
$\text{CH}_2\text{CH}_2\text{CH}_3$	32.57	32.49	32.45	32.42
C11 linoleic	26.25	26.22	25.91	25.83
C8 and 11 oleic	27.85	27.75	27.57	27.46
C8 and 14 linoleic			129.75	129.47
C9 oleic	129.95	129.91	130.01	129.81
C10 oleic	130.19	130.18	128.38	128.41
C9 linoleic	128.90	128.76	128.14	128.11
C10 linoleic	128.49	128.37		
C12 linoleic				

\* Chemical shift (ppm) relative to external TMS.

† Resonance coincident with phytol carbons 15a and 16.

# Resonance coincident with phytol carbons 9 and 13.

Table VI

 $^{13}\text{C}$  Chemical shifts\* for phytol

Carbon number	Chemical shift at 52° C			Chemical shift at 11° C		
	Neat	D <sub>2</sub> O dispersion (20%+2% SDS)	1:1 phytol -	Neat	D <sub>2</sub> O dispersion (20%+2% SDS)	1:1 phytol -
			lecithin vesicles (20% in D <sub>2</sub> O)			lecithin vesicles (20% in D <sub>2</sub> O)
1	58.73	58.91	58.78	58.31	58.34	58.08
2	124.80	124.91	124.45	124.54	124.60	-
3	137.35	137.90	138.41	136.83	137.17	137.91
4	40.27	40.54	40.25	40.15	40.31	39.63
14	39.80	40.06	40.05	39.40	39.75	28.35
15	28.28	28.53	28.56	28.15	28.29	28.35
6	37.19	37.48	37.51	37.05	37.27	37.78
8,10,12	37.84	38.11	37.95	37.67	37.79	37.78
7,11	33.12	33.38	33.35	32.98	33.15	32.99
9	24.87	25.13	25.33	24.83	24.91	25.65
5	25.64	25.92	25.33	25.42	26.03	25.65
13	25.15	25.38		25.09	25.24	
3a	16.32	16.55	16.41	16.12	16.27	16.09
7a, 11a	20.10	20.34	20.19	19.91	20.05	19.80
15a, 16	23.01	23.23	23.15†	22.93	23.06	22.90

\* Chemical shift (ppm) from external TMS.

† Resonance coincident with penultimate carbon lecithin chain.

D<sub>2</sub>O by sonication in the presence of 2 mole% sodium dodecylsulphate, and for phytol incorporated into EYL vesicles. The assignments are taken from those made by Goodman et al (139).

The upfield portion of the <sup>13</sup>C spectrum of 20% w/v EYL vesicles containing a 1:1 mole ratio of lecithin:phytol at 52°C is reproduced in Figure 8. One notable feature of this spectrum is the sharp resonance lines. This is in contrast to the broadening effect which is observed for cholesterol-lecithin mixed vesicles (12,18). In view of recent work by Finer (5) and Bloom et al (6), such small linewidths must be due to rapid vesicle tumbling, more rapid lateral diffusion of lecithin molecules in the plane of the bilayer or decreased ordering of the lecithin fatty acyl chains. The first case implies a decrease in vesicle size upon incorporation of phytol since the rotational correlation time for the tumbling of vesicles as a whole may be estimated from the Stokes-Einstein relation (140,141),

$$\tau_R = 4\pi\eta r^3/3kT \quad \text{IV-2}$$

where  $\eta$  is the viscosity experienced by the vesicle,  $k$  is the Boltzmann constant,  $T$  is the absolute temperature and  $r$  is the radius of the vesicle. The size of the lecithin-phytol vesicles is not accurately known, however, an approximation may be made from the relative numbers of <sup>31</sup>P nuclei on the inside and outside layers of the vesicle. These results, which are discussed in Section 4I, indicate that the vesicle sizes are similar, although, admittedly,

this method is rather crude. In addition, Sepharose 4B chromatography of mixed EYL vesicles suggested the presence of small vesicles along with some larger liposomes. These results are discussed in Section 5B. The second possibility that an increase in the lecithin lateral diffusion rate occurs will be discussed later (Section 4I), in more detail.

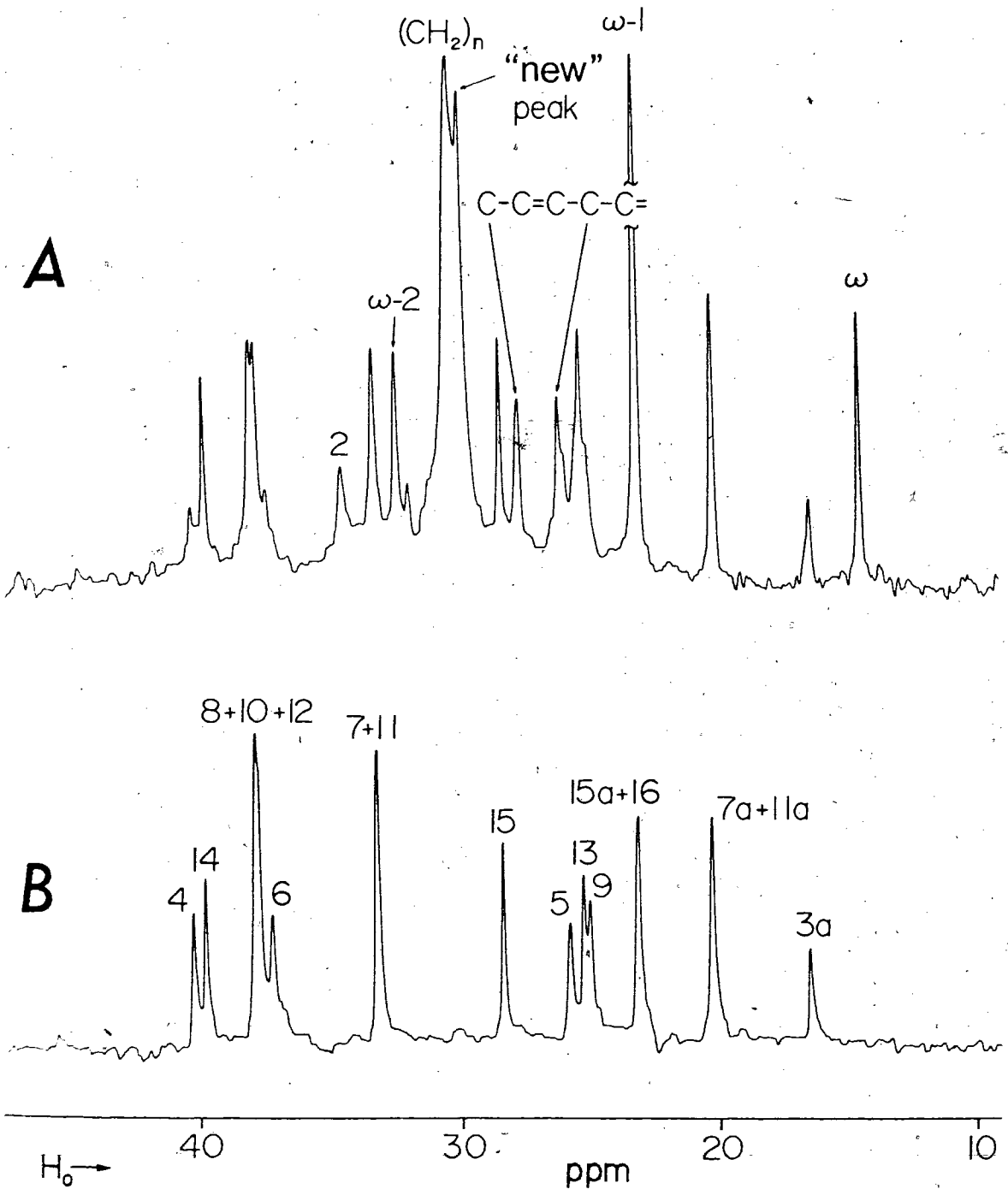
A second noteworthy feature of the lecithin-phytol system is the splitting of the main methylene envelope of lecithin into two distinct peaks by the addition of phytol. In addition to the  $(\text{CH}_2)_n$  resonance at 30.39 ppm observed with lecithin alone, a "new" peak of nearly equal intensity which cannot originate from the intercalated phytol (see Fig.8) is observed approximately 0.5 ppm upfield in the lecithin-phytol system.

While it is possible that the appearance of this new peak is simply a consequence of increased spectral resolution upon the incorporation of phytol, because of its shift, an alternative explanation involves a gamma shift (142,143). For  $^{13}\text{C}$  resonances of fatty acids, an upfield shift results when 1,4 carbons in the chain are placed in gauche juxtaposition (13). There exists a steric induced charge perturbation in the  $\text{H}-^{13}\text{C}$  bond due to non-bonded repulsion existing between electrons centred on hydrogen atoms which are proximated by a gauche conformation of the intervening  $\alpha-\beta$ , C-C bond. In the hydrophobic regions of fully saturated lipid bilayers,

Figure 8. Proton noise decoupled  $^{13}\text{C}$  NMR spectra for the region 5ppm to 45 ppm at  $52^\circ\text{C}$ .

A. 20% w/v egg yolk lecithin vesicles in  $\text{D}_2\text{O}$  with the incorporation of an equal mole ratio of phytol. B. sonicated dispersion of 20% w/v phytol in  $\text{D}_2\text{O}$  with the addition of 2 mole % SDS





the all trans conformation is usually the lower energy form since this allows for the tightest packing of adjacent lipid molecules. Laser Raman studies (144,145) of sonicated dipalmitoyl (16:0) and dioleoyllecithin (18:1) above the gel-liquid crystalline transition temperature,  $T_m$ , have indicated the presence of 4-5 gauche configurations per fatty acid residue or a total of 8-10 per lecithin molecule (146). Thus, as the temperature is lowered, and the trans states are populated to a greater extent, a downfield shift would be expected. Indeed, the "new" peak in the lecithin-phytol admixture does shift to lower field by approximately 0.1 ppm on going from 52°C to 11°C. Although such behaviour is consistent with a  $^{13}\text{C}$  gamma shift, it is not proof of such. However, the matter does not rest there. One additional piece of evidence which bears upon the origin of this "new" peak is the fact that it is not present in DPL-phytol (2:1 mole ratio) mixed vesicles at 52°C ( $T_m$  of DPL = 41°C (147)). This may indicate a slightly different molecular packing of phytol in EYL vs DPL due to the presence of unsaturation in the EYL fatty acid chains. The clarification of this point would require the use of specifically labeled  $^{13}\text{C}$  lecithin molecules.

$^{13}\text{C}$   $T_1$  relaxation times of lecithin carbons for EYL and EYL-phytol 1:1 mole ratio vesicles at 52 and 11°C are given in Table VII. The relaxation times reflect the order and/or the rate of motion of the lecithin molecules. An examination of these values for pure EYL vesicles shows that the relaxation times are in agreement with

Table VII

lecithin  $^{13}\text{C}$  relaxation times for egg yolk lecithin and  
lecithin-phytol 1:1 mixed vesicles.

Carbon	$T_1$ (s) at 52°C		$T_1$ (s) at 11°C	
	Lecithin	Lecithin + phytol	Lecithin	Lecithin + phytol
Choline				
$\text{N}^+(\text{CH}_3)_3$	0.88( $\pm 0.07$ )	1.16( $\pm 0.08$ )	0.24( $\pm 0.02$ )	0.38( $\pm 0.03$ )
$\text{N}^+\text{CH}_2$	0.51( $\pm 0.04$ )	0.52( $\pm 0.05$ )	0.24( $\pm 0.02$ )	0.17( $\pm 0.01$ )
$\text{CH}_2\text{OP}$	0.50( $\pm 0.04$ )	0.53( $\pm 0.04$ )	0.21( $\pm 0.01$ )	<0.07
Chain				
C1	2.80( $\pm 0.21$ )	2.22( $\pm 0.24$ )	1.81( $\pm 0.14$ )	0.80( $\pm 0.06$ )
C2	0.28( $\pm 0.02$ )	0.87( $\pm 0.06$ )	0.09( $\pm 0.01$ )	0.10( $\pm 0.01$ )
C3	0.32( $\pm 0.03$ )	+	+	+
$(\text{CH}_2)_n$	0.59( $\pm 0.05$ )	1.03(upfield)( $\pm 0.07$ )	0.23( $\pm 0.02$ )	0.25(upfield)( $\pm 0.02$ )
		0.76(downfield)( $\pm 0.05$ )		0.18(downfield)( $\pm 0.01$ )
CH <sub>3</sub>	4.12( $\pm 0.29$ )	4.00( $\pm 0.32$ )	1.58( $\pm 0.11$ )	1.72( $\pm 0.12$ )
$\text{CH}_2\text{CH}_3$	2.25( $\pm 0.18$ )	2.44*( $\pm 0.17$ )	0.73( $\pm 0.05$ )	0.76*( $\pm 0.05$ )
$\text{CH}_2\text{CH}_2\text{CH}_3$	1.11( $\pm 0.08$ )	1.64( $\pm 0.11$ )	0.50( $\pm 0.04$ )	0.41( $\pm 0.03$ )
C11 linoleic	1.22( $\pm 0.11$ )	1.15( $\pm 0.08$ )	0.35( $\pm 0.02$ )	0.25( $\pm 0.02$ )
C8 and 11 oleic				
C8 and 14 linoleic	0.76( $\pm 0.07$ )	1.11( $\pm 0.08$ )	0.28( $\pm 0.03$ )	0.25( $\pm 0.02$ )
C9 oleic	0.90( $\pm 0.06$ )	1.20( $\pm 0.08$ )	0.30( $\pm 0.02$ )	0.55( $\pm 0.05$ )
C10 oleic	0.05( $\pm 0.10$ )	1.33( $\pm 0.12$ )	0.26( $\pm 0.02$ )	0.51( $\pm 0.04$ )
C9 linoleic				
C10 linoleic	0.90( $\pm 0.06$ )	1.36( $\pm 0.10$ )	0.33( $\pm 0.02$ )	0.41( $\pm 0.04$ )
C12 linoleic	1.39( $\pm 0.12$ )	1.56( $\pm 0.11$ )	0.53( $\pm 0.04$ )	0.42( $\pm 0.03$ )

\* Resonance coincident with phytol carbons 15a and 16.

+ Resonance coincident with phytol carbons 9 and 13.

previous studies (7) in that  $T_1$  increases upon increased distance from the bilayer surface, culminating with a large increase for the last few carbons in the chain, i.e.  $C2 < C3 < (CH_2)_n < w-2 < w-1 < w$ .<sup>\*</sup> This is consistent with a more fluid environment in the centre of the hydrophobic membrane interior. In addition  $T_1$  for these carbons decreases upon decreasing temperature as expected for purely dipolar relaxation. Activation energies for these processes calculated from  $^{13}C$   $T_1$ 's at three temperatures have been discussed in Section 4A.

At 52°C, the incorporation of phytol into the bilayer results in an increase in ~75% of the  $T_1$  values for the lecithin carbons. (Compare columns 2 and 3, Table VII). Such increases reflect increased internal motion due to the intercalated phytol. This is especially evidenced by the increase in relaxation time of the main methylene envelope carbons, from a value of 0.59-sec in the absence of phytol to values of 0.77 sec and 1.03 sec for the two peaks which are resolved in the presence of phytol. This corresponds to increases of 29 and 75% respectively. An increase from 1.11 to 1.64 sec (48%) is observed for the w-2 carbons. As the terminal carbon is approached (e.g. w-2 to w), the effect of the interjacent phytol is lessened since at this temperature, even in the absence of phytol, there is significant freedom of motion of the chain termini. ( $T_m$  of EYL - 5°C (148)).

---

<sup>\*</sup>In this nomenclature, the terminal methyl carbons of the fatty acid chains are designated as w, the penultimate carbons by w-1, etc.

These results are in direct contrast to those obtained for the incorporation of cholesterol into dioleoyl lecithin vesicles which results in decreased  $^{13}\text{C}$   $T_1$ 's due to an increase in lipid packing (9). It appears therefore that the intercalation of phytol causes a decrease in lipid packing and a concomitant increase in  $^{13}\text{C}$   $T_1$ 's.

The increased freedom of motion in the bilayer is also evidenced by substantial increases in the relaxation times for the phytol backbone carbons when incorporated into the membrane (compare columns 3 and 4, Table VIII). Increases are shown to be on the order of 80-100% for carbons 4-13. Lesser increases are found for the phytol methyl groups which are proposed to be in closest proximity with the lecithin fatty acid chains.

The effect of temperature on the motions of the lecithin-phytol bilayer is extremely interesting, especially the effects on the hydrophilic lecithin headgroup. In the absence of phytol, a decrease from 0.50 to 0.21 sec is observed for the choline  $\text{CH}_2\text{OP}$  carbon (approximately 2-fold decrease) on going from 52 to 11°C. In the presence of phytol, this reduction is much greater. The  $^{13}\text{C}$   $T_1$  for  $\text{CH}_2\text{OP}$  decreases from 0.53 sec to less than 0.07 sec. Thus, phytol causes a much greater loss in motional freedom for this carbon. It should be noted that this differential decrease as the temperature is lowered is smaller for the adjacent  $\text{CH}_2\text{N}^+$  (0.51 sec to 0.24 sec, and 0.52 sec to 0.47 sec in the absence and presence of phytol

Table VIII

 $^{13}\text{C}$   $T_1$  relaxation times for phytol

Carbon number	Neat		1:1 phytol- lecithin vesicles		Neat		$\text{D}_2\text{O}$ dispersion		1:1 phytol- lecithin vesicles	
1	0.42(±0.03)		0.81(±0.06)		0.10(±0.01)		0.15(±0.01)		0.15(±0.01)	
2	0.48(±0.03)		0.58(±0.05)		0.19(±0.01)		0.18(±0.01)		0.18(±0.01)	
3	3.06(±0.21)		2.85(±0.22)		1.18(±0.09)		0.95(±0.07)		1.18(±0.08)	
4	0.33(±0.03)		0.54(±0.04)		0.10(±0.01)		0.13(±0.01)		0.17(±0.02)	
14	0.72(±0.05)		1.05(±0.07)		0.20(±0.01)		0.31(±0.03)		0.19(±0.01)	
15	1.51(±0.11)		1.54(±0.12)		0.32(±0.02)		0.34(±0.03)		0.22(±0.02)	
6	0.29(±0.02)		0.20(±0.01)		0.07(±0.01)		0.12(±0.01)		0.21(±0.01)	
8,10,12	0.40(±0.03)		0.49(±0.04)		0.07(±0.01)		0.20(±0.01)		0.45(±0.03)	
7 and 11	0.50(±0.04)		0.75(±0.05)		0.10(±0.01)		0.20(±0.01)		0.45(±0.03)	
9	0.31(±0.02)		0.22(±0.02)		0.09(±0.01)		0.13(±0.01)		0.54(±0.05)	
5	0.32(±0.02)		0.31(±0.02)		0.13(±0.01)		0.13(±0.01)		0.54(±0.05)	
13	0.60(±0.05)		0.44(±0.03)		0.12(±0.01)		0.63(±0.05)		0.81(±0.07)	
3a	2.22(±0.16)		1.73(±0.15)		0.85(±0.06)		0.63(±0.05)		0.81(±0.07)	
7a and 11a	0.95(±0.07)		1.04(±0.07)		0.32(±0.03)		0.55(±0.04)		0.46(±0.03)	
15a and 16	2.00(±0.19)		1.69(±0.13)		0.63(±0.07)		0.47(±0.04)		0.76*(±0.05)	

\* Resonance coincident with penultimate carbon of lecithin chain.

respectively), while the  $N^+(CH_3)_3$  relaxation time is increased in the phytol-lecithin admixture, even at  $11^\circ C$ .

At first glance, such a trend indicates that the phytol hydroxyl must extend into the hydrophilic region of the bilayer. As the temperature is lowered, the lipid packing becomes more ordered, as monitored by the  $T_1$ 's. Upon addition of phytol at the lower temperature the  $T_1$  for the choline  $CH_2OP$  shows a much accelerated decrease. Such a marked decrease in  $CH_2OP$  motional freedom is consistent with hydrogen bonding of the phytol hydroxyl to the negatively charged phosphate of a lecithin molecule. The extension into the hydrophilic region of an intercalated phytol molecule, causing an expansion of the bilayer, results in a decreased ionic attraction of the negatively charged phosphate of one lecithin molecule to the positively charged trimethylammonium group of adjacent, but now more distant, lecithin molecules. The  $T_1$  of the  $N^+(CH_3)_3$  carbons would then increase, as is observed, due to this lessened ionic attraction.

At  $11^\circ C$ , the temperature dependent increase in lipid packing leads to varying effects on the relaxation rates with incorporated phytol. The  $T_1$ 's of the 9,10-unsaturated (oleic residue) carbons increase while that for the 12-unsaturated carbon (linoleic residue) decreases. Similarly, the main methylene envelope  $(CH_2)_n$  which is considerably broadened at  $11^\circ C$  experiences a differential effect.

The "new" peak at high field (30.03 ppm) has approximately the same  $T_1$  as the  $(\text{CH}_2)_n$  resonance in the absence of phytol, while the relaxation time of the low field peak (30.30 ppm) is reduced by approximately 22%. It must be remembered that the  $T_1$  values obtained for this envelope is the average of a number of methylene carbons, and thus specific effects at different distances along the hydrocarbon chains may tend to be masked.

The phytol backbone at 11°C, on the other hand, displays greater mobility in the lecithin vesicle than when dispersed in  $\text{D}_2\text{O}$ . This is evidenced by increases in the  $T_1$  values up to C14 (compare columns 6 and 7 Table VIII). Methyl carbons 7a and 11a, in contrast, are more hindered since they are proximate to the fatty acid chains of lecithin, and the  $T_1$  values drop from 0.55 to 0.46 (16%) at 11°C (i.e. when packing requirements become more stringent as the transition temperature,  $T_m$  is approached).

It has been reported that approximately one third of the theoretical maximum nuclear Overhauser enhancement (NOE) of 124% (149) in the  $^{13}\text{P}$  NMR spectra of EYL vesicles is accounted for by dipolar interactions between the lecithin phosphate, and the  $\text{N}^+(\text{CH}_3)_3$  protons of adjacent phospholipid molecules (35). Since the NOE is a measure of the dipolar contribution to the relaxation rate, and since this relaxation mechanism depends on the inverse sixth power of the internuclear distance, the removal of the  $\text{N}^+(\text{CH}_3)_3$  protons from



the proximity of the EYL phosphorus nuclei allows another relaxation mechanism (chemical shift anisotropy) to become dominant (35,75), resulting in a decrease in the NOE. Therefore, it was thought that a lateral expansion of the bilayer (a pushing apart of adjacent lecithin molecules), as is proposed to occur upon the intercalation of phytol, should result in a decreased NOE for the lecithin  $^{13}\text{P}$  nuclei.

EYL vesicles (10% w/v) and mixed EYL-phytol vesicles (10% w/v) (2:1 mole ratio, EYL:phytol) were prepared using 0.05M Tris buffer, pH=7.44 in  $\text{D}_2\text{O}$ , which was 0.05M in KCl and  $10^{-4}\text{M}$  in EDTA. Proton decoupled  $^{31}\text{P}$  NMR spectra were recorded at  $30^\circ\text{C}$ , as well as coupled spectra, and spectra with gated decoupling (150) to suppress the NOE. The NOE was measured by a comparison of the area of the completely decoupled  $^{31}\text{P}$  resonance with the area for gated or no decoupling. The average of at least eight spectral determinations were used. Pure EYL vesicles yielded an NOE of 55% while the  $^{31}\text{P}$  nuclei in the mixed EYL-phytol vesicles experienced an average enhancement of 33%. Although the NOE decreases consistent with a lateral expansion of the bilayer caused by the intercalation of phytol, large errors ( $\pm 20\%$ ) are inherent in these measurements, and therefore no definite conclusions may be reached. It was found by  $^1\text{H}$  NMR that under the experimental conditions used, that the phytol hydroxyl proton does not exchange with  $\text{D}_2\text{O}$ . Thus, it is possible

that the proximity of the phytol hydroxyl proton to the lecithin phosphate provides a dipolar relaxation pathway for the  $^{31}\text{P}$  nuclei which partially overcomes the decrease in NOE caused by less dense lateral packing of the bilayer. The clarification of this point could be achieved with the use of deuterated phytol. Results discussed in the following sections (Sections 4C and 4D) further elucidate the structure of the lecithin-phytol mixed bilayer.

### C. $^{13}\text{C}$ NMR of Dipalmitoyl Lecithin-Phytol Bilayers

$^{13}\text{C}$   $T_1$  relaxation times for synthetic dipalmitoyl lecithin vesicles (20% w/v) and for dipalmitoyl lecithin vesicles with 33 mole% incorporated phytol at  $52^\circ\text{C}$  are presented in Table IX. Assignments for DPL are taken from Levine et al (7). The relaxation times are in agreement with those determined previously (7). Phytol resonances were also resolved, but due to the lesser amount incorporated and the time required for a set of inversion-recovery experiments, these phytol resonances were not generally of sufficient intensity to allow an accurate determination of their relaxation times.

An examination of the  $T_1$  values obtained (Table IX, columns 2 and 3) reveals trends similar to those observed for the incorporation of phytol into EYL bilayers at  $52^\circ\text{C}$ . Increases in the majority of the hydrocarbon chain relaxation times again indicate greater motional freedom in the hydrocarbon region of the model membrane. As with EYL at  $52^\circ\text{C}$ , this is particularly apparent in the increase seen for the

Table IX

$^{13}\text{C}$   $T_1$  relaxation times for dipalmitoyl lecithin, and dipalmitoyl lecithin-phytol mixed vesicles at 52°C.

DPL Carbon	$T_1$ (sec)	
	20% w/v DPL	20% w/v DPL containing 33 mole% phytol
C16	3.11 ( $\pm 0.22$ )	3.32 ( $\pm 0.28$ )
C15	1.59 ( $\pm 0.11$ )	2.07 <sup>a</sup> ( $\pm 0.14$ )
C14	0.80 ( $\pm 0.06$ )	1.23 ( $\pm 0.11$ )
C4-C13	0.42 ( $\pm 0.03$ )	0.77 ( $\pm 0.08$ )
C3	0.38 ( $\pm 0.03$ )	0.38 ( $\pm 0.03$ )
C2	0.25 ( $\pm 0.02$ )	0.23 ( $\pm 0.02$ )
C1	2.17 ( $\pm 0.15$ )	2.35 ( $\pm 0.16$ )
N+(Me) <sub>3</sub>	0.81 ( $\pm 0.16$ )	0.86 ( $\pm 0.06$ )
CH <sub>2</sub> OP (choline)	0.64 ( $\pm 0.04$ )	0.44 ( $\pm 0.03$ )
CH <sub>2</sub> N <sup>+</sup>	0.54 ( $\pm 0.04$ )	0.40 ( $\pm 0.03$ )

<sup>a</sup> Peak coincident with phytol carbons 15a and 16.

C4-13 envelope, the relaxation time of which increases from 0.42 sec to 0.77 sec (83%). Similarly, increases of 56%, and 30% are observed for carbons 14 and 15, respectively. Relaxation rates for carbons 2 and 3, however, remain relatively unchanged.

Once again, an examination of the relative relaxation times of the headgroup carbons is most interesting. A trend is observed similar to that obtained for EYL. The relaxation time for the choline  $\text{CH}_2\text{OP}$  resonance is decreased by 38% in the presence of incorporated phytol (2:1 mole ratio, lecithin:phytol). As seen previously with EYL (see table VII, columns 4 and 5) this decrease is smaller for the adjacent  $\text{CH}_2\text{N}^+$  carbon (26%), and finally, as the  $\text{N}^+(\text{CH}_3)_3$  carbons are approached, a slight increase is seen upon incorporation of phytol. The trend in the relaxation times for the lecithin headgroup carbons is consistent with hydrogen bonding of the phytol hydroxyl function to the negatively charged lecithin phosphate moiety. In addition, the incorporation of phytol affects the bilayer motions throughout the length of the lipid hydrocarbon chains. This suggests that phytol is incorporated into the membrane in a relatively extended form. Results discussed in the following section further elucidate the structure of the lecithin-phytol mixed bilayer.

#### D. Intermolecular Field Effects

The incorporation of phytol into the bilayer is characterized by a relatively large effect on the chemical shifts of the unsaturated

phytol carbons C2 and C3. At 52°C, C2 is shifted upfield by 0.46 ppm, while C3 is shifted downfield by 0.51 ppm from their positions in D<sub>2</sub>O dispersions (Table VI, columns 3 and 4). These shifts cannot be attributed simply to a change in the solvent system, but the characteristic upfield-downfield chemical shift for the olefinic pair can be interpreted in terms of a linear electric field effect (124, 127, 128). The origin of this electric field is the polar surface of the lecithin bilayer; the resulting chemical shifts of the phytol double bond being due to the proximity of the unsaturated carbons of phytol to this interface. Therefore, the magnitude and direction of the electric field induced shifts may be used to investigate the structure of the lecithin-phytol bilayer. This observation is one of the few examples of an intermolecular field effect.

Several studies carried out on bilayers have suggested that the phosphatidyl choline headgroup of lecithin is oriented in a plane perpendicular to the fatty acid chains. Electrostatic and electrokinetic studies (151), X-ray diffraction (152), single crystal X-ray analysis of phosphatidylethanolamine (153), <sup>13</sup>C NMR of EYL with paramagnetic shift reagents (23) and surface dipole moment measurements of lecithin in monolayers (40), plus <sup>31</sup>P NMR lineshape analysis of lecithin dispersions (78-81), all support this orientation of the zwitterion.

From monolayer surface potential measurements, the surface dipole moment per molecule,  $\mu_s$ , is directly proportional to the observed surface potential,  $\Delta V$  (44). In other words, the greater the magnitude of the dipole moment per molecule, the greater is the magnitude of the observed surface potential.

The total surface dipole moment of a lecithin molecule may be thought of as being the sum of four components. These are the carbonyls of the fatty acid chains which produce a negligible vertical component since they are oriented in an approximately horizontal plane, the glycerol C-O bonds, the phosphate group, and the trimethylammonium group. The resultant surface dipole moment is oriented such that the negative pole is pointing outwards into the aqueous phase (40,46). This orientation of the resultant dipole has been confirmed by surface dipole moment measurements of plasmalogen (40).

As discussed in Section 3B, the value of the electric field parallel to the phytol double bond due to the bilayer surface dipole moment may be calculated by the method of Zurcher (123) (Section 3B Equation III-41).

Since the surface dipole moment is the normal component of the dipole averaged over the whole surface, it is assumed in the subsequent treatment that the additional field experienced by the

unsaturated phytol carbons arises from a point directly above the phytol hydroxyl moiety. It is further assumed that phytol is intercalated into the bilayer parallel to the lecithin fatty acid chains in an extended conformation, as is indicated by the  $^{13}\text{C}$   $T_1$  results. In this approximation, the field resolved parallel to the phytol double bond is given by

$$E_1 = 2\mu_1/r^3$$

IV-3

where  $\mu_1$  is the surface dipole moment and  $r$  is the distance from the surface dipole to the midpoint of the C=C bond.

While it would not be expected that the phytol hydroxyl would penetrate into the highly charged plane of the choline headgroup, it is probable that phytol is engaged in hydrogen bonding with the phosphate  $\text{O}^{1/2-}$ . This is consistent with the  $^{13}\text{C}$   $T_1$  relaxation measurements. Calculations using a hydrogen bond length of 1.75Å, the single crystal conformation of dilauroyl phosphatidylethanolamine (153), and the X-ray determined bond lengths of L- $\alpha$ -glycerophosphorylcholine (154), place the phytol hydroxyl approximately 0.88Å below the dipole surface.

Using bond lengths and angles for structurally similar molecules (155, 156), it can be calculated that the distance from the dipole to the midpoint of the phytol C2-C3 double bond is 4.72Å. For a surface dipole moment of 0.6 Debye (45), the value of the electric field experienced by the phytol olefinic carbons using equation IV-3 is calculated to be  $1.4 \times 10^4$  esu-cm/cm<sup>3</sup>.

Substituting this value for the field into equation III-45 and subsequently into equation III-46 using a shift/electron value of 182 ppm/e (157) results in a calculated theoretical chemical shift difference for the phytol unsaturated carbons due to the linear electric field effect of 0.90 ppm (observed = 0.97 ppm). Not only is this calculated value of the right order of magnitude, but more importantly, it is in the correct direction. Carbon 2 of phytol which is nearer the membrane surface experiences an increase in electron density due to the polarization of the olefinic bond, and is, as a result, shifted upfield. C3 which experiences a decrease in electron density is reciprocally shifted downfield, in agreement with the theoretical treatment of Seidman and Maciel (128).

Although subject to a considerable amount of error due to the necessary assumptions, the observed field effect is in qualitative agreement with the structure proposed for the lecithin-phytol bilayer, as shown in Figure 9, since it places the phytol hydroxyl close enough to the headgroup for hydrogen bonding.

Since the observed electric field effect shift is induced by the surface dipole moment of the membrane, any change in this dipole moment should change the observed shift non-equivalence. In this regard, it should be noted that the observed field effect shift for C3 increases from 0.51 to 0.74 ppm as the temperature of the mixed bilayer is lowered from 52 to 11°C. Such an increase is most likely a consequence of increased molecular packing at the lower temperature.



Also, the monolayer surface potential measurements of Shah and Schulman (40) show that at both low and high surface pressures, the surface dipole moment per molecule of EYL is approximately 25% greater than that of DPL. This is reflected in the smaller field effect for DPL than EYL at 52°C (0.70 ppm vs 0.97 ppm).

Finally, the surface dipole was varied to see whether this would lead to concomitant change in the C2, C3 chemical shifts. The method involves the addition of NaCl to the vesicle preparation. It has previously been shown that the addition of 150 mM sodium ions to the subphase of lecithin monolayers increases the surface dipole moment by approximately 40% (45). Therefore, if the DPL-phytol vesicles are prepared containing 150 mM NaCl, the magnitude of the field effect induced chemical shift should increase. This is observed to be true; the additional shift nonequivalence of the phytol olefinic carbons increases to 0.94 ppm from 0.70 ppm (i.e. by 36%) in the presence of 150 mM NaCl, exactly as predicted by equations III-46 and IV-3. Therefore, the effect of temperature, a change in the nature of the phospholipid, and the effect of added ions all support the interpretation that the characteristic upfield-downfield chemical shift for the phytol olefinic pair upon incorporation into lecithin bilayers is indeed due to an intermolecular linear electric field effect caused by the membrane surface dipole moment. In addition, the magnitude and direction of this effect are in qualitative agreement with the proposed structure of the lecithin-phytol bilayer which is depicted in Figure 9.

80a

Figure 9. Space filling molecular models illustrating the proposed structure of the lecithin-phytol bilayer.

E. <sup>13</sup>C NMR of EYL-Vitamin E and Phytanic Acid Bilayers

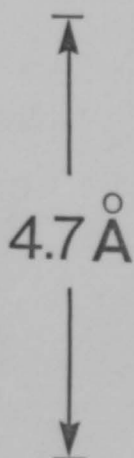
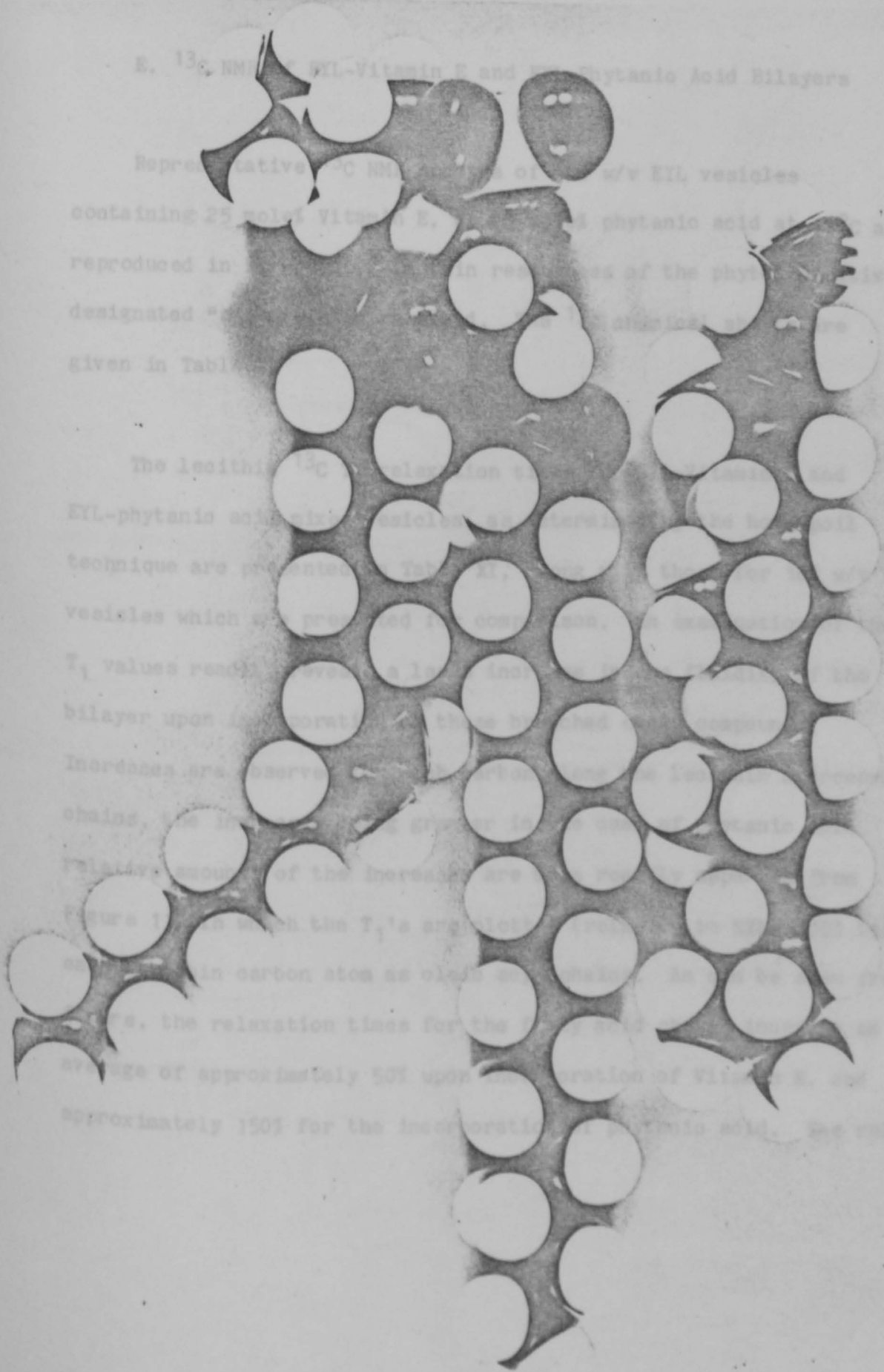
Representative <sup>13</sup>C NMR spectra of EYL vesicles

containing 25% solid Vitamin E, and phytanic acid are reproduced in Figures 1 and 2. The spectra are designated "a" and "b" and are given in Table I.

The lecithin <sup>13</sup>C relaxation times for the EYL-phytanic acid vesicles are presented in Table II. The vesicles which were prepared in the presence of Vitamin E, the T<sub>1</sub> values reach a value of approximately 1000 ms. The bilayer upon incorporation of the solid, the T<sub>1</sub> values increase and are observed to be in the range of 1000-2000 ms. The increase in the T<sub>1</sub> values is due to the presence of the solid chains, the increase in the T<sub>1</sub> values is due to the presence of the solid chains, the increase in the T<sub>1</sub> values is due to the presence of the solid chains.

Figure 1 shows the T<sub>1</sub>'s are approximately 1000 ms. In the presence of the solid, the relaxation times for the solid chains are approximately 1500 ms. The relaxation times for the solid chains are approximately 1500 ms. The relaxation times for the solid chains are approximately 1500 ms.

Figure 2 shows the T<sub>1</sub>'s are approximately 1000 ms. In the presence of the solid, the relaxation times for the solid chains are approximately 1500 ms. The relaxation times for the solid chains are approximately 1500 ms. The relaxation times for the solid chains are approximately 1500 ms.



## E. $^{13}\text{C}$ NMR of EYL-Vitamin E and EYL-Phytanic Acid Bilayers

Representative  $^{13}\text{C}$  NMR spectra of 10% w/v EYL vesicles containing 25 mole% Vitamin E, or 25 mole% phytanic acid at  $11^\circ\text{C}$  are reproduced in Figure 10. Certain resonances of the phytol additives, designated "a", are also resolved. The  $^{13}\text{C}$  chemical shifts are given in Table X.

The lecithin  $^{13}\text{C}$   $T_1$  relaxation times for EYL-Vitamin E and EYL-phytanic acid mixed vesicles, as determined by the homospoil technique are presented in Table XI, along with those for 10% w/v EYL vesicles which are presented for comparison. An examination of the  $T_1$  values readily reveals a large increase in the fluidity of the bilayer upon incorporation of these branched chain compounds. Increases are observed for each carbon along the lecithin hydrocarbon chains, the increases being greater in the case of phytanic acid. The relative amounts of the increases are more readily apparent from Figure 11, in which the  $T_1$ 's are plotted (relative to EYL=1.00) for each lecithin carbon atom as oleic acyl chains. As can be seen from the figure, the relaxation times for the fatty acid chains increase an average of approximately 50% upon incorporation of Vitamin E, and approximately 150% for the incorporation of phytanic acid. The relative

Figure 10: Proton noise decoupled  $^{13}\text{C}$  NMR spectra of lecithin-Vitamin E, and lecithin-phytanic acid vesicles at  $11^\circ\text{C}$ . A. 10% w/v EYL vesicles containing 25 mole% Vitamin E. B. 10% w/v EYL vesicles containing 25 mole% phytanic acid. The resonances designated "a" are due to intercalated Vitamin E or phytanic acid in A or B respectively.

A

B

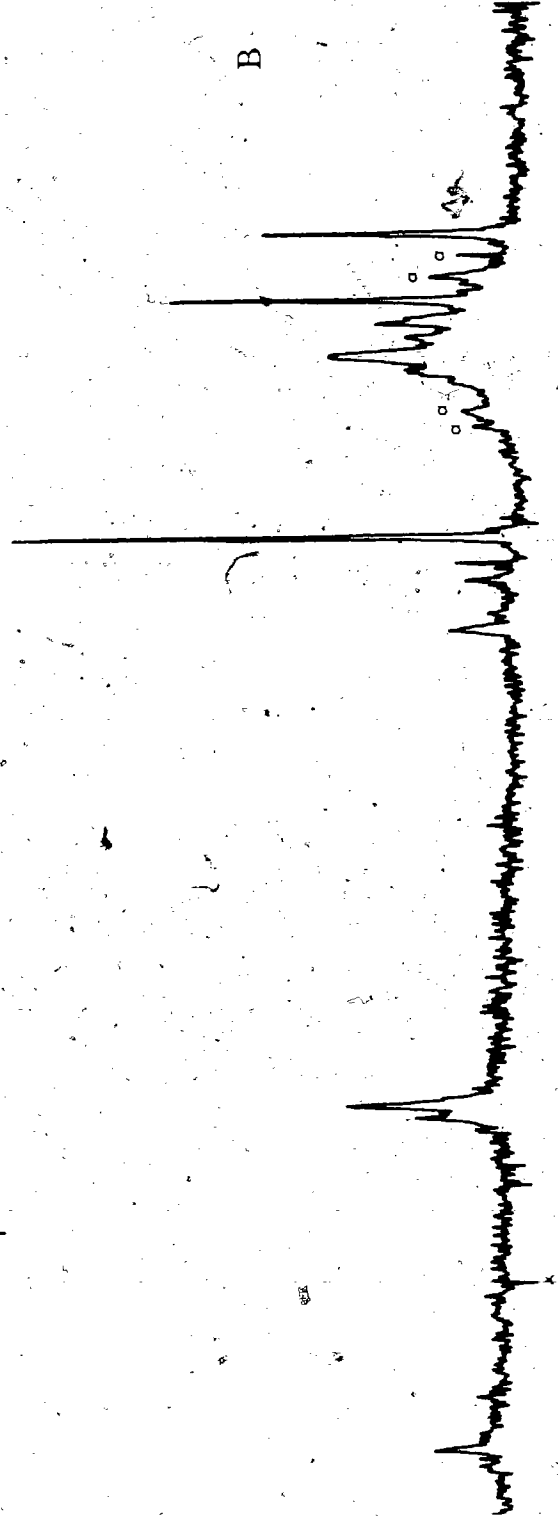
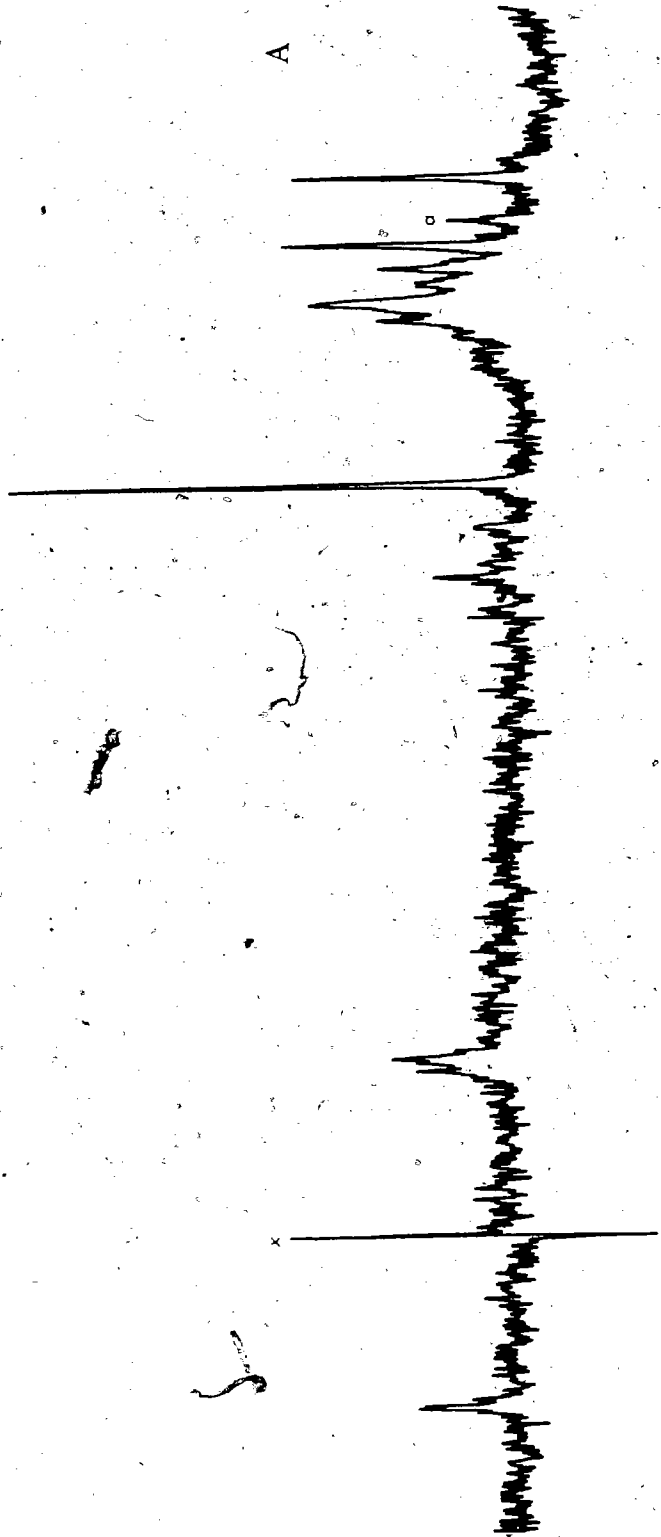


Table X

$^{13}\text{C}$  chemical shifts for 10% w/v EYL vesicles and for vesicles containing 25 mole% Vitamin E or phytanic acid at  $11^\circ\text{C}$ .

Carbon	EYL	EYL + 25mole% Vitamin E	EYL + 25mole% phytanic acid
Choline $\text{N}+(\text{CH}_3)_3$	54.15	54.29	54.33
$\text{N}+\text{CH}_2$	66.17	66.15	66.40
$\text{CH}_2\text{OP}$	59.79	59.77	59.75
Chain $\text{CH}_3$	14.26	14.31	14.34
$\text{CH}_2\text{CH}_3$	23.02	22.84	22.93
$\text{CH}_2\text{CH}_2\text{CH}_3$	32.35	32.40	32.48
$(\text{CH}_2)_n$	30.28	30.28	30.30
$\text{C}_2$	34.27	34.26	34.30
$\text{C}=\text{O}$	173.66	173.66	173.81
$-\text{C}^*\text{H}_2-\text{CH}=\text{CH}-\text{C}^*\text{H}_2-$	27.60	27.88	27.56
C11 linoleic	25.74	25.88	25.86
$-\text{CH}=\text{C}^*\text{H}-\text{CH}_2-\text{CH}_2-$	129.52	129.59	129.83
$-\text{CH}=\text{C}^*\text{H}-\text{CH}_2-\text{C}^*\text{H}=\text{CH}-$	127.93	127.96	128.06

Table XI

$^{13}\text{C}$  relaxation times<sup>a</sup> for lecithin, lecithin-Vitamin E, and lecithin-phytanic acid bilayers<sup>c</sup>  
at 11°C

Carbon	EYL	EYL + 25 mole% Vitamin E	EYL + 25 mole% phytanic acid
$\text{CH}_3$	$2.05 \pm 0.12$	$2.76 \pm 0.17$	$2.98 \pm 0.25$
$\text{CH}_2\text{CH}_3$	$0.66 \pm 0.04$	$0.80 \pm 0.05$	$1.75 \pm 0.08$
$\text{CH}_2\text{CH}_2\text{CH}_3$	$0.30 \pm 0.02$	$0.55 \pm 0.03$	$0.90 \pm 0.05$
$(\text{CH}_2)_n$	$0.30 \pm 0.02$	$0.45 \pm 0.03$	$0.81 \pm 0.05$
C2	$0.12^b \pm 0.01$	$0.13^b \pm 0.01$	$0.35 \pm 0.02$
C=O	$1.62 \pm 0.12$	$2.31 \pm 0.14$	$2.01 \pm 0.23$
$-\text{C}^*\text{H}_2-\text{CH}=\text{CH}-$	$0.24 \pm 0.02$	$0.47 \pm 0.03$	$0.58 \pm 0.05$
$-\text{CH}=\text{CH}-\text{C}^*\text{H}_2-\text{CH}=\text{CH}-$	$0.25 \pm 0.02$	$0.60 \pm 0.04$	$1.06 \pm 0.06$
$-\text{CH}=\text{C}^*\text{H}-\text{CH}_2-\text{CH}_2$	$0.33 \pm 0.02$	$0.53 \pm 0.04$	$0.74 \pm 0.04$
$-\text{CH}=\text{C}^*\text{H}-\text{CH}_2-\text{C}^*\text{H}=\text{CH}$	$0.58 \pm 0.05$	$0.71 \pm 0.04$	$1.10 \pm 0.07$
$\text{N}(\text{CH}_3)_3$	$0.24 \pm 0.03$	$0.41 \pm 0.02$	$0.39 \pm 0.02$
$\text{NCH}_2$	$0.13^b \pm 0.01$	$0.27 \pm 0.02$	$0.24 \pm 0.02$
$\text{CH}_2\text{OP}$ (choline)	$0.12^b \pm 0.01$	$0.21 \pm 0.01$	$0.14^b \pm 0.01$

<sup>a</sup> Measured by homospoil method

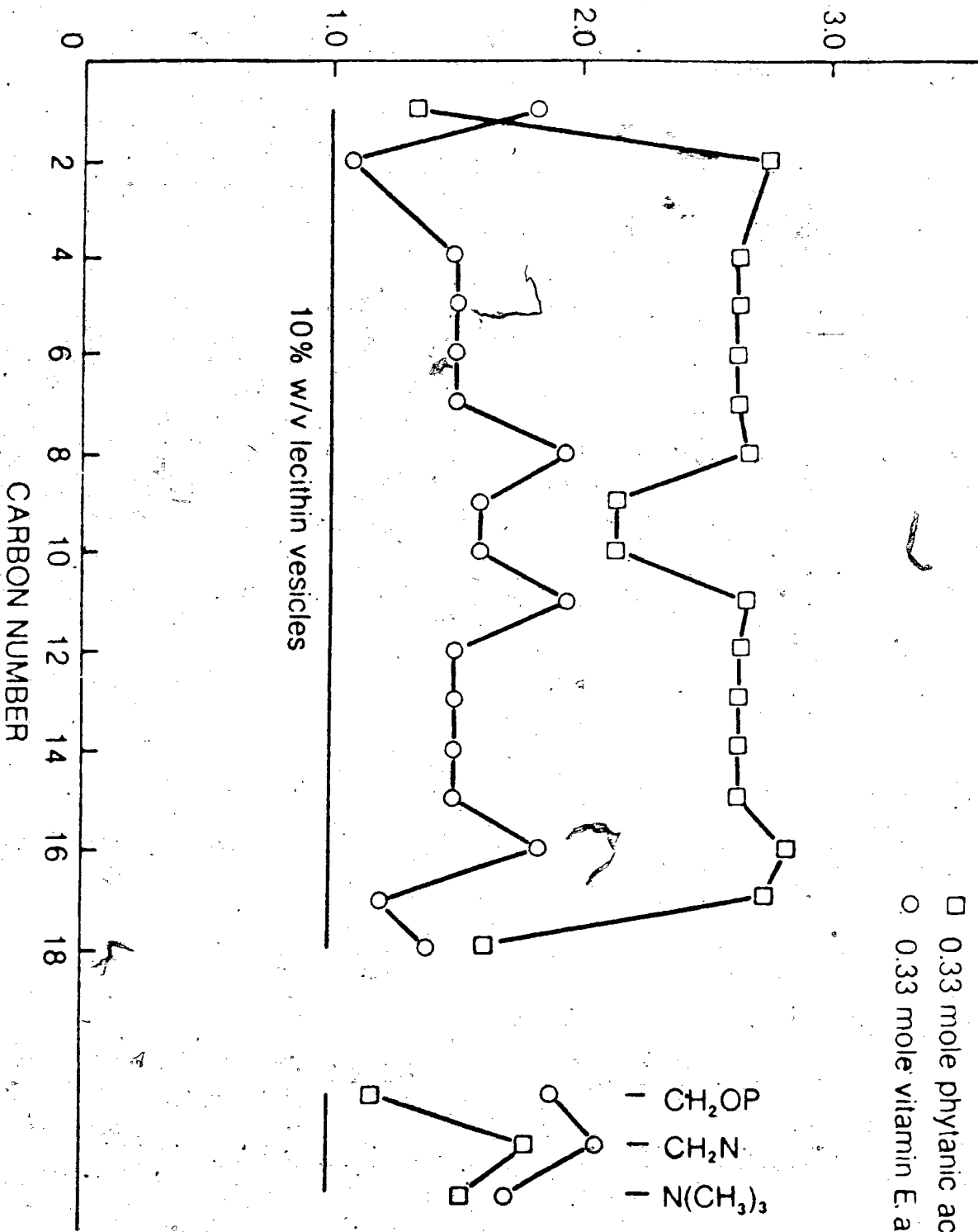
<sup>b</sup> Measured by inversion-recovery method

<sup>c</sup> 4000 transients



Figure 11. The relative  $^{13}\text{C}$   $T_1$  relaxation times for fatty acid carbons of lecithin and mixed lecithin-phytyl compound vesicles in  $\text{D}_2\text{O}$  at  $11^\circ\text{C}$ .  $\square$  containing 25 mole% phytanic acid.  $\circ$  containing 25 mole% Vitamin E. The  $^{13}\text{C}$   $T_1$  values for 10% w/v pure EYL vesicles have been given the relative value of 1.00.

RELATIVE T<sub>1</sub> RELAXATION TIME



— CH<sub>2</sub>OP  
 — CH<sub>2</sub>N  
 — N(CH<sub>3</sub>)<sub>3</sub>

value for the main methylene envelope was given to all carbons contributing to this resonance. It is possible that the apparent symmetry of the relative  $T_1$ 's about the region from C8 to C11 may be due to penetration of the methyl branches of the phytol chains into pockets created by the cis double bonds of the lecithin fatty acyl tails, but this hypothesis cannot be proven with the data available.

More specifically, the  $T_1$  for the main methylene envelope increases from 0.30 to 0.55 sec upon incorporation of Vitamin E, and to 0.81 sec upon intercalation of phytanic acid, while the antepenultimate carbon experiences increases from 0.30 to 0.55 sec for the lecithin-Vitamin E and to 0.90 sec for lecithin-phytanic acid mixed bilayers. Similarly, increases are also detected for the penultimate carbon from 0.66 to 0.80 and 1.75 sec, and for the terminal methyl carbon from 2.05 to 2.76 and to 2.98 sec. Increases are also observed for the olefinic carbons of oleic acid residues from 0.33 to 0.53 and 0.74 sec.

These large increases in relaxation times indicate an increase in motion within the bilayer structure, phytanic acid giving rise to the greater effect.

The increased mobility of the lecithin hydrocarbon chains, at 11°C upon the addition of Vitamin E and phytanic acid can be explained in terms of the difficulty in accommodating the branched

chain compounds in an ordered bilayer arrangement. Since the London attractive forces between the hydrocarbon chains of lipid bilayers are highly distance dependent, even a slight expansion of the bilayer would lead to a large decrease in the interaction of adjacent lipid molecules.

An examination of the  $^{13}\text{C}$   $T_1$ 's for the lecithin headgroup reveals information concerning the membrane surface. For these carbons, the order of the  $T_1$  increase is reversed (see Fig. 11); that is, Vitamin E produces larger effects, while the effects of phytanic acid are less pronounced. Particularly interesting is the effect on the carbon atom adjacent to the lecithin phosphate i.e.  $\text{CH}_2\text{OP}$ . While the incorporation of phytanic acid increases the  $^{13}\text{C}$  relaxation time from 0.12 sec to only 0.14 sec, the addition of Vitamin E results in an increase to 0.21 sec (75%).

A rationalization of this fact may be made by a consideration of the relative depth at which phytanic acid and Vitamin E sit in the membrane. It has been shown in Section 4D, by the use of a linear electric field effect, that phytol sits sufficiently close to the membrane hydrophilic region to engage in hydrogen bonding with the lecithin phosphate moiety. Phytanic acid with its hydrophilic carboxyl function would also be expected to extend into the aqueous phase, and may be engaged in hydrogen bonding with the lecithin phosphate. Such an interaction would tend to anchor the carbon atoms of the lipid

headgroup and decrease their motional freedom. Vitamin E, on the other hand, with a single hydroxyl function on its bulky chromanol ring system would not be expected to penetrate as far into the hydrophilic region. It is possible that the position of the chromanol may parallel that occupied by cholesterol (158,159), with the hydroxyl function at the site of the fatty acid ester carbonyl. It is unlikely that the Vitamin E is engaged in hydrogen bonding with the carbonyl since it is known that hydrogen bonding deshields carbonyl carbons (160), resulting in a downfield  $^{13}\text{C}$  shift. No significant shift in the lecithin carbonyl is observed upon the addition of Vitamin E. Therefore the possibility of hydrogen bonding is remote.

It has previously been reported (12) that the incorporation of cholesterol into EYL results in a downfield shift of  $\sim 2$  ppm for the lecithin carbonyls. However when 33 mole% cholesterol was incorporated into EYL vesicles at  $30^\circ\text{C}$ , no significant shift was observed. It has subsequently been suggested that although the cholesterol hydroxyl lies at a depth equal to that of carbonyls, its primary function is simply to provide amphiphilic character and an orienting influence through solvation by water at the polar interface (161). Such may also be the case for  $\alpha$ -tocopherol.

In any event, Vitamin E is not expected to interact directly with the lecithin headgroup but the large increases in  $T_1$  for the headgroup carbons may be explained by a decreased ionic interaction of

the negatively charged lecithin phosphate group for the positively charged trimethylammonium moiety of an adjacent lipid molecule. This decrease in ionic interaction is proposed to be due to an expansion of the bilayer due to the intercalation of the phytol compounds. This will be discussed in more detail in the following section (Section 4F). The smaller increases in  $T_1$  for headgroup carbons in the case of phytanic acid is consistent with hydrogen bonding of the phytanic acid carboxyl moiety to the lecithin phosphate. This would then tend to anchor the headgroup. Note that the difference between the increases caused by Vitamin E and phytanic acid is lessened as the trimethylammonium carbons are approached (Fig. 11).

We have seen that the incorporation of Vitamin E (25 mole%) dramatically affects the  $^{13}\text{C}$   $T_1$  relaxation times of the lecithin carbons of a phospholipid bilayer. In order to determine the effect of a smaller amount of  $\alpha$ -tocopherol,  $^{13}\text{C}$   $T_1$  relaxation times were determined at  $52^\circ\text{C}$  for mixed vesicles containing a 10:1 mole ratio of EYL:Vitamin E. These values are reported in Table XII for both the admixture and for EYL alone. A comparison of these values indicates little change. This is not unexpected due to the smaller amount of  $\alpha$ -tocopherol incorporated, as compared with the incorporation of 25 mole%  $\alpha$ -tocopherol which produced substantial perturbation. However, as will be shown in Section 4G, the disruption caused by the intercalation of as little as 3 mole% Vitamin E is manifested in a significant increase in the permeability of the mixed membrane.

Table XII

$^{13}\text{C}$   $T_1$  relaxation times for 20% w/v EYL vesicles and  
20% w/v EYL vesicles containing a 10:1 mole ratio  
lecithin:Vitamin E at 52°C.

Carbon	Lecithin	Lecithin + Vitamin E
Choline $\text{N}^+(\text{CH}_3)_3$	0.88	0.78
$\text{N}^+(\text{CH}_2)$	0.51	0.55
$\text{CH}_2\text{OP}$	0.50	0.50
Chain $\text{CH}_3$	4.12	3.63
$\text{CH}_2\text{CH}_3$	2.25	2.10
$\text{CH}_2\text{CH}_2\text{CH}_3$	1.11	1.12
$(\text{CH}_2)_n$	0.59	0.56
C2	0.28	0.33
C=O	2.80	1.93
C9 oleic	0.90	0.84
C10 oleic	1.05	1.10
C9 linoleic		
C11 linoleic	1.22	1.15
C8 and 11 oleic	0.76	0.70
C8 and 14 linoleic		
C12 linoleic	1.39	1.44
C10 linoleic	0.90	1.07

## F. Phytol Compounds and Membrane Packing

The preceding sections on the effect of phytol, Vitamin E and phytanic acid have been interpreted in terms of the difficulty in accommodating these branched chain structures in an ordered bilayer structure. It was seen that at 11°C, the effects increased in the order phytol < Vitamin E < phytanic acid. This section will discuss this interpretation in terms of further known properties of these and other molecules.

Monolayers of phytol,  $\alpha$ -tocopherol, and phytanic acid occupy molecular areas of 55, 60 and 61 Å<sup>2</sup> per molecule at 0.5 dyne/cm, respectively (46), while cholesterol is known to form stable monolayers under the same conditions with molecular areas of approximately 40 Å<sup>2</sup> per molecule. Thus, the area requirements for the phytol molecules is much higher. Such large monolayer areas must be due to the branched nature of the chains, since the unbranched C18 acid, stearic acid occupies monolayer areas of the order of 24 Å<sup>2</sup> per molecule (46).

Above the lecithin gel-liquid crystalline transition temperature, cholesterol is known to fit into cavities created by thermal motion of the fatty acyl chains causing an "intermediate fluid" condition (42,47). Thus, mixed monolayers of lecithin and cholesterol do not follow the additivity rule since cholesterol occupies pockets in the



membrane and causes little proportional increase in the area/molecule of mixed monolayers. Such behaviour has been correlated with a decrease in permeability above  $T_m$  (99,162). Very recently the monolayer behaviour of Vitamin E in lecithin monolayers has been studied (50). It was found that in monolayers of distearoyl- or dioleoyl-lecithin the additivity rule was well followed up to 50 mole% incorporated  $\alpha$ -tocopherol. This indicates that unlike cholesterol,  $\alpha$ -tocopherol is not able to fit into the cavities between adjacent lecithin molecules, and displaces its full area requirement in mixed lecithin- $\alpha$ -tocopherol systems. Such behaviour necessarily involves an increase in lipid-lipid separation due to intercalated Vitamin E.

The total interaction energy due to London-Van der Waals dispersion forces between the long hydrocarbon tails of phospholipids is proportional to the inverse fifth power of the intermolecular distance (163). Thus even a small lateral expansion of the lipid bilayer would result in a large decrease in the interaction energies of adjacent lipid molecules. As an example, it has been found that the presence of a single methyl group in isostearic acid reduces the interaction energy from that of stearic acid by a factor of three (163). This decrease in intramolecular attraction would be expected to become even more severe for more highly branched molecules such as phytol, Vitamin E and phytanic acid.

Such decreases in intramolecular attractions and increases in phospholipid-phospholipid packing distances due to the incorporation of phytol, Vitamin E, and phytanic acid are consistent with the the  $^{13}\text{C}$   $T_1$  relaxation results. Thus, phytol, with a monolayer area of  $55\text{\AA}^2$  per molecule, causes the least perturbation of the three. Although  $\alpha$ -tocopherol has nearly the same area requirements as phytanic acid (60 vs  $61\text{\AA}^2$ /molecule), because of its extremely hydrophobic nature it is not expected to penetrate as far into the region of the lecithin headgroup, but due to its intercalation, simply decrease the ionic attraction of the negatively charged phosphate of one lecithin molecule for the trimethylammonium group of an adjacent, but now more distant, lecithin molecule. Phytanic acid causes the greatest increase in  $^{13}\text{C}$   $T_1$  relaxation times since in addition to its large surface area requirement, it penetrates furthest into the hydrophilic region, further interfering with the normal lecithin-lecithin headgroup ionic interaction.

In order to determine that the effects on  $^{13}\text{C}$   $T_1$  relaxation times are in fact due to the branched nature of the phytyl chain, relaxation times were determined for the incorporation of the unbranched C16 acid, palmitic acid, into EYL vesicles, for comparison with those determined for lecithin with incorporated phytanic acid, and for those of lecithin alone. These are presented in Table XIII. An examination of these values clearly shows that the incorporation of 25 mole% palmitic acid has little effect on the fluidity of the

Table XIII

$^{13}\text{C}$   $T_1$  relaxation times for 10% w/v EYL vesicles and  
10% EYL vesicles containing 25 mole % incorporated  
palmitic acid at 11°C. .

Carbon	$T_1$ (sec)	
	Lecithin	Lecithin + 25mole% Palmitic Acid
Choline $\text{N}^+(\text{CH}_3)_3$	0.24	0.25
$\text{N}^+\text{CH}_2$	0.13	0.16
$\text{CH}_2\text{OP}$	0.12	0.12
Chain $\text{CH}_3$	2.05	1.76
$\text{CH}_2\text{CH}_3$	0.66	0.64
$\text{CH}_2\text{CH}_2\text{CH}_3$	0.30	0.37
$(\text{CH}_2)_n$	0.30	0.26
C2	0.12	0.13
C=O	1.62	1.63
$\text{C}^*\text{H}_2\text{-CH=CH-}$	0.24	0.27
C11 linoleic	0.25	0.25
$\text{-CH=C}^*\text{H-CH}_2\text{-CH}_2\text{-}$	0.33	0.35
$\text{-CH=C}^*\text{H-CH}_2\text{-C}^*\text{H=CH-}$	0.58	0.40

bilayer as evidenced by  $^{13}\text{C}$   $T_1$ 's, in direct contrast to the effect of the branched acid, phytanic acid. Since palmitic acid has a very small area requirement ( $\sim 24\text{\AA}^2/\text{molecule}$ ), it is able to fit into the cavities created by thermal fluctuations of the lecithin fatty acid chains above the gel-liquid crystalline transition temperature and, because it is unbranched, causes little perturbation of the London-van der Waals attractive forces. Thus, incorporation of phytol, Vitamin E, and phytanic acid perturb the normal phospholipid packing, resulting in increased fluidity of the bilayer.

Changes in bilayer fluidity and chain packing have been associated with changes in membrane permeability (9). Therefore, an investigation was conducted into the effects of the incorporation of phytol, Vitamin E and phytanic acid on membrane permeability. The results of this study are presented in the succeeding sections (Sections 4G-4I).

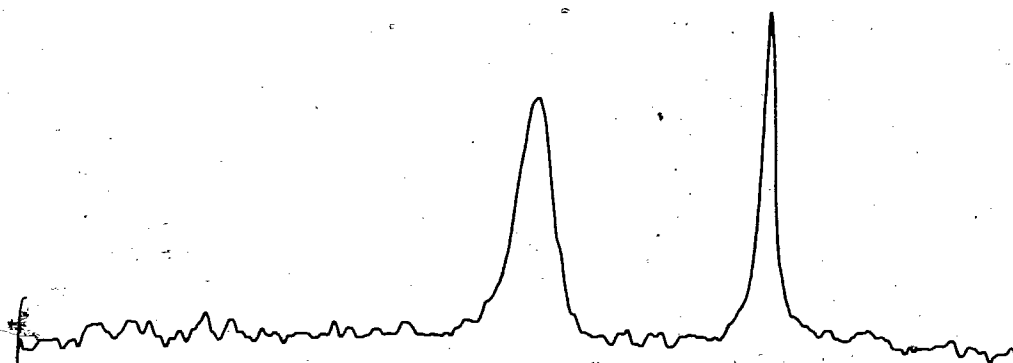
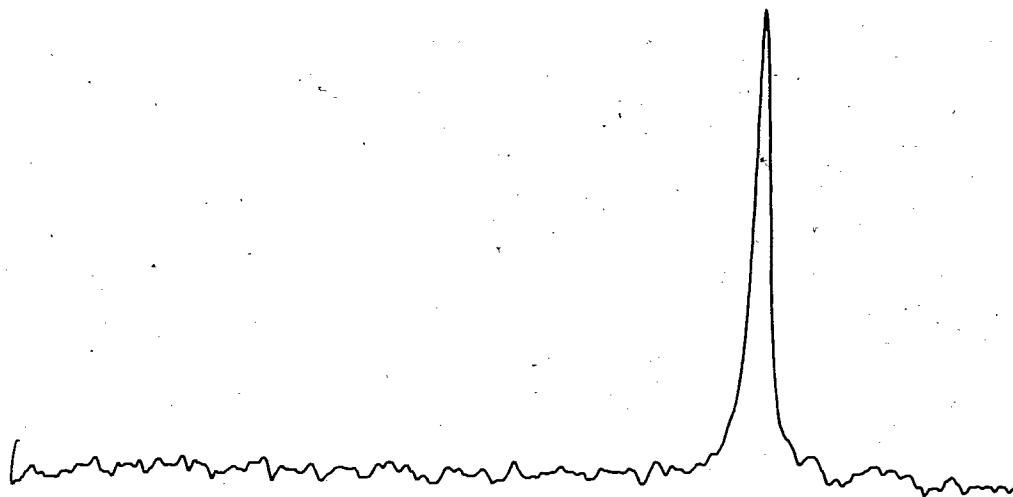
#### G. Permeability Studies by $^{31}\text{P}$ NMR

Bystrov and co-workers (26,27,164,165) discovered that it is possible to differentiate the inner and outer surfaces of phospholipid vesicles using  $^{31}\text{P}$  and  $^1\text{H}$  NMR with the aid of added lanthanide shift reagents. The  $^{31}\text{P}$  NMR chemical shifts of the phosphorus nuclei (or  $\text{N}^+(\text{CH}_3)_3$  protons in the case of  $^1\text{H}$  NMR) in the inner and outer layers of phospholipid vesicles are very nearly

equivalent, and a single resonance is observed. When the paramagnetic lanthanide  $\text{Pr}^{3+}$  is added to preformed lecithin vesicles, the resonance signal of phosphorus nuclei on the outside layer is broadened and shifted downfield, while the phosphorus nuclei on the inside layer facing towards the enclosed volume remain unaffected. Due to this lanthanide induced shift (LIS), the independent observation of both the "inside" and "outside" lecithin molecules is possible. This is illustrated in Figure 12. The relative areas of the two peaks is a measure of the relative number of phospholipid molecules on the inner and outer layers of the vesicles.

Previous workers (165,166) have used  $^1\text{H}$  NMR and LIS to study the permeability of phospholipid vesicle systems. As the paramagnetic lanthanide  $\text{Pr}^{3+}$  crosses the bilayer, the  $\text{N}^+(\text{CH}_3)_3$  protons are shifted downfield to reside under the low field peak. The rate of change of the chemical shift difference between the two resonances with time was used as a measure of the rate of permeation of the praseodymium cations. It is known that the observed shifts induced by lanthanides in the  $^{31}\text{P}$  NMR spectra are much larger than those of protons. This is consistent with a model in which the lanthanide ion associates with the lecithin phosphate moiety (167). Chemical shift data in the presence of shift reagent suggest that the lanthanide binds strongly to ~1% of the lecithin molecules (168). Thus, in order for all lecithin on the outside of the bilayer to be affected by  $\text{Pr}^{3+}$ , there most probably exists a sequential exchange of lecithins

Figure 12.  $^{31}\text{P}$  NMR spectra of 10% w/v egg yolk lecithin vesicles at 33 C. Top: Before the addition of  $\text{Pr}^{3+}$ . Bottom: Immediately after the addition of 150 ul of 0.1 M  $\text{Pr}(\text{NO}_3)_3 \cdot 5\text{H}_2\text{O}$ . Elapsed time = 13 min.



liganded to lanthanide at the surface of the bilayer, without the necessity for complete dissociation of the ion from the vesicle surface (168).

As mentioned previously, the rate of disappearance of the upfield, or "inside"  $^{31}\text{P}$  resonance signal can be used to study the traverse of the  $\text{Pr}^{3+}$  through the bilayer, and hence, monitor the membrane permeability. The larger chemical shift differences for added lanthanide with  $^{31}\text{P}$ , and the simplicity of the phosphorus spectra of phospholipids makes  $^{31}\text{P}$  NMR even more conducive to such studies than  $^1\text{H}$  NMR. It was found that due to the severely broadened nature of the downfield peak, however, that it was difficult to employ the difference in chemical shifts of the upfield and downfield peaks with time as a measure of permeability because of the uncertainty involved in measuring the chemical shift of the downfield peaks. Also, at 40.5 MHz, it was found that the upfield peak did not shift evenly, as a whole to lower field with time, but that as the paramagnetic  $\text{Pr}^{3+}$  crossed the bilayer with time, the intensity of the upfield peak decreased, as part of the intensity was transferred to a very broad absorbance of intermediate chemical shift. This broad absorbance grew with time and shifted downfield, under the downfield resonance, as the upfield peak intensity diminished. Therefore the decrease in the area of the sharp upfield peak (unaffected by  $\text{Pr}^{3+}$ ) with time was used as a measure of the bilayer permeability, i.e. a more direct pseudo first order rate of disappearance of the "inside" resonance signal was employed.



Since changes in the tightness of chain packing when the structure of the lecithin molecule is varied in lipid vesicles, as expressed by  $^{13}\text{C}$  relaxation times, can be correlated directly with permeability (168), variations in chain packing due to intercalated phytol, Vitamin E, and phytanic acid should also parallel permeability for these mixed vesicle systems. Therefore the effect of phytol, Vitamin E, phytanic acid, and palmitic acid on membrane permeability to lanthanide ion was studied by  $^{31}\text{P}$  NMR.

Figure 13 illustrates the decay of the upfield  $^{31}\text{P}$  resonance with time for lecithin with 25 mole% incorporated phytol, and for lecithin with 25 mole% Vitamin E. The upper traces represent the spectra immediately after  $\text{Pr}^{3+}$  addition. The upfield peak is due to  $^{31}\text{P}$  nuclei facing the enclosed vesicle volume, while the downfield peak is due to outside phosphorus nuclei which are exposed to the added lanthanide. Note that the rate of decay of the upfield resonance is not equal for the two systems.

Plots of the disappearance of the "inside"  $^{31}\text{P}$  resonance signal as paramagnetic  $\text{Pr}^{3+}$  crosses the bilayer vs time are shown in Figure 14 for pure EYL, EYL with 25 mole% incorporated phytol, EYL with 25 mole% Vitamin E, and EYL with 25 mole% phytanic acid. From the relative slopes of the graphs, it is clear that the addition of these phytol compounds greatly increases the permeability of the membrane. These rates are quantified in Table XIV. An examination of these rates

Figure 13.  $^{31}\text{P}$  NMR spectra of 10% w/v egg yolk lecithin vesicles containing 25 mole% phytol or 25 mole% Vitamin E at the indicated times after the addition of 0.005 M  $\text{Pr}^{3+}$ .

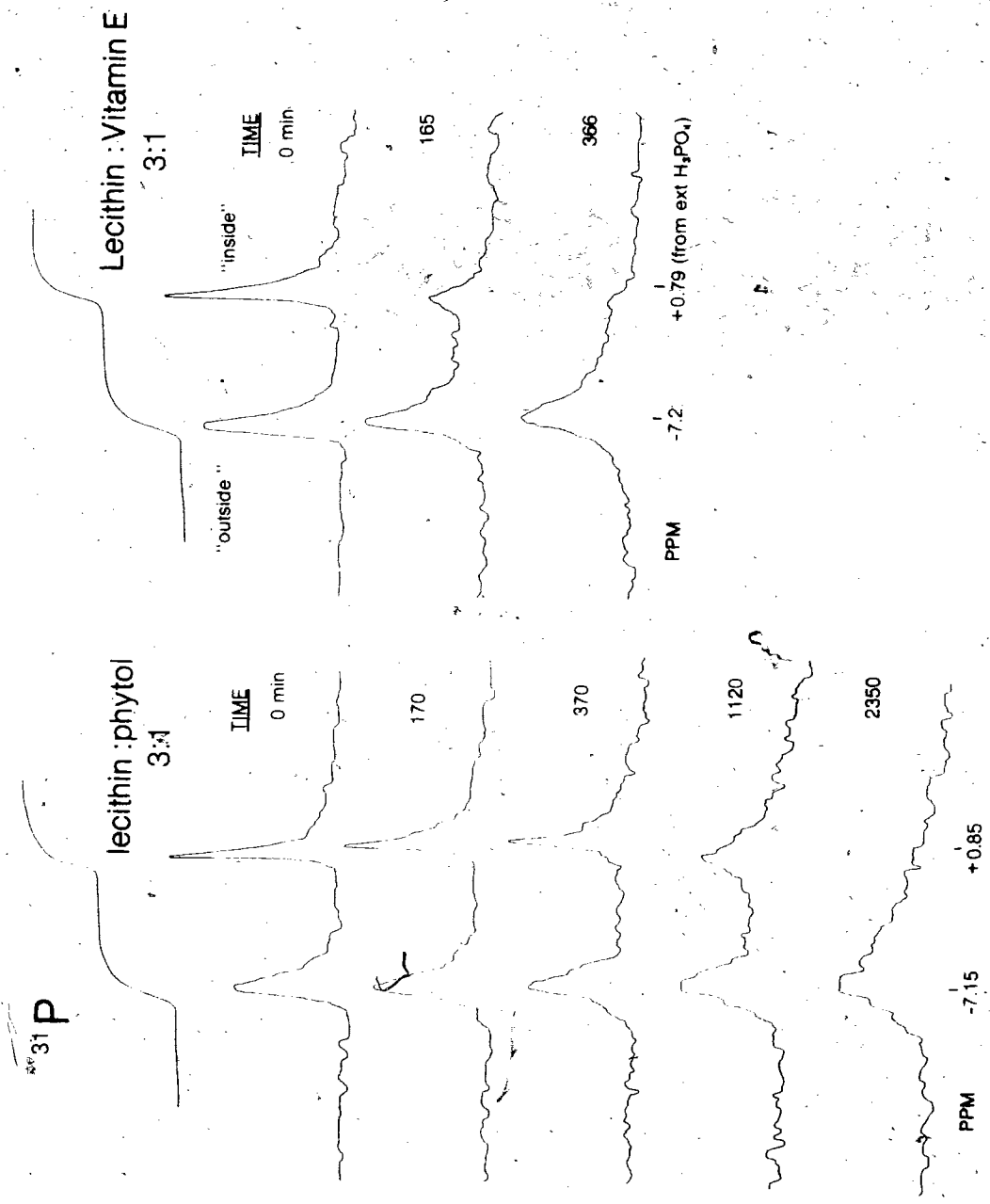


Figure 14. Percent total of "inside"  $^{31}\text{P}$  NMR signal relative to its initial value vs. time for various lecithin-phytyl compound mixed vesicles. (A) egg lecithin alone + 0.005 M  $\text{Pr}^{3+}$ , (B) egg lecithin with 25 mole% incorporated phytol + 0.005 M  $\text{Pr}^{3+}$ , (C) egg lecithin with 25 mole% incorporated Vitamin E + 0.005 M  $\text{Pr}^{3+}$ , (D) egg lecithin with 25 mole% incorporated phytanic acid + 0.005 M  $\text{Pr}^{3+}$ . Because of the extreme slope with phytanic acid, lines (C) and (D) are reproduced in the insert using an expanded time scale.

RELATIVE INTENSITY (PERCENT)

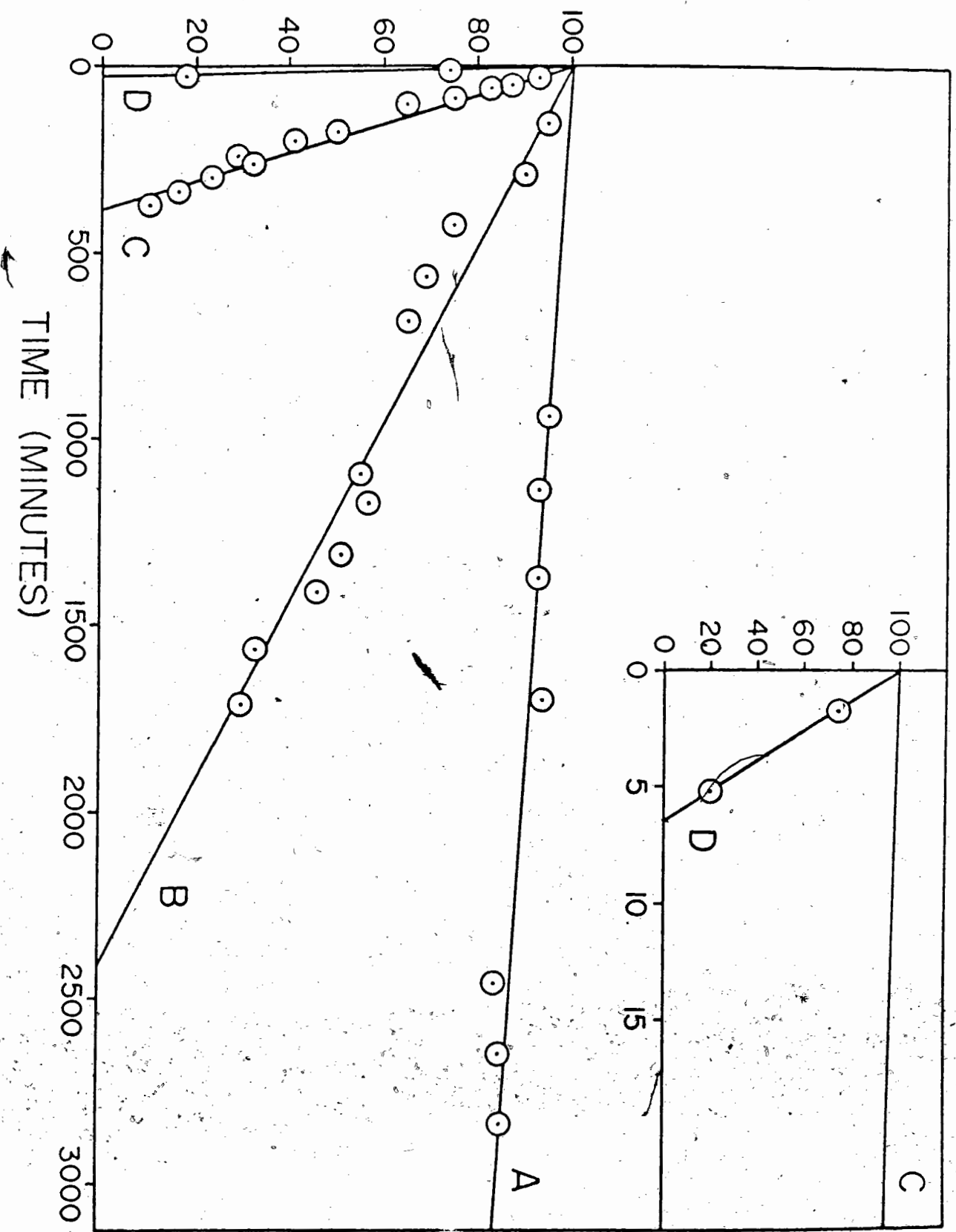


Table XIV

Leak rates for lecithin and lecithin-phytyl compound vesicles at 33°C. Lecithin:additive = 3:1 mole ratio

	<sup>31</sup> P Chemical Shift pre Pr <sup>3+</sup> (PPM up- field <sup>a</sup> from 85 % H <sub>3</sub> PO <sub>4</sub> )	"Inside" <sup>31</sup> P signal decay (% total/min)	Relative Rate	Half life -(days)
EYL	0.87	5.35x10 <sup>-3</sup>	1.00	6.5
EYL + Phytol	0.85	4.17x10 <sup>-2</sup>	7.79	0.83
EYL + Vitamin E	0.79	2.55x10 <sup>-1</sup>	47.66	0.14
EYL + Phytanic Acid	0.91	15.50	2897	0.0022

<sup>a</sup> 800 transients; pulse width = 10us (56° flip angle)

shows that the incorporation of 25 mole% phytol increases the vesicle leak rate by approximately 8 times, 25 mole% Vitamin E by approximately 48 times, and 25 mole% phytanic acid by nearly 2900 times over the rate obtained for pure egg lecithin vesicles. Half lives were calculated from the observed rates and are also given in Table XIV.

After the disappearance of the upfield "inside" resonance due to  $\text{Pr}^{3+}$  entering the vesicles, sufficient EDTA was routinely added to complex with accessible  $\text{Pr}^{3+}$  and spectra redetermined. Again two peaks were resolved, the upfield peak now due to phosphorus nuclei on the outside of the bilayer which are directly exposed to the added EDTA. Such behaviour indicates two things. Firstly, the disappearance of the upfield resonance with time after the initial addition of  $\text{Pr}^{3+}$ , can not be due to vesicle rupture. If the destruction of vesicles were responsible for the disappearance of the upfield protected signal, the subsequent addition of EDTA should result in a single upfield peak since all  $\text{Pr}^{3+}$  should be accessible for complexation. In addition, this behaviour indicates that these mixed vesicles are not appreciably permeable to EDTA during the time required for the determination of a spectrum (3-10 min). Thus, the  $^{31}\text{P}$  LIS procedure indeed monitors the permeability of lecithin vesicles.

The  $^{31}\text{P}$  NMR method lends itself best to diffusion studies which may be followed to completion during a time interval of 0-4 days. As can be seen, the observed half life for pure EYL vesicles is of the order of over one week. It was understandably not practical to conduct experiments of such duration. Therefore the observed rate for EYL is subject to considerably more error than for the more rapid rates in the case of the aforementioned mixed vesicle preparations. This is due to the smaller changes in peak areas in the time available. Repeated determinations of the permeability of pure EYL vesicles, which were run as standards for each determination, yielded rates from approximately  $2 \times 10^{-3}$  to  $5 \times 10^{-3}$  %/min. The standard deviations as computed from a least squares treatment of the experimental data were typically on the order of 20-30% of the calculated rate. The decay rates for the mixed vesicle systems are much more easily measured over a much wider change of spectral area and are considered to be accurate to  $\pm 10\%$ . It is clear that the incorporation of phytol, Vitamin E, and phytanic acid greatly increases the permeability of EYL bilayers. The effects of these compounds on permeability parallels their effect on the fluidity of the bilayer as shown by  $^{13}\text{C}$   $T_1$  relaxation times, i.e. phytanic acid > Vitamin E > phytol > lecithin alone.

In previous sections, the increase in  $^{13}\text{C}$   $T_1$  relaxation times was correlated with monolayer areas for the phytol compounds, and for mixed EYL-Vitamin E monolayers. It is interesting to note that the



reduction in permeability of liposomes containing cholesterol has been correlated with the low mean molecular area of lecithin-cholesterol mixed monolayers (169,170).

Once again, in order to illustrate the effect of the large effects of the molecular packing due to the branched chains, the permeability of EYL vesicles with 25 mole% incorporated palmitic acid was studied. Over a three day period, the upfield  $^{31}\text{P}$  signal decayed to ~90% of its original value, yielding a rate of  $2.4 \times 10^{-3}$  %/min, which is on the order of that obtained for EYL alone.

Experiments were also carried out to determine the effect of temperature on the permeability of lecithin-phytol (3:1 mole ratio) mixed vesicles. The results are shown in Table XV. Raising the temperature from  $11^{\circ}\text{C}$  to  $52^{\circ}\text{C}$  results in a rate increase of almost two orders of magnitude. In Fig.15 the logarithms of the rates were plotted against the inverse of the absolute temperature (Arrhenius plot). The plot is linear, yielding an activation energy of  $20.3 \pm 0.2$  kcal. It is extremely interesting that activation energy for  $\text{Pr}^{3+}$  permeation is in quite close agreement not only with that reported for  $\text{Na}^{+}$  permeation through lecithin-phosphatidic acid bilayers (99), but also with that reported for the transverse diffusion (flip-flop) of spin labeled lecithin molecules across phospholipid bilayers (19.3 kcal) (65). The implications of the magnitude of the activation energy for permeation through the lecithin-phytol bilayer will be discussed in Section 4I.

Table XV

Permeation rates of  $\text{Pr}^{3+}$  into EYL vesicles containing  
25 mole% phytol at various temperatures.

Temperature ( $^{\circ}\text{K}$ )	Permeability <sup>a</sup> (%/min)
325	$525 \times 10^{-3} \pm 25 \times 10^{-3}$
306	$42 \times 10^{-3} \pm 2 \times 10^{-3}$
284	$6.7 \times 10^{-3} \pm 3.8 \times 10^{-3}$

<sup>a</sup> The errors reflect the standard deviation in the  
individually determined rates.

107a


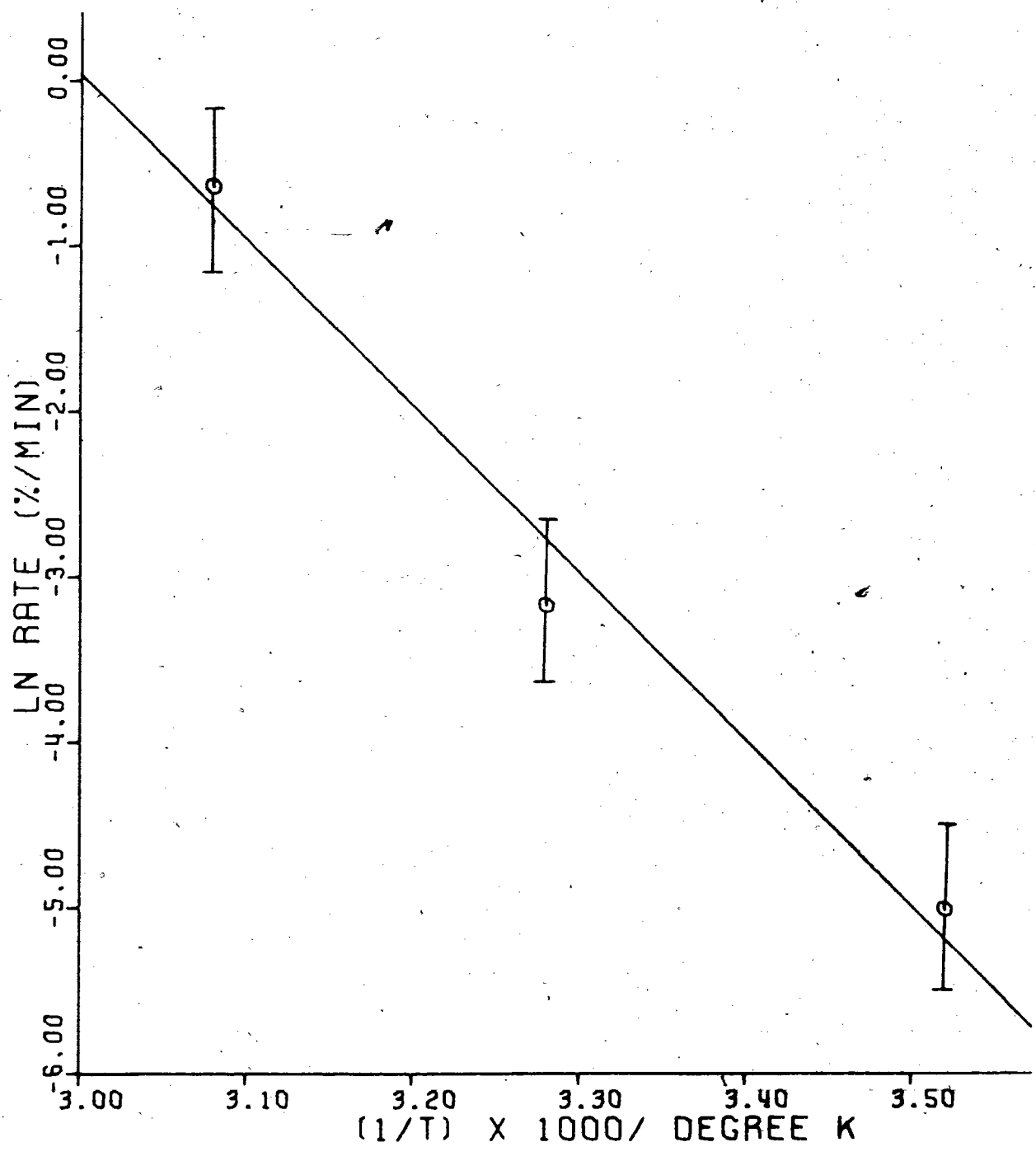


Figure 15. Arrhenius plot of vesicle leak rate vs. the inverse of absolute temperature for 10% w/v egg yolk lecithin vesicles containing 25 mole% phytol.



The rates of  $\text{Pr}^{3+}$  permeation (relative to egg yolk lecithin =1.00) for mixed vesicles containing various amounts of  $\alpha$ -tocopherol are given in Table XVI. The table shows that even the incorporation of a small amount of Vitamin E (3 mole%) results in the increase of the inward diffusion of  $\text{Pr}^{3+}$  to approximately three hundred percent of its original value. Thus, amounts of  $\alpha$ -tocopherol, which approach the physiological ratios of  $\alpha$ -tocopherol/total lipid and  $\alpha$ -tocopherol/phospholipid found in the human aorta (171,172), exert a large effect on the permeability properties of the membrane.

The relative rate of  $\text{Pr}^{3+}$  permeation vs mole% Vitamin E incorporated is plotted in Figure 16. The rates show roughly a logarithmic increase with increasing Vitamin E concentration, indicating that it is the intercalation of Vitamin E which is responsible for the permeability changes.

Thus, it is clear that the rate of  $\text{Pr}^{3+}$  diffusion through the EYL-phytyl compound membranes is dependent both on temperature and on the relative concentration of the membrane components. A more complete discussion of this permeation is presented in Section 4I, following the results obtained for cholesteryl ester-EYL mixed membrane systems.

Table XVI

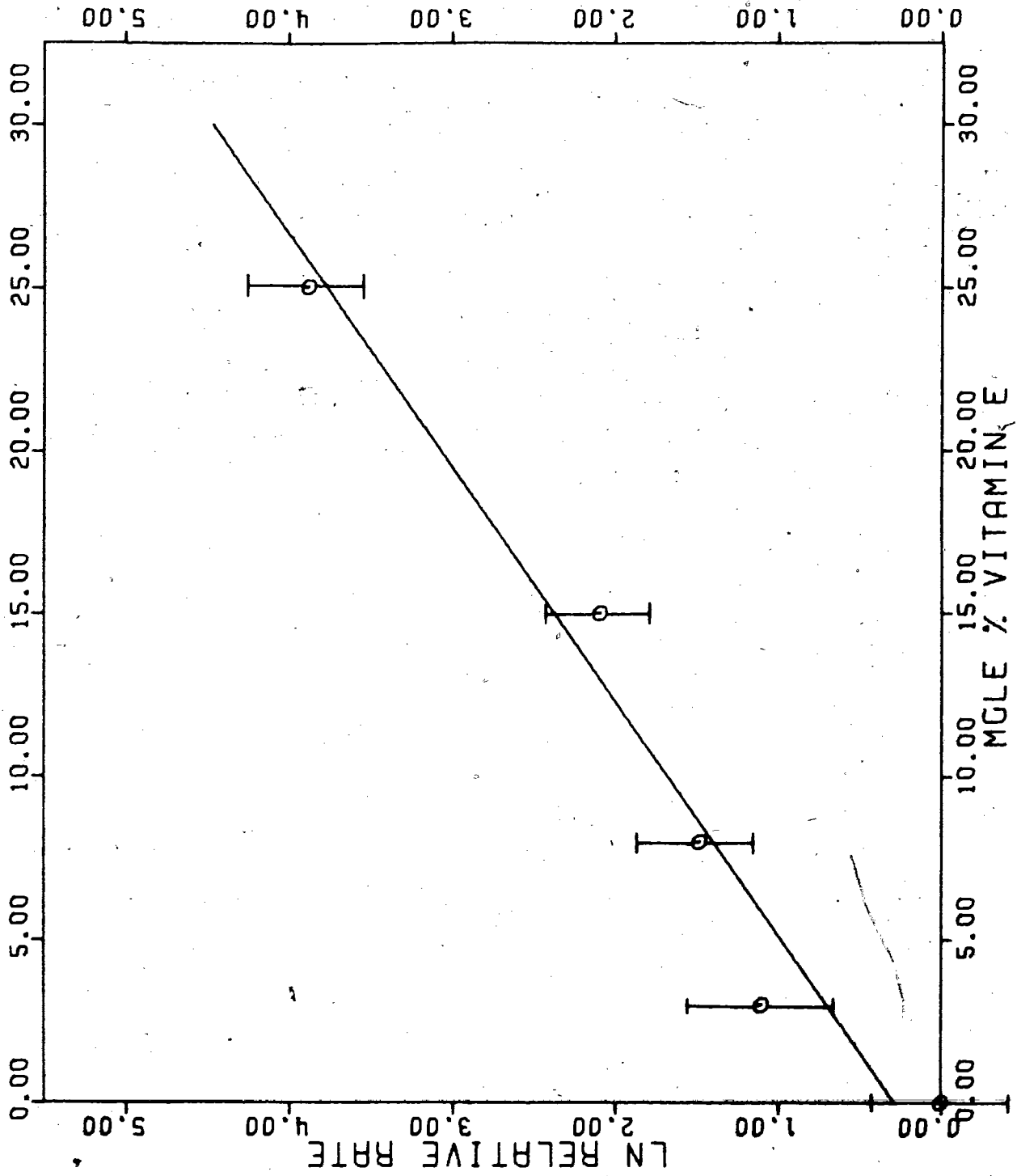
Permeation rates of  $\text{Pr}^{3+}$  into EYL vesicles containing various concentrations of incorporated Vitamin E at  $33^\circ\text{C}$

(relative to EYL = 1.00)

Mole% Vitamin E	Relative Permeability
25	47.8
15	8.1
8	4.4
3	3.0
0	1.0

110a

Figure 16. Effect of Vitamin E concentration on the permeability of 10% w/v egg yolk lecithin vesicles at 33°C.





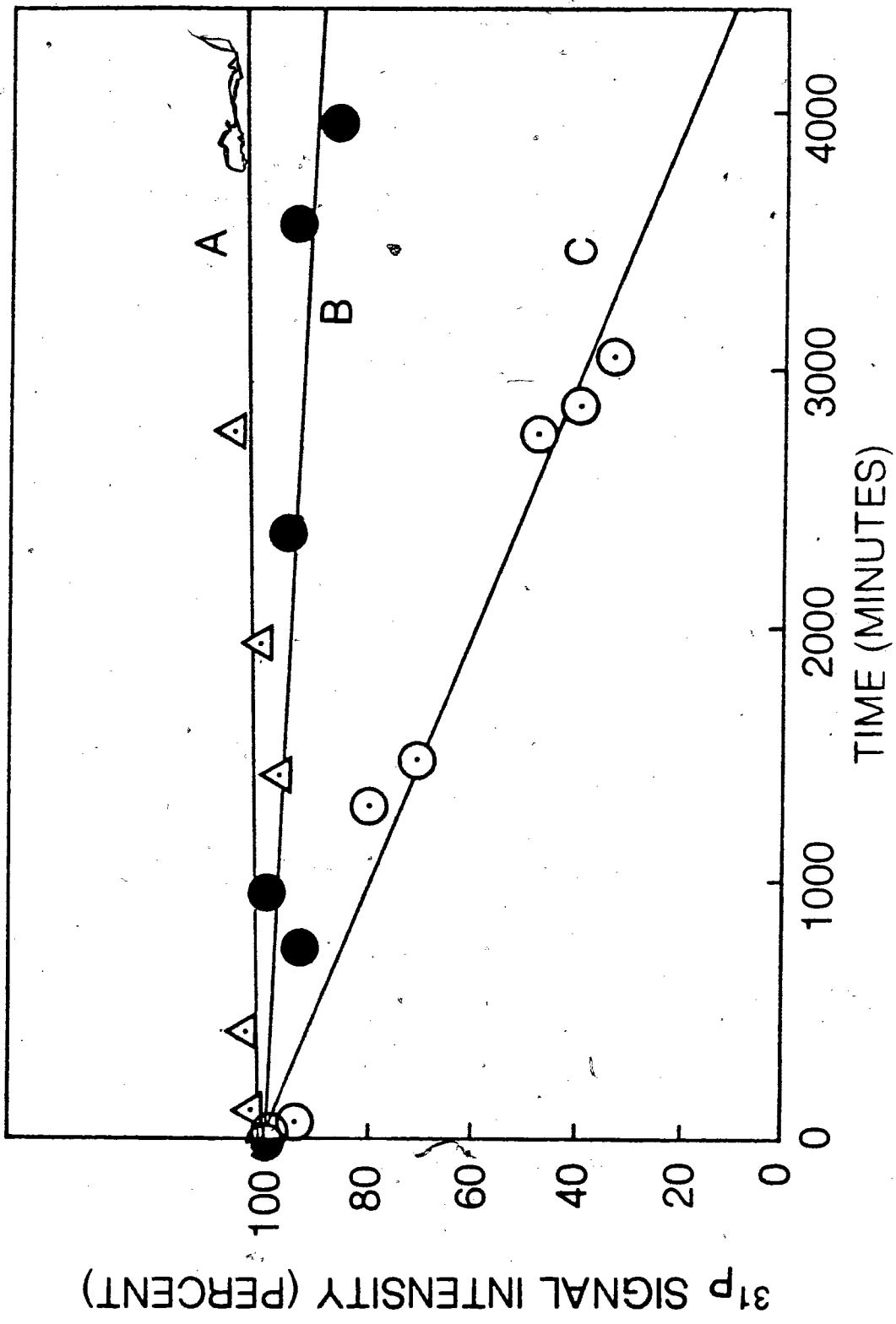
#### H. $^{31}\text{P}$ NMR Permeability Studies of EYL-Cholesterol Ester Vesicles

As discussed in Chapter 1, areas of increased cholesteryl ester content in the aorta membrane have been associated with increased permeability. Since any change in membrane permeability may have implications in atherogenesis, the effect of the incorporation of a small amount (5 mole%) of cholesteryl palmitate in EYL vesicles was investigated using the  $^{31}\text{P}$  NMR method described in Section 4G. These results, an important part of the atherosclerosis investigation, are presented first here, since they too bear on the succeeding mechanistic discussion.

When  $\text{Pr}^{3+}$  is added to preformed EYL vesicles, the rate of infusion of praseodymium across the bilayer is proportional to the rate of disappearance of the upfield  $^{31}\text{P}$  NMR signal. Least squares plots of the rate of disappearance of this peak vs time are shown in Figure 17 for EYL alone, EYL with 25 mole% incorporated cholesterol, and EYL with 5 mole% incorporated cholesteryl palmitate. From the relative slopes of the graphs, it is calculated that the effect of 5 mole% incorporated cholesteryl palmitate increases the membrane permeability by approximately 10 times.

On the other hand, the decrease in the upfield  $^{31}\text{P}$  signal intensity for EYL with 25 mole% incorporated cholesterol is exceedingly slow. This is in agreement with previous work which

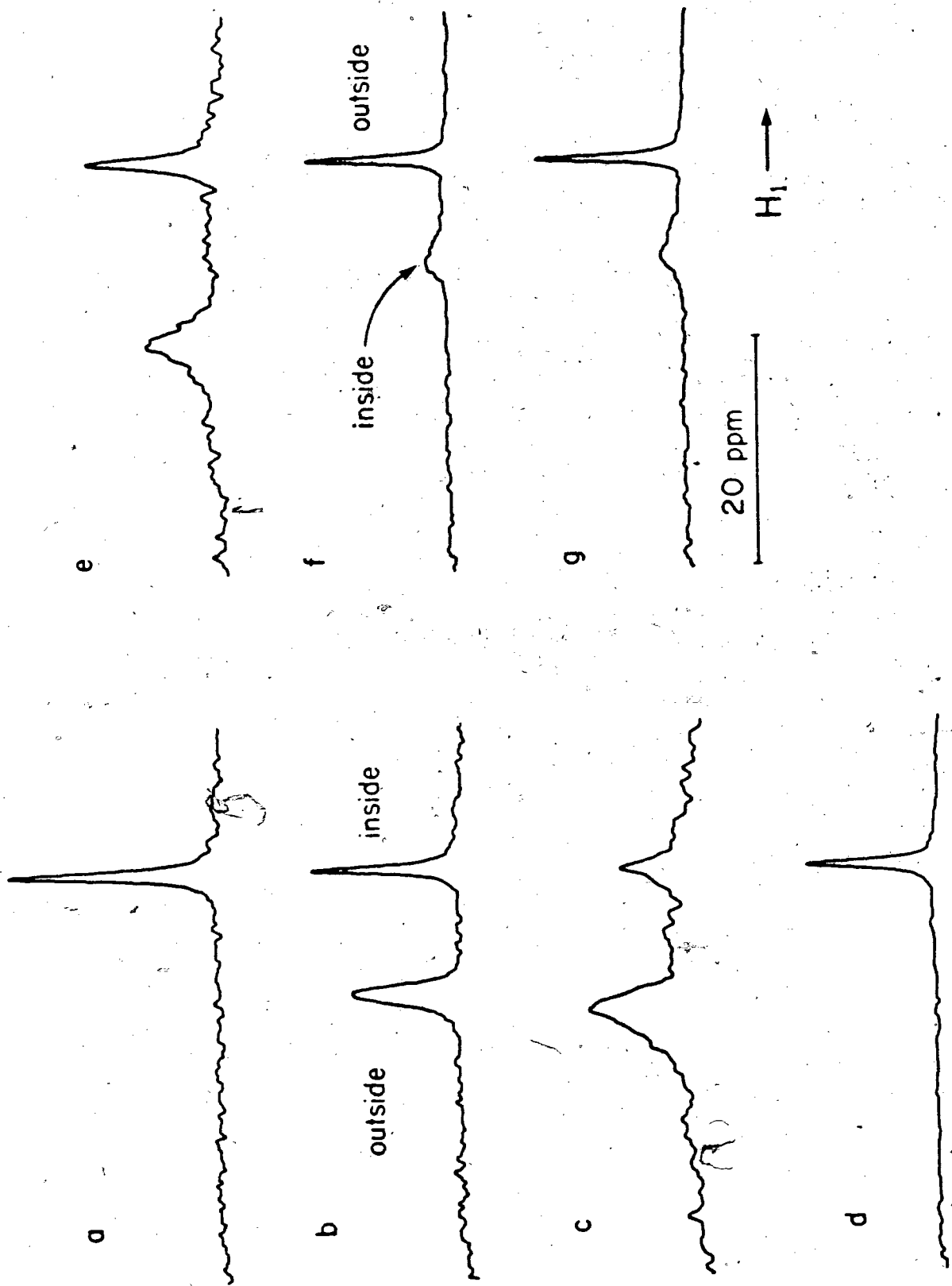
Figure 17. Relative intensity of "inside"  $^{31}\text{P}$  NMR signal (initial value = 100%) vs. time for pure and mixed vesicles containing cholesterol or cholesteryl palmitate. (A) 10% egg yolk lecithin containing 25 mole% cholesterol. (B) 10% w/v egg yolk lecithin. (C) 10% egg yolk lecithin containing 5 mole% cholesteryl palmitate.



showed that the incorporation of cholesterol decreases the permeability of lecithin vesicles to cations (99). In fact, the relative intensity of the upfield resonance of EYL-cholesterol vesicles increased by approximately 6 % in the 4000 minutes of this experiment. This is indicative only of the inherent error in measurement. Although it is clear that the incorporation of cholesterol results in a decreased permeability, the  $^{31}\text{P}$  method is not sufficiently sensitive to quantify such a slow process. However, more rapid rates of permeation such as are observed with cholesteryl palmitate incorporation involve much larger changes in relative spectral area, leading to decreased error. Linear least squares analysis of the data gave slopes of  $-20.0 \times 10^{-3} \pm 8 \times 10^{-4} \text{ %/min}$  and  $-2.0 \times 10^{-3} \pm 0.6 \times 10^{-3} \text{ %/min}$  for EYL-cholesteryl palmitate and pure EYL vesicles, respectively. Therefore, a ten fold permeability increase to  $\text{Pr}^{3+}$  is caused by the incorporation of a very small amount of cholesteryl palmitate (5 mole%). The course of the permeability study is illustrated in Figure 18. Initially, a single  $^{31}\text{P}$  resonance signal is observed (Fig. 18a). The addition of 150 ul of 0.1M  $\text{Pr}^{3+}$  results in a downfield shift of approximately 11 ppm (LIS) of the outside phosphorus nuclei which are exposed to the added lanthanide (Fig. 18b). As the paramagnetic  $\text{Pr}^{3+}$  traverses the bilayer the relative intensity of the upfield peak decreases (compare Figs. 18b and c). After the disappearance of the upfield peak, 300 ul of 0.2M EDTA was added to complex with the accessible  $\text{Pr}^{3+}$ , the spectrum underwent an immediate change. In contrast to the two peaks

Figure 18.  $^{31}\text{P}$  NMR spectra at  $33^\circ\text{C}$  of egg yolk lecithin cholesteryl palmitate vesicles

- a. 10% w/v egg yolk lecithin vesicles containing 5 mole% cholesteryl palmitate.
- b. Sample a immediately after the addition of 150  $\mu\text{l}$  of 0.1 M  $\text{Pr}^{3+}$  ; time = 0 min.
- c. Sample b after time = 3044 min.
- d. Sample c immediately after addition of 300  $\mu\text{l}$  0.2 M EDTA (Total time = 3103 min.)
- e. Sample d after the addition of 500  $\mu\text{l}$   $\text{Pr}^{3+}$  (Total time = 3119 min.)
- f. 10% w/v EYL vesicles with 0.005 M encapsulated  $\text{Pr}^{3+}$  immediately following addition of 300  $\mu\text{l}$  of EDTA.
- g. Sample f. after time = 679 min.



which were observed with the phytyl compounds, the spectrum consisted of a single sharp upfield resonance at the same chemical shift as native phospholipid (Fig.18d). This indicates that all the  $\text{Pr}^{3+}$  which was initially present was available for complexation with the added EDTA within the time required to determine the spectrum (approx. 10 min.). Subsequent addition of excess of  $\text{Pr}^{3+}$  again resulted in two  $^{31}\text{P}$  resonances, with the same relative areas as had been observed immediately following the initial addition of the shift reagent (Fig.18c). This demonstrates that the above results for permeability are not due to membrane rupture, but are instead due to changes in the permeability properties of the membrane upon incorporation of cholesteryl ester. Since the vesicles are still intact, as shown by the addition of the second aliquot of  $\text{Pr}^{3+}$  (Fig.18e), and since EDTA was able to complex with all of the initial portion of  $\text{Pr}^{3+}$  which had previously traversed the membrane, the cholesteryl ester-EYL mixed vesicles must be extremely permeable to EDTA, i.e. a half life of less than 10 minutes may be calculated.

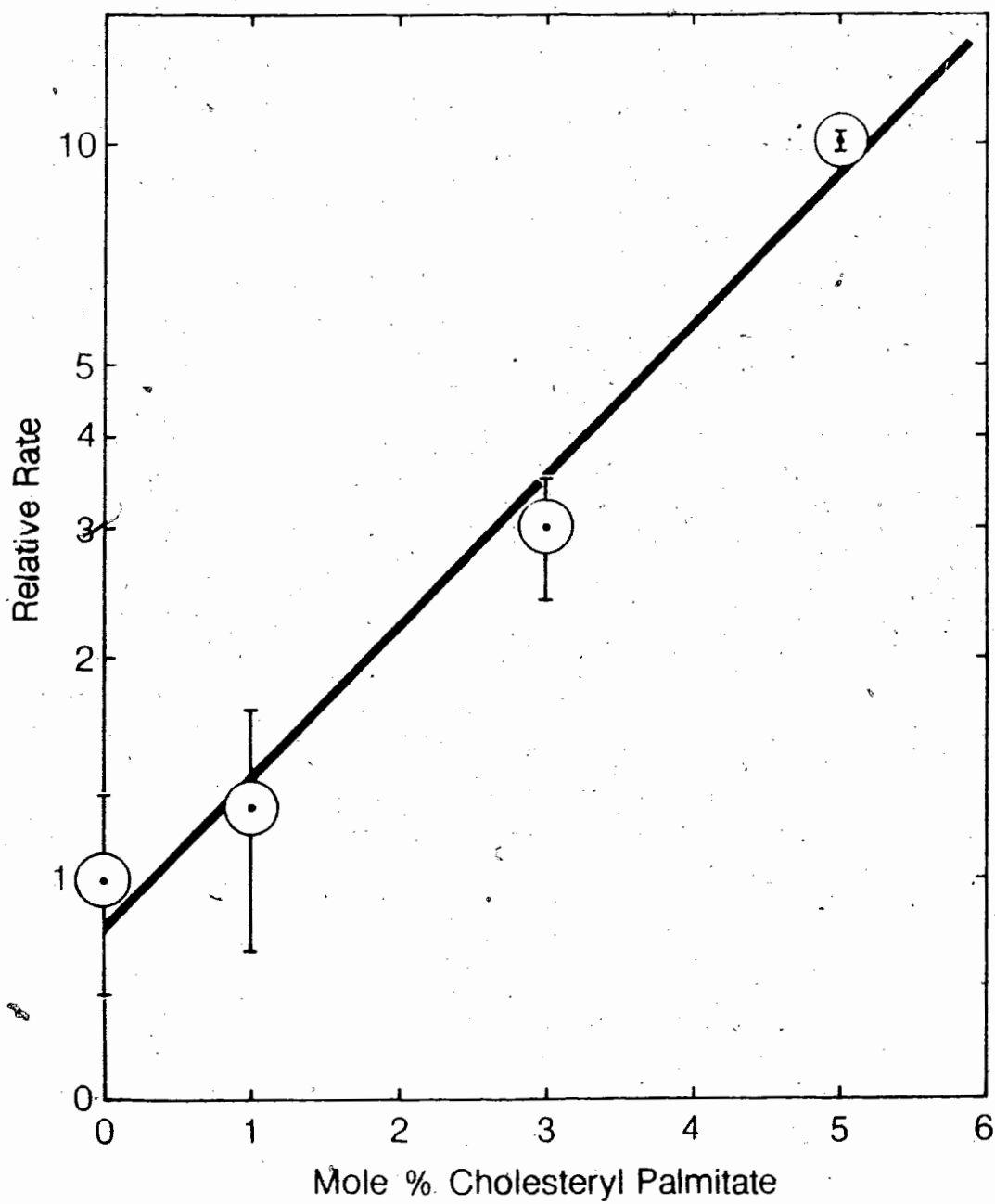
As stated in Section 4G, extremely rapid rate of permeation of EDTA was not found for mixed vesicles of phytyl compounds with EYL. Therefore, a separate experiment was performed in order to estimate the rate of infusion of EDTA into pure EYL vesicles. Vesicles were prepared with a  $\text{Pr}^{3+}$  concentration of 0.005M both inside, and outside. Subsequent addition of 300 ul of 0.2M EDTA resulted in two resonances (Fig.18f), the upfield resonance due to outside  $^{31}\text{P}$

nuclei and the downfield resonance due to inside  $^{31}\text{P}$  nuclei which are exposed to encapsulated  $\text{Pr}^{3+}$ . By following the rate of increase of the relative area of the sharp upfield resonance as EDTA enters the vesicles and subtracting the rate at which  $\text{Pr}^{3+}$  diffuses out, an approximation of the rate of EDTA influx may be made. Figure 18g shows the spectrum of the same sample 679 minutes after the addition of EDTA. The relative areas of the peaks of the spectra in Figures 18f and 18g are very similar indicating that very little change has occurred in the ionic environment of the inside or outside phosphorus nuclei during the intervening time period. Therefore pure EYL vesicles exhibit low permeability to both  $\text{Pr}^{3+}$  and EDTA. Subtracting the previously determined rate of  $\text{Pr}^{3+}$  permeation into pure EYL vesicles from the observed rate of increase of the upfield resonance for pure EYL vesicles with encapsulated  $\text{Pr}^{3+}$  yields a rate of  $5.8 \times 10^{-3} \pm 4.1 \times 10^{-3}$  %/min for EDTA penetration into pure EYL vesicles. This is in direct contrast to the extremely rapid permeation of EDTA through EYL vesicles containing 5 mole% cholesteryl palmitate (half life <10 minutes).

Proof that the increased permeability of the membrane to  $\text{Pr}^{3+}$  is due to the incorporation of cholesteryl palmitate is seen in Figure 19. Figure 19 shows the relative rate of inward diffusion of  $\text{Pr}^{3+}$  versus several concentrations of cholesteryl palmitate. The rate increases in a roughly logarithmic fashion with increases in the cholesteryl ester concentration. These results are similar to those



Figure 19. Effect of cholesteryl palmitate concentration on the permeability of egg yolk lecithin vesicles at 33°C.



obtained for the intercalation of various concentrations of Vitamin E (Section 4G). It is interesting to note that while the incorporation of 5 mole% cholesteryl palmitate increases the permeability of EYL vesicles approximately ten fold, the same increase would require the incorporation of approximately 15 mole% Vitamin E.

A further set of experiments were carried out with the unsaturated cholesteryl ester, cholesteryl linoleate, in order to determine the effect of the nature of the fatty acid chain on membrane permeability. To within experimental error, there was no increase in permeability up to 5 mole% cholesteryl linoleate incorporation. The dissimilar influence on  $\text{Pr}^{3+}$  inward diffusion can be explained by examining the structure of each ester at  $33^{\circ}\text{C}$ . At  $33^{\circ}\text{C}$ , the temperature of the NMR experiment, cholesteryl palmitate is in a solid crystalline phase, whereas cholesteryl linoleate exists in either a smectic or cholesteric liquid crystal phase (173). It appears that the thermodynamic stability of the different phases of cholesteryl esters may be of importance in biological systems (174). Whether the differential effects of the saturated and unsaturated esters are due to segregation of the cholesteric phase of the linoleate (See Section 5C), or whether it is simply a function of increased flexibility of the unsaturated ester is not known. This question may be answered in part by an interacting spin label study employing nitroxide labeled esters in their cholesteric phase.

In summary, the incorporation of small amounts of cholesteryl palmitate in the solid state increases membrane permeability, while esters in a more fluid state do not. It is known that cholesterol:lecithin dispersions with a cholesterol:lecithin ratio of greater than 1:1 stimulate intracellular formation of cholesterol esters, possibly to divert excess crystalline cholesterol into a more fluid liquid crystal form (174). Therefore, in addition to the importance of the free cholesterol/cholesteryl ester ratio (Section 1C); the properties of the aortic membrane will be influenced by the relative amounts of saturated and unsaturated esters which are present during the initial stages of atherosclerosis.

#### I. Mechanism of Vesicle Permeability

Several possible mechanisms exist for the transfer of ions from the bulk phase, across the bilayer to the inside of phospholipid vesicles. These include mechanisms involving vesicle fusion, carrier mediated transport, and simple passive self diffusion through transient pores in the membrane.

During fusion of DPL-phosphatidylserine vesicles it had been suggested that these structures are temporarily open, allowing for an influx of external contents into the vesicle interior (175). However, vesicle fusion in that study was subsequently found to be due to an unidentified impurity in the phosphatidylserine (175). Fusion has been

found not to be an important process in the case of pure EYL vesicles. As well, studies of transverse and lateral diffusion rates, and measurement of transmembrane potentials (65,66,69,72,176) have taken advantage of the fact that the process of fusion is negligible, both for phospholipid vesicles, and vesicles prepared from biological membranes.

The operation of a fusion mechanism would result in an increase in vesicle size. An estimate of the diameter of the vesicles may be made from the ratio of the intensities of the outside to inside  $^{31}\text{P}$  resonances in the presence of shift reagent (28,177), and in these studies, no increase of vesicle size is detected. In addition, after the disappearance of the upfield peak due to permeation of the added lanthanide, in favourable cases, the relative areas of the inside and outside phosphorus resonance signals may be redetermined following the addition of EDTA. The relative intensities of the inside and outside phosphorus resonances before and after the  $\text{Pr}^{3+}$  permeation are presented in Table XVII. In the case of cholesteryl palmitate-EYL mixed vesicles, the post experimental value was determined after the addition of a second aliquot of  $\text{Pr}^{3+}$  because of the rapid rate of permeation of EDTA which results in a single upfield resonance. Post experimental values for pure EYL, EYL with incorporated cholesterol, and EYL with incorporated palmitic acid are unavailable due to the extremely slow rate of  $\text{Pr}^{3+}$  permeation.

Table XVII

NMR signal intensity of inward facing  $^{31}\text{P}$  nuclei.

Membrane	Intensity (% total)	
	Initial	Post $\text{Pr}^{3+}$ permeation.
EYL	42	a
EYL + 25 mole% phytol	41	39
EYL + 25 mole% Vitamin E	37	39
EYL + 5 mole% cholesteryl palmitate	37	37
EYL + 25 mole % palmitic acid	40	a
EYL + 25 mole % cholesterol	45	a

a Measurement not possible due to extremely slow rate of permeation of  $\text{Pr}^{3+}$

Assuming a bilayer thickness of  $50\text{\AA}$ , an equal packing density of phospholipid on the inside and outside layers, and a homogeneous distribution of the added nonphospholipid membrane components, simple calculations indicate that these vesicles are less than  $500\text{\AA}$  in diameter. In actual fact tighter packing may exist on the inside of the bilayer (28), resulting in an overestimation of the true vesicle size. Thus, the value of  $500\text{\AA}$  serves as an upper limit of the vesicle diameter.

In addition, the narrow  $^{31}\text{P}$  lineshape is indicative of small vesicles undergoing rapid isotropic tumbling. Since there is large chemical shift anisotropy contribution to the linewidth of larger liposomes (76-81) due to the slower reorientation of these larger particles,  $^{31}\text{P}$  resonances arising from phosphorus nuclei in such a state would be broadened into the spectral baseline. Thus possible complications due to initial size inhomogeneity is avoided.

Thirdly, the similarity of the ratio of inside and outside phosphorus resonances before and after the permeability studies indicate that little change has occurred in vesicle size during the course of the experiments. If significant fusion had occurred, the ratio of outside and inside would tend towards unity. If "leaky" fusion was the mechanism whereby  $\text{Pr}^{3+}$  enters the vesicles this fusion process would occur at an extremely rapid rate, especially in the case of EYL-phytanic acid mixed vesicles. ( $t_{1/2}$  for  $\text{Pr}^{3+}$

permeation ~3 minutes). Rapid fusion would result in a great increase in particle size in a short time period. Such a size change might be expected to manifest itself as increased linewidth with time in  $^{13}\text{C}$  NMR spectra caused by a slower tumbling rate of very large vesicles. However no differences were observed in the linewidths of resonances in the  $^{13}\text{C}$  spectra of phytanic acid-EYL vesicles over a period of approximately 30 hours. Therefore, the possibility of a fusion type of mechanism is extremely remote.

Elimination of the possibilities of vesicle rupture (see Sections 4G and 4H) and vesicle fusion show that the observed disappearance of the upfield  $^{31}\text{P}$  resonance signal with time after the addition of  $\text{Pr}^{3+}$  is due to a traversal of the membrane by this cation.

The suggestion has been made that the formation of an ion-lipid complex, followed by transverse diffusion (flip-flop) of the complex to the opposite side of the bilayer may be responsible for ion flux across phospholipid membranes (65,178). Unfortunately, it is not possible to directly monitor the flip-flop of an ion-lipid complex, and therefore, such a mechanism has, as yet, no direct proof. It is only possible to compare rates and activation energies of transverse diffusion with rates and activation energies of ion permeation. Since rate of inside-outside transition of spin labeled lecithin in EYL bilayers is of the order of  $24 \text{ hr}^{-1}$ , the rate for unlabeled lecithin may be much slower due to the greater polarity of native phospholipid.



Other membrane components may undergo much more rapid inside-outside transitions.  $^{14}\text{C}$ -labeled stearate exchanges between two ~~stearate~~ stearate monolayers with a half life of 25 minutes at  $25^{\circ}\text{C}$  (179). However, this system does not offer a very satisfactory comparison with phospholipid bilayers because of large differences in nature of the ionic interactions of the hydrophilic region.

It may be merely coincidental that the activation energy for  $\text{Pr}^{3+}$  permeation of lecithin-phytol mixed bilayers ( $20.3 \pm 0.2$  kcal) is in such good agreement with that of phospholipid "flip-flop" (19.3 kcal) as measured by Kornberg and McConnell (65), since the spin labeled phospholipid used in that study is less polar than EYL and therefore may give rise to an artificially lowered activation energy. However, the perturbation of the bilayer by intercalated phytol may also result in a lessened activation energy for phospholipid transmigration, and thus a carrier mechanism may not be necessarily excluded.

The third, and most probable mechanism involves passive self-diffusion across the bilayer. This mechanism involves a translocation of an ion from a medium of high dielectric constant (external bulk solution) to a medium of low dielectric constant (bilayer membrane interior). Such a process would be unfavourable for charged species in general, and may account for the high activation

energy (approx. 20 kcal/mole) observed with the lectihin-phytol system.

The entry of the ion into the membrane interior may occur through transient pores caused by thermal motion of the bilayer, for example, lateral diffusion parallel to the membrane surface. Migration of a phospholipid through an interstitial site in the plane of the membrane would force together phospholipids in its path, leaving a transient lattice vacancy (110). As discussed in Section 4F there are indications of a lateral expansion of the bilayer upon incorporation of the branched chain phytol compounds. Such an expansion of the bilayer should decrease the ionic attraction of the negatively charged phosphate moiety of one lecithin molecule for the trimethylammonium group of an adjacent phospholipid and may lead to an increase in transient pore formation and an increase in lateral diffusion rates. It has been demonstrated by Cullis (36), that the intercalation of 30 mole% cholesterol decreases the lateral diffusion rate of EYL above the gel-liquid crystalline transition temperature by approximately 50%, as well as decreasing membrane permeability to  $\text{Na}^+$ ,  $\text{Cl}^-$ , and glucose (99). Thus, the permeability, fluidity and rates of lateral diffusion of membrane components appear to be interrelated. In any case, increased fluidity of the bilayer should lead to increased permeability, the increase in fluidity being caused by the intercalation of compounds such as cholesteryl palmitate, phytol, phytanic acid or Vitamin E. Indeed, the membrane permeability

increases with increasing Vitamin E concentration over the range of 3 to 25 mole%. Membrane fluidity should also increase with increasing Vitamin E concentration.

It has been suggested that the incorporation, in the membrane, of certain molecules whose polarity or polarizability is greater than that of the lipid could stabilize an ion in the lipid phase to a greater extent than water molecules (180). It might be assumed that any slightly polar molecules with a higher solubility in lipid than a hydrated ion would increase the permeability of such ions. If the polarity of the interjacent molecules used in this study was the major contributing factor in the increase of ion permeability, it would be expected that similar increases in permeability would be observed for the intercalation of palmitic acid and phytanic acid. Obviously this is not the case. The permeability of EYL vesicles is unchanged in the presence of 25 mole% palmitic acid but increased approximately 3000 fold in the presence of 25 mole% phytanic acid. Therefore the major contributing factor to the permeability increases is steric in nature, i.e. a function of molecular packing in the mixed bilayer systems (see Section 4F).

As discussed previously, deviations from normal lipid packing caused by the intercalation of the phytol compounds should result in an expansion of the bilayer and an increased average separation of lecithin molecules. This decrease in packing density is manifested in

an increased membrane permeability, likely through a mechanism of simple passive diffusion. However, the possibility of a contribution to the observed rate of a flip-flop carrier mechanism cannot be entirely excluded since a lateral expansion of the bilayer should result in decreased steric hindrance to lipid transmembrane migration.

## CHAPTER 5

## RESULTS AND DISCUSSION: PART II

## CHOLESTERYL ESTERS AND ATHEROSCLEROSIS

## A. ESR of Oriented Lipid Multiplayers

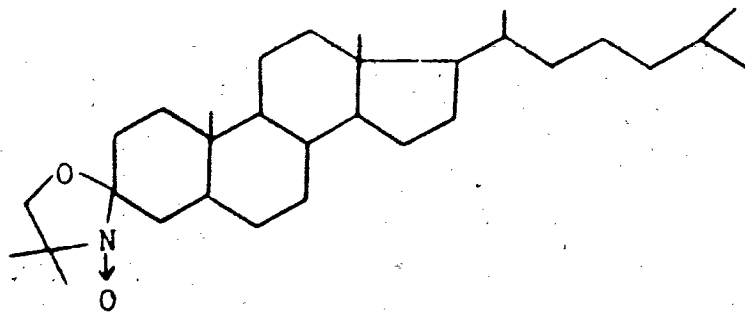
## 1. Orientation of cholesteryl esters in phospholipid multilayers

Oriented lipid multilayers were prepared as described in Section 2.B.3. The structures of the spin probes used - cholestane, I, 5-doxylpalmitic acid, II, 16 doxylstearic acid, III, and IV, and V, the corresponding cholesteryl esters of II, and III, respectively, are shown in Figure 20. The values of the hyperfine splitting constants for these labels incorporated into EYL multilayers are given in Table XVIII, where  $T_{||}$  and  $T_{\perp}$  are defined by the orientation of the sample such that the normal to the flat cell surface is parallel, and perpendicular, respectively, with respect to the direction of the applied magnetic field, i.e. parallel and perpendicular, respectively, to the known direction of the  $2p\pi$  orbitals of the fatty acid nitroxides. The order parameter,  $S$ , was calculated from these hyperfine splittings using equation III-66 in the case of the fatty acid probes whose nitroxide  $2p\pi$  orbital is parallel to the long molecular axis, and using equation III-67, in the case of the cholestane spin probe whose  $2p\pi$  orbital is perpendicular to the long molecular axis. The fatty acyl chains of the labeled esters were

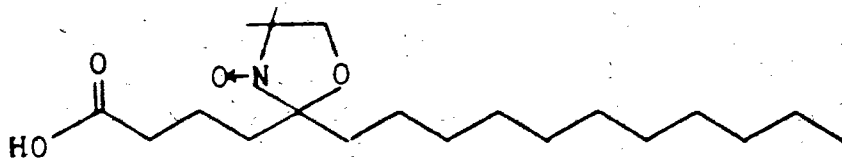
Figure 20. The structure of various nitroxide spin probes.

I, 3-doxylcholestane; II, 5-doxylpalmitic acid; III, 16-doxylstearic acid;

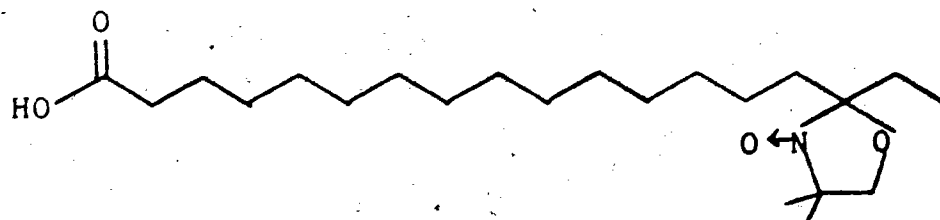
IV, the cholesteryl ester of II; V. the cholesteryl ester of III.



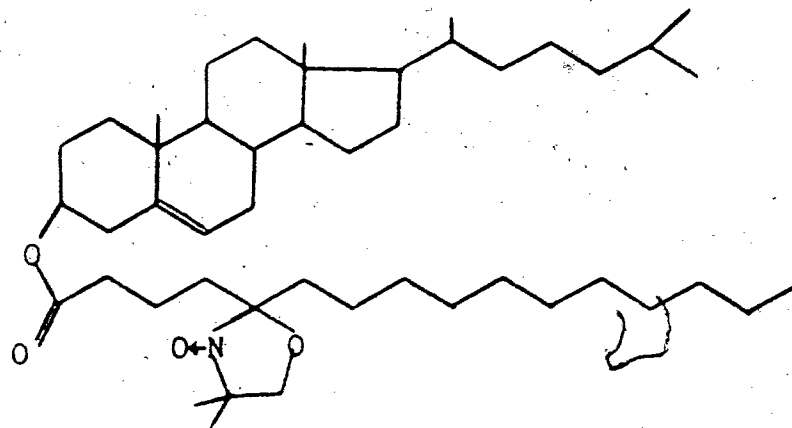
I



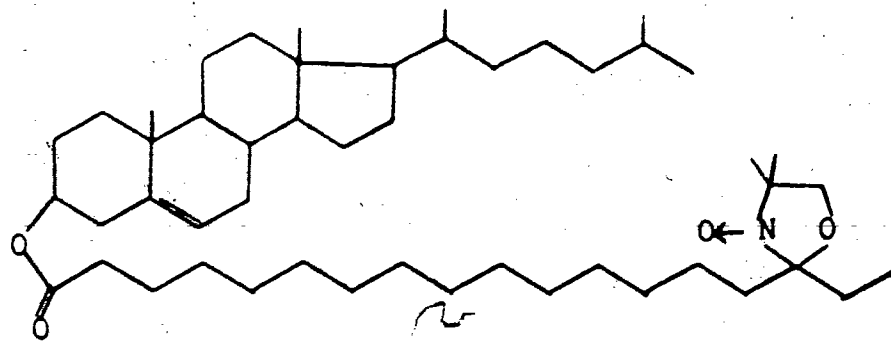
II



III



IV



V

assumed initially to have the same orientation as the free acid labels. As well, the principle values of the hyperfine splitting tensor of the esters were assumed to correspond to those of the acids, i.e.  $T_{xx} \approx T_{yy} \approx 6$  gauss, and  $T_{zz} \approx 32$  gauss (60) for both of the esters and the acids. The order parameters for the two spin labeled acids, and for cholestane (Table XVIII) are in agreement with the literature values (51, 54, 60, 111, 135, 181, 182). Note that the order parameter for the cholestane spin probe is quite high, since the nitroxide is situated near the membrane surface. It should also be noted that the order parameter of the 5-doxylpalmitic acid is much larger than that of the 16-doxylstearic acid. Once again, this behaviour is characteristic of the fluidity gradient which exists along the fatty acid chains of the membrane interior (see Fig. 21).

The hyperfine splittings and order parameters for the two esters, IV, and V incorporated into lecithin multilayers are given in Table XVIII. For the 16-doxylstearate ester, V, a low positive order parameter is calculated, similar to that for the corresponding acid, III, indicative of the fact that the nitroxide  $2p\pi$  orbital is preferentially oriented perpendicular to the multilayer surface, and that it is undergoing rapid motion which tends to average the components of the hyperfine splitting tensor. Such observations are consistent with the doxyl group for both III, and V occupying a position near the fluid central region of the bilayer. This interpretation is substantiated by the results of ascorbate reduction experiments which are discussed later in this section.



Table XVIII

Spectral parameters of spin labels I-V in lecithin multilayers at 23°C.

Lecithin	Spin Probe	$T_{\parallel}^a$	$T_{\perp}$	$S^b$
EYL	I	8.7	17.4	$0.68 \pm .03$
	II	24.8	10.4	$0.54 \pm .04$
	III	15.2	13.8	$0.055 \pm .004$
	IV	14.4	15.7	$-0.049 \pm .004$
	V	15.2	14.4	$0.029 \pm .007$
DPL <sup>c</sup>	I	7.0	16.8	$0.82 \pm .004$
	II	18.0	11.0	$0.30 \pm .03$
	III	17.4	12.5	$0.20 \pm .02$
	IV	13.0	16.0	$-0.113 \pm .015$
	V	14.5	14.2	$0.012 \pm .003$

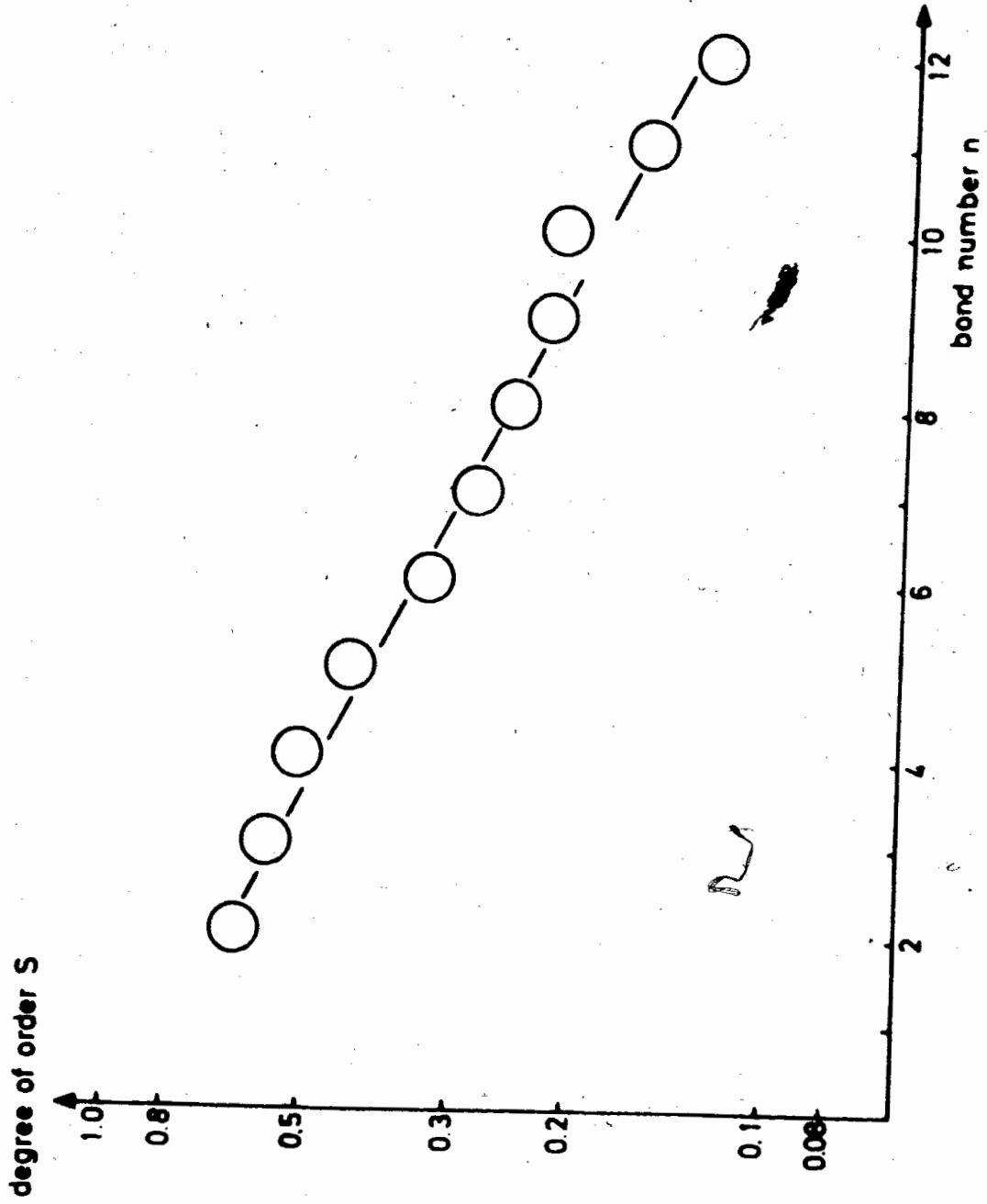
<sup>a</sup> The values of the hyperfine splittings are in gauss.

<sup>b</sup> The order parameter,  $S$ , was calculated for a number of samples. The error indicated reflects the variation in the individual determinations.

<sup>c</sup> DPL multilayers were prehydrated with 0.15 M NaCl for at least 60 minutes prior to recording the spectra.

132a

Figure 21. Positional dependence of the order parameter in a lipid bilayer as detected by fatty acid spin probes using Equation III-66. Taken from reference 131.



The 5-doxylpalmitate ester, IV, however, exhibits a low and negative order parameter since  $T_{\perp} > T_{\parallel}$ . The corresponding acid, II, was found to have a large positive order parameter of 0.54. These results indicate that the nitroxide  $2p\pi$  orbital of the ester, IV, is oriented differently from the corresponding acid, II, i.e. the sign of the order parameter as calculated from Equation III-58 changes if the orbital is oriented such that it makes an angle of slightly greater than  $45^{\circ}$  with the bilayer normal. Thus the orientation of the nitroxide of the 5-doxylpalmitate ester more closely resembles that of cholestane, I, than the corresponding acid, II.

Other evidence which bears upon the orientation and mobility of IV is that the peak to peak linewidth of the low field resonance is approximately 8 gauss, as compared with a linewidth of approximately 2 gauss for the 16-doxylstearate ester. Such broadening may be indicative either of slower motional reorientation of the spin probe or a superposition of resonances due to different orientations within the membrane. Indeed, IV has been shown to exhibit complex behaviour with doublet low and high field resonances for sample orientations between  $0$  and  $90^{\circ}$  with respect to the magnetic field (183). A complete analysis of these spectra requires computer simulation of the experimental spectra in order to separate the effects of order and motion. Such spectral complexity is unique to IV, and has not been observed for the 16-doxylstearate ester incorporated into phospholipid multilayers (183).

Ascorbate reduction experiments which are discussed later in this section indicate that the doxyl group of IV is situated nearer to the bilayer surface than that of V.

The effect of cholesterol on the order parameter of IV, and V was also studied, and the results are shown in Figures 22 and 23. The effect of cholesterol incorporation into the bilayer over the range of 0-40 mole% of the total lipid increases the order parameter of V from a value of 0.029 to a value of 0.26, with the greatest increase between 30 and 40 mole% added cholesterol, consistent with the known condensing effect of cholesterol on the hydrophobic region of phospholipid membranes. The order parameter of IV changed from -0.049 in the absence of cholesterol to -0.13 in the presence of 49.5% cholesterol i.e. the incorporation of cholesterol increases the absolute value of the order parameter, but its sign remains negative, indicative of an orientation of the  $2p\pi$  orbital at an angle of less than  $45^\circ$  with the bilayer surface.

The effect of added cholesteryl palmitate on the order parameter of the cholestane spin label, I, was also investigated. The results, which are shown in Figure 24, reveal a slight decrease in the order parameter upon incorporation of cholesteryl palmitate, with an abrupt break at approximately 5 mole% cholesteryl palmitate. In light of the results described in Section 5B, and that of previous workers (184-186), it is probable that ester present in excess of 5 mole%

Figure 22. Interactions between cholesteryl-5-doxylpalmitate, cholesterol and egg yolk lecithin at 23°C. Multilayers containing 1 mole% IV in egg yolk lecithin and specified concentrations of cholesterol were treated with  $10^{-2}$  M ascorbate. First half life (solid line) and order parameter (dashed line) are plotted against cholesterol concentration.

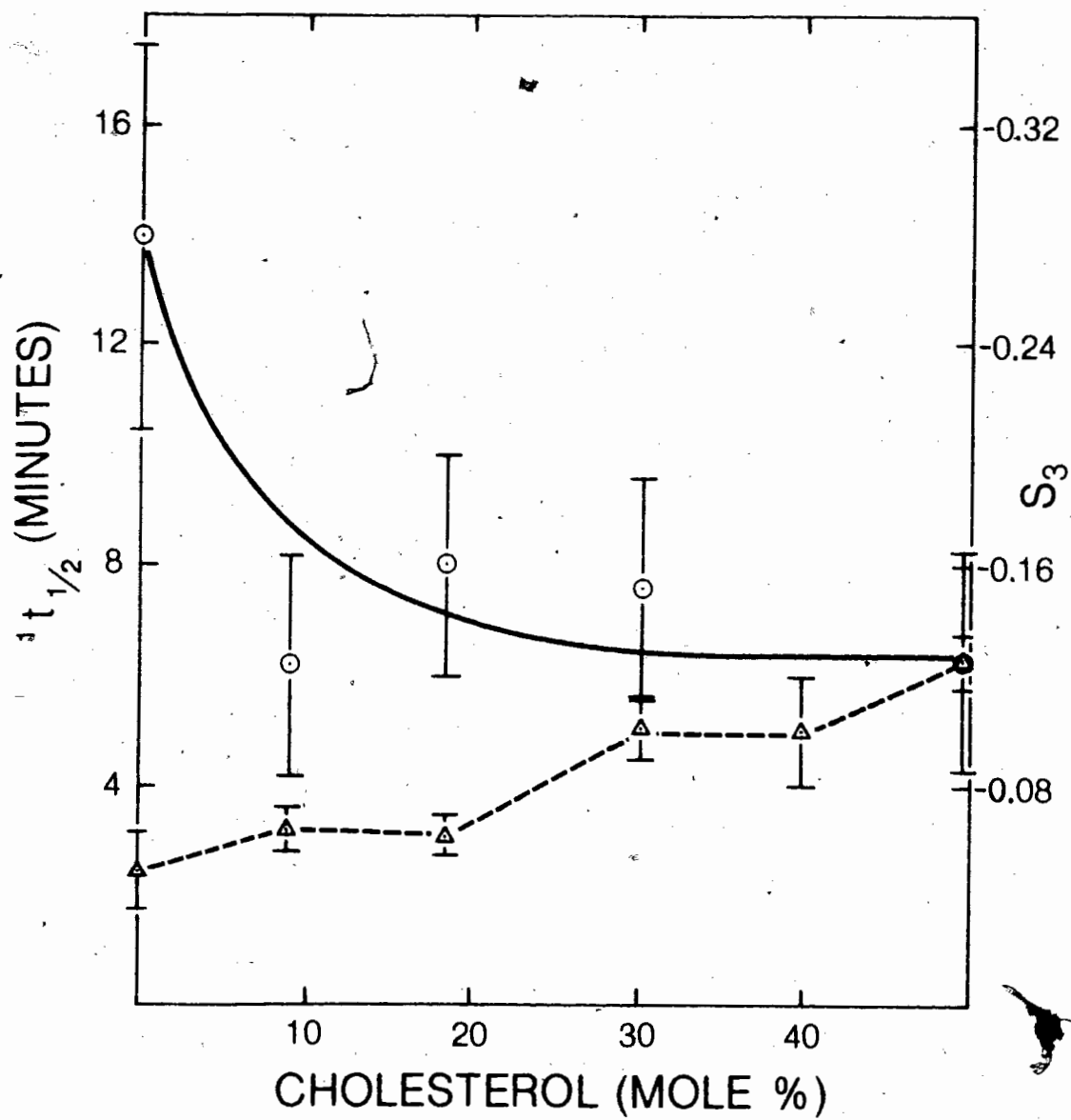


Figure 23. Interactions between cholesteryl-16-doxyLstearate, cholesterol and egg yolk lecithin at 23°C. Multilayers containing 1 mole% V in egg yolk lecithin and specified concentrations of cholesterol were treated with  $10^{-2}$  M ascorbate. First half life (solid line) and order parameter (dashed line) are plotted against cholesterol concentration.



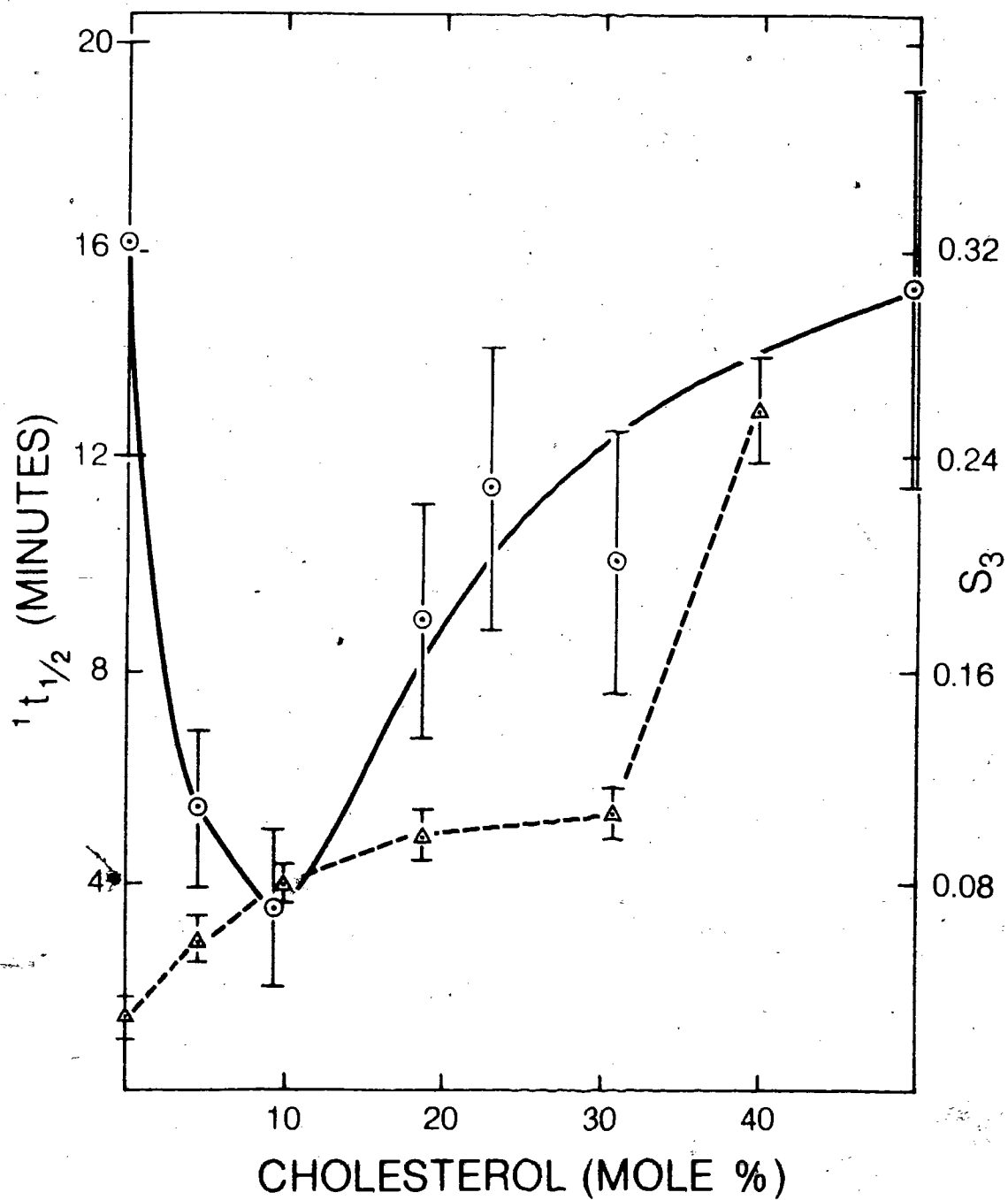
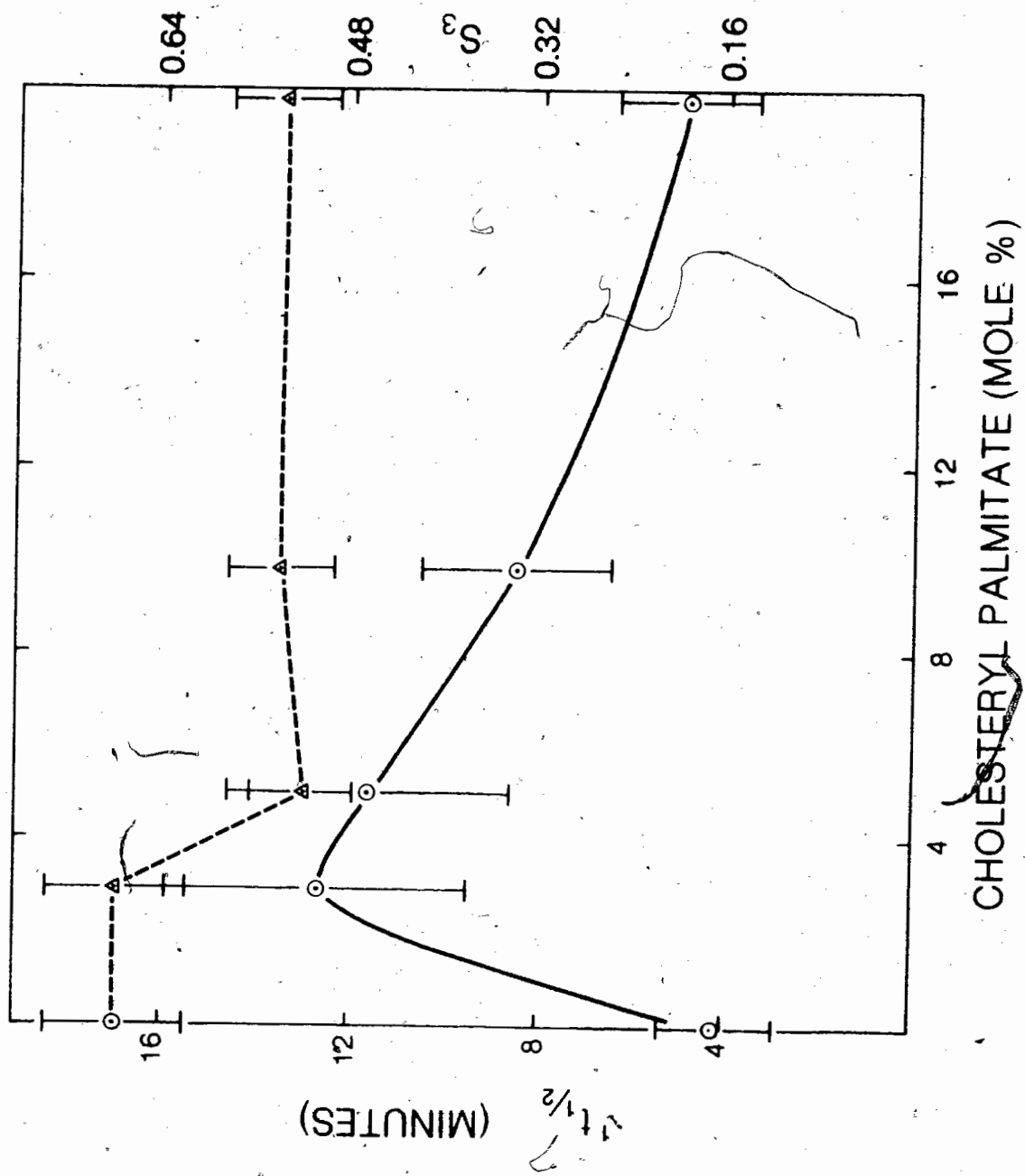


Figure 24. Interactions between 3-doxylcholestane, cholesteryl palmitate and egg yolk lecithin at 23°C. Egg yolk lecithin multilayers containing 1 mole% 3-doxylcholestane, and specified concentrations of cholesteryl palmitate were treated with  $10^{-2}$  M ascorbate. First half life (solid line) and order parameter (dashed line) are plotted against cholesteryl palmitate concentration.



forms a separate phase which does not interact strongly with the lecithin lamellar phase. However, the incorporation of up to 5 mole% cholesteryl palmitate decreases the order parameter of I, consistent an increase in membrane motional freedom and permeability as discussed in Section 5.A.3.

Sodium ascorbate rapidly reduces nitroxide spin labels to the corresponding hydroxylamine with concomitant loss of ESR signal intensity. This property has been utilized by Schreier-Muccillo et al (73) to follow the rate of ascorbate permeation into oriented lipid multilayers containing various spin probes, and as a spectroscopic ruler to determine the depths at which the labeled sites lie beneath the membrane surface (73).

In the present investigation it was found that the rate of disappearance of the low field component of the nitroxide ESR spectrum did not follow first order kinetics but rather the quadratic

$$\ln(\text{peak height}) = a - bt + ct^2 \quad \text{V-1}$$

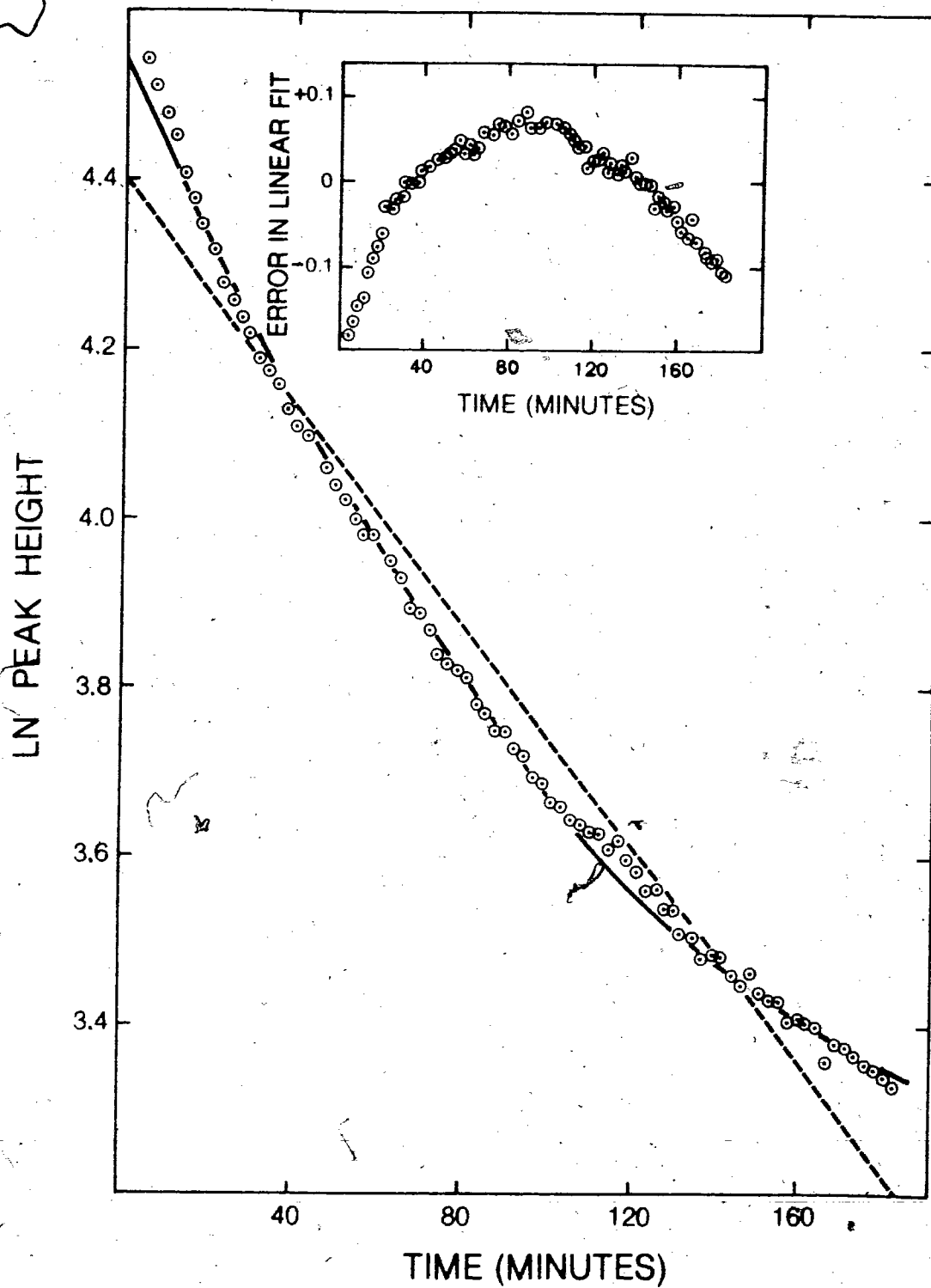
was both necessary and sufficient to describe the data. The inadequacy of a simple first order treatment is demonstrated in Figure 25 where the dotted line describes a linear fit of  $\ln(\text{peak height})$  vs time, and the solid line is a least squares computer fit of the data to Equation V-1. The insert in Figure 25 more clearly depicts the systematic error in the linear treatment. Therefore, it is obvious that the half life of ascorbate reduction in this approximation

Figure 25. Ascorbate induced ESR signal decay vs. time.

Egg yolk lecithin multilayers containing 1 mole% 16-doxyl-stearic acid were treated with  $10^{-3}$  M ascorbate.

Least square fits, linear (straight line) and quadratic (curved line) were computed for  $\ln(\text{peak height})$  vs. time.

The insert shows the systematic error of the linear fit (computed value - observed value) vs. time.



depends upon the initial time lag between ascorbate addition and the recording of the first spectrum as well as upon the total length of time for which data are acquired. Therefore, the experimental data was fitted to the quadratic shown in Equation V-1, and the rate described by the first half life,  $t_{1/2}$ , of the decay of the ESR signal intensity which is given by

$$\ln 2 - b(t_{1/2}) + c(t_{1/2})^2 = 0 \quad \text{V-2}$$

where  $t_{1/2}$  is the time required for the spectral amplitude to decay to 50% of its extrapolated zero time value.

Kornberg and McConnell (65) have previously described the rate of ascorbate reduction of the nitroxide moiety of headgroup labeled lecithin. They observed that the rate of signal decay initially followed first order kinetics, but that deviation from this behaviour occurred at large time due to reoxidation of the nitroxide. It is highly unlikely that the deviation from linearity of Figure 25 is due to reoxidation of the nitroxide since unlike the previous study (65) which used EYL vesicles up to 2 days old, the use in the present investigation of saturated dipalmitoyl lecithin (DPL), for which reoxidation by oxidized lipid is not possible, resulted in deviations from linearity similar to that shown by Figure 25. In addition, all reductions were carried out with freshly prepared, thoroughly deoxygenated ascorbate solutions. Therefore, the deviation from linearity must be a consequence of the mechanism of ascorbate permeation.

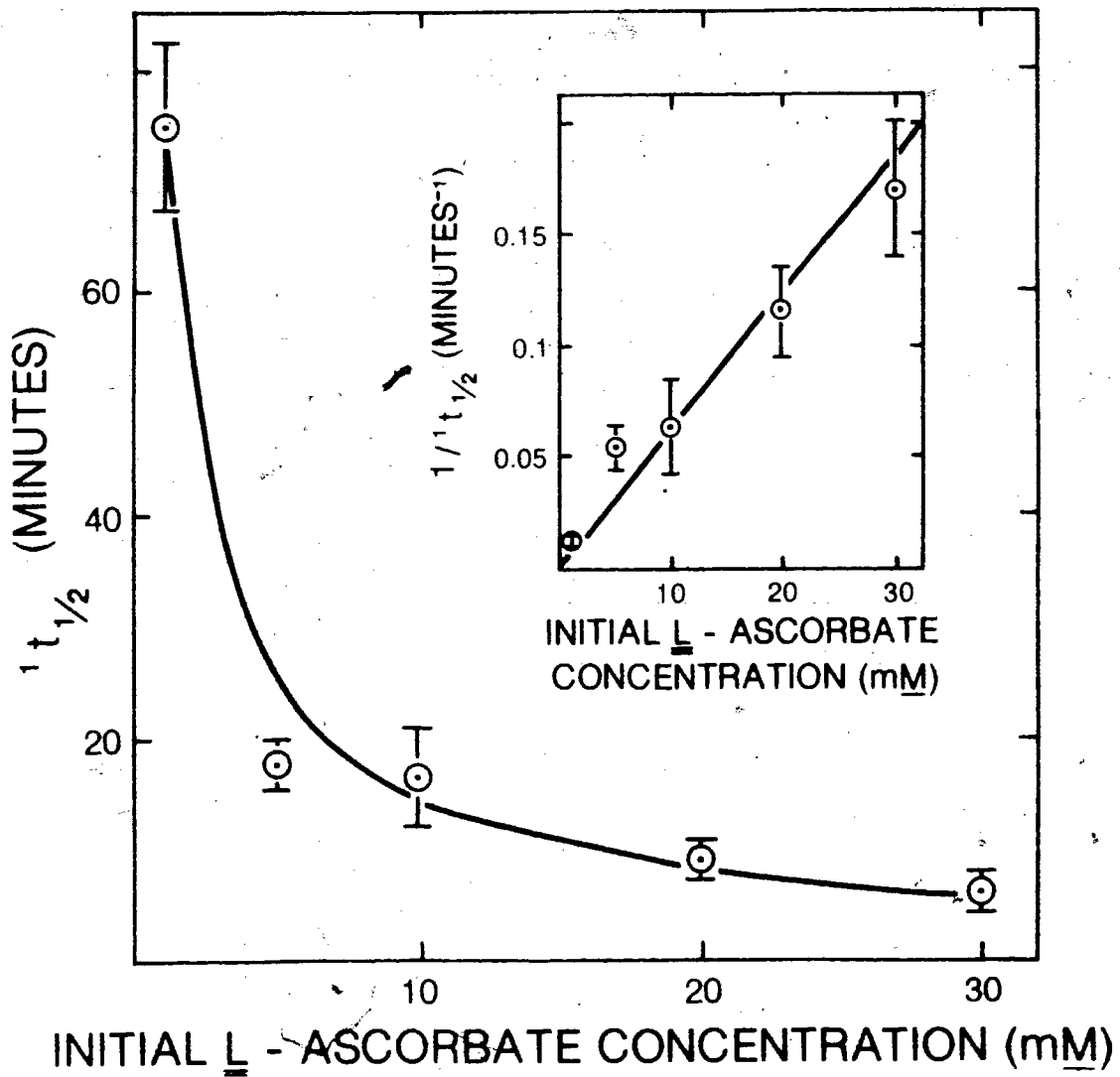
The mechanism of ascorbate permeation was further investigated using the fatty acid probe, III. The variation of the first half life on the initial ascorbate concentration for reduction of III incorporated into EYL multilayers is shown in Figure 26. The spin label concentration was held constant at 1 mole%. The inverse of the first half life increases in a roughly linear fashion with increasing ascorbate concentration over the range of  $1 \times 10^{-2}$  to  $3 \times 10^{-2}$  M. That the half life is dependent on the inverse of the initial ascorbate concentration is in agreement with the prediction of Schreier-Muccillo et al (73). However the permeation model proposed by these workers also predicts a dependence of the reduction rate on the fractional area of the bilayer occupied by the nitroxide, and thus on the initial spin label concentration, according to the relationship

$$dh/dt = -\Phi N F_{asc} \times f_{SL}^{\circ} h \quad \text{V-3}$$

where  $\Phi$  is the flux of ascorbate to the spin label in mole  $\text{cm}^{-2}\text{sec}^{-1}$ ,  $N$  is Avogadro's number,  $F_{asc}$  is the molecular area of the ascorbate ion,  $f_{SL}^{\circ}$  is the initial fractional area occupied by the spin label in the plane of the bilayer, and  $h$  is the height of the ESR resonance. The first term in Equation V-3,  $\Phi N F_{asc}$ , is the fractional area in the plane of the bilayer swept out by the ascorbate per second. Therefore, Equation V-3 states that the rate of decay of the ESR line height is proportional to the product of the fractional area occupied by the ascorbate ions, and the fractional area occupied by the spin label i.e. to the probability of a collision resulting in the chemical reaction.



Figure 26. Effect of initial ascorbate concentration on the first half life of ascorbate reduction. Egg yolk lecithin multilayers containing 1 mole% 16-doxylstearic acid were treated with the specified concentrations of ascorbate. The insert shows a linear correlation between the inverse of the first half life and the initial ascorbate concentration.



However, in the present investigation, it was found that the rate of decay of the ESR signal was invariant to the amount of the spin label, III, incorporated into the membrane, over the range of 1-3 mole%, the first half life remaining constant at approximately 16+2 min. This lack of dependence of the rate on the initial spin label concentration infers that the reaction rate is independent of the fractional area in the plane of the bilayer which is occupied by the nitroxide, possibly as a consequence of rapid lateral diffusion of the acid, III, in the plane of the membrane. If, indeed, such were the case, the slowing of lateral diffusion through the use of DPL below its gel-liquid crystalline phase transition temperature might be expected to induce a rate dependence on the initial nitroxide concentration.

The flux of ascorbate to the site of the spin label has been given to be (73)

$$\Phi = D (K_p C_0) / x \text{ mole cm}^{-2} \text{sec}^{-1} \quad \text{V-4}$$

where  $C_0$  is the initial ascorbate concentration at the surface of the bilayer,  $x$  is the depth at which the nitroxide is situated beneath the surface,  $D$  is the diffusion coefficient, and  $K_p$  is the partition coefficient of the ascorbate between the aqueous phase and the membrane interior. It has been assumed that the partition coefficient is invariant with time. However, the possibility exists that the higher order effects on the observed rates may be due to a time dependence of the partition coefficient i.e. the lowering of the

amount of unreacted ascorbate which may be solubilized in the bilayer, as the reaction proceeds.

In order to test this hypothesis, EYL multilayers were prepared incorporating 1 mole% of the acid label, III, and hydrated for approximately 1 hr with  $10^{-2}M$   $\delta$ -gluconolactone (1,2,3,4,5-pentahydroxycaproic acid lactone) which was 0.15M in NaCl. The ESR cell was then rinsed and filled with  $10^{-2}M$  ascorbate, 0.15M NaCl, and the rate of decay of the ESR signal monitored in the usual way. It was thought that if the preincubation of the multilayers with the lactone (which is structurally similar to ascorbate, but unreactive towards nitroxide spin labels) altered the first half life of ascorbate reduction, this would be indicative of a change in the partition coefficient of unreacted ascorbate as the permeation proceeds. The first half life was found to be approximately 26 min. Thus, the presence of a molecule structurally similar to ascorbate slows the rate of reduction of the spin label from a half life of approximately 16 min to a half life of approximately 26 min. Thus the partition coefficient of unreacted ascorbate may not be constant, but rather may have a time dependence of the form

$$K_p = f(K_p^0, t)$$

V-5

where  $K_p^0$  is the initial partition coefficient in the absence of reacted ascorbate. However, it must be remembered that the gluconolactone was not added in the form of a salt and therefore might not resemble closely enough the structure of sodium ascorbate.

The first half lives,  $t_{1/2}$ , of ascorbate reduction of the spin probes I-V in EYL, and DPL multilayers at 23°C are shown in Table XIX. In EYL, cholestane, I, yielded a  $t_{1/2}$  value of approximately 4 minutes, confirming that the nitroxide is very near the membrane surface. The other labels, II-V, however, yielded very similar  $t_{1/2}$  values, all on the order of 14-16 min. This is in contrast with the results of previous workers (73) who found half lives of ascorbate reduction of 5-doxylstearic acid and 16-doxylstearic acid, incorporated into EYL multilayers, of 9.5 and 32 minutes, respectively. Whether the discrepancy between the previous results and those presented here are due to slight differences in experimental conditions, or differences in the treatment of the experimental data is not known. Since the previous results were obtained at 19°C, which is very close to the temperature of 23°C used in the present study, it is unlikely that the discrepancy is due to large temperature induced changes in the fluidity of the membrane. In the present investigation, since rate of disappearance of the ESR signal did not follow first order kinetics, it was found necessary to fit the experimental ascorbate reduction data to a quadratic equation, Equation V-1. As discussed previously in this section, this treatment minimizes errors introduced through the time lag between the addition of ascorbate and the onset of data accumulation, as well as eliminating the dependence of the calculated first half life on the total time for which data is acquired.

Table XIX

First half lives of reaction with ascorbate for spin probes  
in lecithin multilayers at 23°C.

Spin Probe	$^1t_{1/2}$ (min) <sup>a</sup>	
	EYL	DPL <sup>b</sup>
3-doxylcholestane, I	4.1 ± 1.7	-
5-doxylpalmitic acid, II	16.5 ± 4.0	16.5 ± 4.0
16-doxylstearic acid, III	16.5 ± 4.0	50.0 ± 10.0
cholesteryl-5-doxylpalmitate, IV	14.0 ± 4.0	42.3 ± 8.0
cholesteryl-16-doxylstearate, V	16.2 ± 4.0	71.0 ± 12.0

<sup>a</sup> ascorbate concentration =  $10^{-2}M$

<sup>b</sup> Multilayers containing DPL were hydrated with 0.15 M

NaCl. pH 6.83, for 60-90 minutes prior to ascorbate addition.

It has been shown previously by Godici and Landsberger (17,18) using  $^{13}\text{C}$  NMR that stearic acid spin-labeled at the 5- or 16- position intercalates into the EYL bilayer membrane in an extended form such that C5 is much nearer the hydrophilic region than is C16. Therefore, the similar rates of ascorbate reduction of II-V in the present study reflect the fluid nature of EYL bilayers at  $23^{\circ}\text{C}$ . Once the ascorbate enters the hydrophobic region, it rapidly diffuses through the fluid membrane core, possibly by the mechanism of "kink diffusion" first proposed by Trauble (187)..

In DPL multilayers, on the other hand, wide variations in the half lives were obtained since at  $23^{\circ}\text{C}$ , DPL is in the gel state. From Table XIX it can be seen that the half lives of ascorbate reduction are in the order  $\text{II} < \text{IV} < \text{III} < \text{V}$ . The rate of reduction for the 5-labeled acid ( $^1t_{1/2}=16.5$  min) is much more rapid than that of the 16-labeled acid ( $^1t_{1/2}=50.0$  min). It should also be noted that the half lives obtained for both the esters, IV and V, are much longer than for the corresponding acids, II and III i.e. 42.3 min vs 16.5 min for the C5 species, and 71.0 vs 50.0 for the C16 species. Since it is known (17,18) that the nitroxide of III lies deep within the membrane core near the lecithin fatty acid chain termini, the slower rate observed for the ester, V, cannot be due to its occupying a position nearer the middle of the bilayer, but must be due either to packing differences for the two molecules, or to the proximity of the ester chain to the cholesterol moiety. In view of

the  $\text{Pr}^{3+}$  permeation studies which were presented in Section 4H, it is unlikely that the saturated ester spin probes pack in a more dense fashion with lecithin than do the corresponding acids. However, it must be remembered that what is being monitored in the ascorbate permeation studies is the rate at which ascorbate reaches the site of the nitroxide and not the actual permeability through the membrane. Bearing this fact in mind, it is more probable that the longer half lives for the esters are caused by the cholesterol moiety i.e. the manifestation of a conformational effect.

In conclusion, based on the ascorbate reductions of the spin labeled esters in DPL, C5 of the fatty acyl chain of the ester is situated nearer to the membrane surface than is C16.

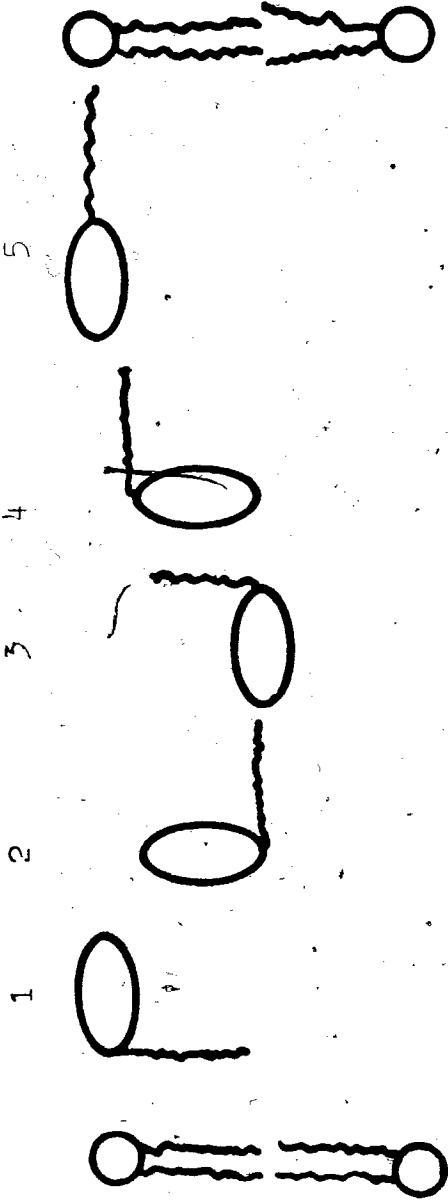
Nine possibilities exist for the orientation of cholesteryl esters within the membrane. These orientations which are depicted in Figure 27 are:

1. an L-shaped configuration with the cholesterol moiety at and parallel to the surface of the membrane with the acyl tail intercalating the lecithin fatty acid chains.
2. an L-shaped configuration with the cholesterol long axis parallel to the bilayer normal, and the ester chain at the centre of the bilayer, parallel to the membrane surface.

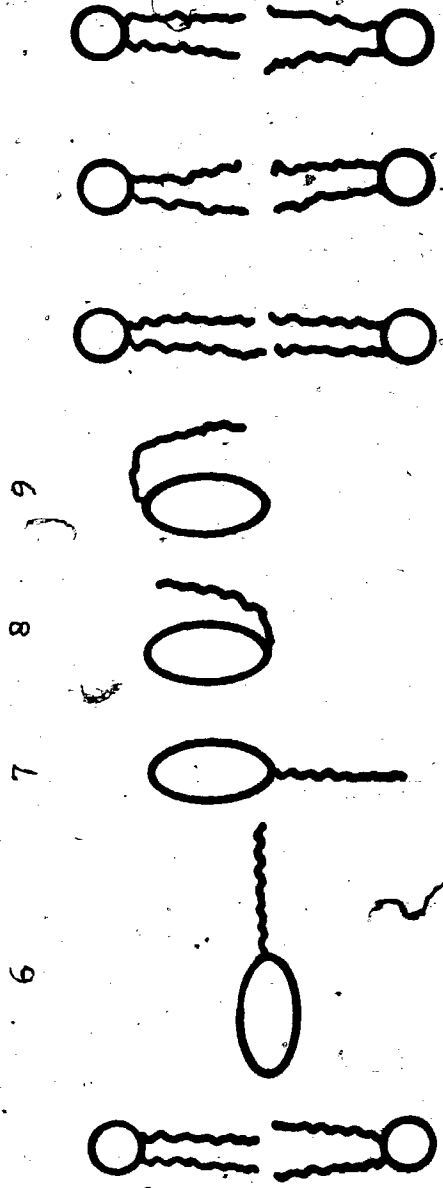


Figure 27. Possible orientations of cholesteryl esters incorporated into lipid bilayers.

AQUEOUS



AQUEOUS



AQUEOUS

3. an L-shaped configuration with the cholesterol moiety in the region of the lecithin chain termini, parallel to the membrane surface, and with the ester chain perpendicular to the membrane surface.

4. an L-shaped configuration with the cholesterol moiety intercalating the lecithin fatty acid chains, and the ester tail at, and parallel to the membrane surface.

5. an extended linear conformation at and parallel to the membrane surface.

6. an extended linear conformation in the centre of the bilayer parallel to the membrane surface.

7. an extended linear conformation spanning the bilayer, with the long molecular axis paralleling the lecithin fatty acid chains, with the steroid and fatty acid tails of the ester at opposite aqueous interfaces of the bilayer.

8. an inverted "horseshoe" conformation with the tail of the cholesterol moiety and the methyl terminus of the ester fatty acyl chain near the membrane surface.

9. a "horseshoe" conformation with the carbonyl group of the ester linkage near the membrane surface and both the steroid moiety and the acyl chain penetrating the hydrophobic region of the bilayer.

Possibilities 1 and 5 may be summarily eliminated since they place the hydrophobic cholesterol moiety in an aqueous environment.

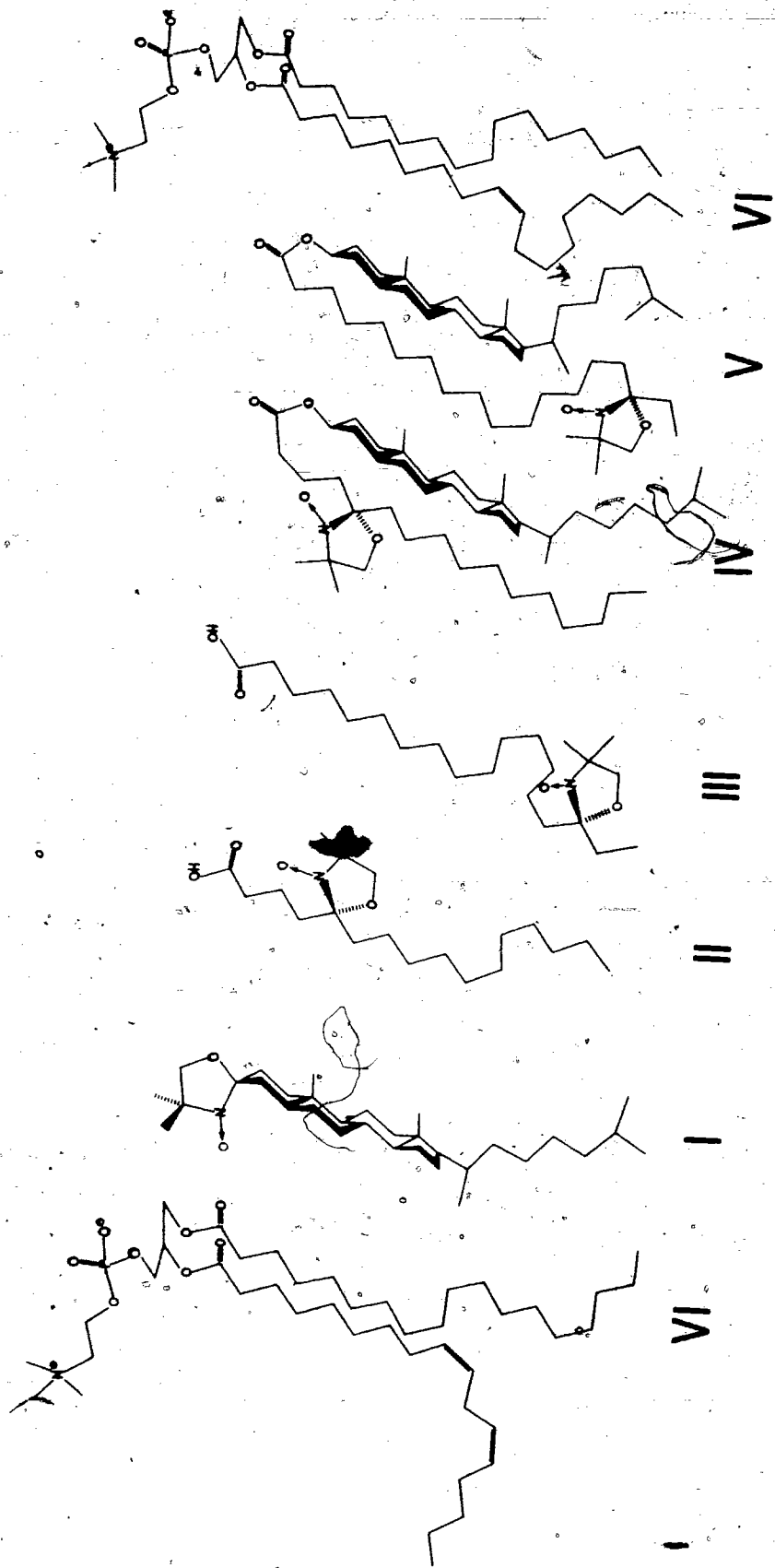
Free cholesterol is virtually insoluble in water, as are cholesteryl esters (186). The remaining seven possibilities must be considered in light of the experimental evidence available. Possibility 4 may be eliminated since it places the fatty acyl tail of the ester in an aqueous environment where the ascorbate reduction of the label should be extremely rapid i.e. at least as rapid as the half life of approximately 4 min found with cholestane. Since it has been shown by the ascorbate reduction experiments in DPL that C16 of the ester is nearer the centre of the bilayer than C5, possibilities 3, 7, and 8 may also be discarded since they require that C5 be further from the membrane surface than C16. Orientations 2 and 6 require that C5 and C16 of the ester fatty acyl chain lie at the same depth in the centre of the membrane. These results appear to be consistent with the rates of ascorbate permeation found in EYL multilayers (half lives for IV, and V of  $14-16 \pm 4$  min). However, it must be remembered that due to the fluid nature of EYL multilayers, the depths of the corresponding acid labels II, and III could not be distinguished in spite of their known orientation (17,18). Therefore, on the basis of the ascorbate reduction rates in DPL where it was possible to distinguish between the rates of reduction of the acid probes II, and III because of their different depths in the bilayer, possibilities 2 and 6 are eliminated. Both 2, and 6 require that C5 and C16 of the ester chain are at the same depth, deep in the centre of the bilayer. However, IV gave a half life of ascorbate reduction of  $42 \pm 8$  min in DPL, while V gave a half life of  $71 \pm 12$  min and therefore C16 of the ester fatty acyl tail must lie deeper within the bilayer than C5.

The sole remaining conformation is 9, a horseshoe with the ester linkage near the membrane surface. This orientation is also consistent with the order parameters for IV; and V which were discussed previously in this section, in that V exhibits a low positive order parameter indicative of the fluid environment in the centre of the bilayer. The 5-doxy palmitate ester, IV, exhibits a low negative order parameter i.e. the nitroxide  $2p\pi$  orbital is oriented at an angle of less than  $45^\circ$  from the plane of the membrane surface, more closely resembling the orientation of the  $2p\pi$  orbital of the cholestane probe, I, than of its corresponding acid, II. This is consistent with the proposed horseshoe ester configuration first put forth by Janiak et al (185) since it places the C5 position near the apex of the horseshoe which would tend to align the nitroxide  $2p\pi$  orbital more closely parallel to the membrane surface, resulting in a negative order parameter as calculated using Equation III-66. The proposed conformations of IV, and V are shown in Figure 28, along with the known orientations of I-III.

## 2. Effect of cholesterol

The effect of added cholesterol on the order parameters of IV, and V has been discussed in Section 5.B.1, and the data for IV are shown in Figure 22, along with the effect of cholesterol on the first half life of ascorbate reduction. Increasing concentrations of cholesterol increases the magnitude of the order parameter while

Figure 28. Orientation and relative depths of various spin probes in lecithin multilayers. Structures VI represent egg yolk lecithin containing saturated and unsaturated fatty acid residues.



decreasing the first half life of the nitroxide reduction to a value on the order of 4-6 minutes. The largest decrease is seen to occur at approximately 10 mole% intercalated cholesterol. Since it is known that cholesterol decreases the angle which the long axis of the phospholipids make with the surface plane, the increase in the magnitude of the order parameter and the rate of reduction of the spin label may be due to a reorientation of the steroid and fatty acid moieties of the ester. Such a reorientation would not only tend to decrease the angle which the nitroxide  $2p\pi$  orbital makes with the lamellar plane, but would also result in the label being rotated closer to the bilayer surface resulting in a shorter  $t_{1/2}$ . The elucidation of this point would require computer simulation of the complex spectra of IV obtained at intermediate angles, and varying concentrations of intercalated cholesterol.

The effect of increasing cholesterol concentrations on the rate of reduction of the nitroxide of the 16-doxylstearate ester, V, was also investigated. The results are shown in Figure 23 along with the changes in the order parameter which were discussed in Section 5.B.1. While increasing amounts of cholesterol increased the order parameter, as was the case for the 5-doxylpalmitate ester, IV, the effects on the rate of ascorbate permeation are somewhat different. The first half life decreases from a value of approximately 16 min in the absence of cholesterol to 5.4 min at a concentration of 4.7 mole%. Increasing the cholesterol concentration to 9.1 mole% resulted in a further



decrease to 3.5 min. Further increases in cholesterol concentrations however, caused the  $t_{1/2}$  to increase. Thus a minimum in the  $t_{1/2}$  curve is observed at a cholesterol concentration of approximately 9 mole%. This suggests that cholesterol induces at least two changes in the structure of the cholesterol ester-lecithin membrane, one at low concentrations, and another at higher concentrations.

Behaviour of this type is not without precedent. The incorporation of up to 8 mole% cholesterol into DPL model membranes causes an increase in bilayer thickness, while incorporation of further amounts results in subsequent decreases (147). However, the data available at the present time does not allow the formulation of a detailed model which is consistent with the results obtained for both ester spin probes.

### 3. Effect of cholesteryl palmitate on cholestane

In view of the dichotomy of the effects of incorporated cholesterol on the  $t_{1/2}$  for V, the converse effects of increasing concentrations of unlabeled cholesterol palmitate on the rate of ascorbate permeation to the site of the cholestane nitroxide were explored. The results are depicted in Figure 24, as are the effects on the order parameter which were discussed in Section 5.B.1. The incorporation of 2.9 mole% cholesteryl palmitate results in a

threefold decrease in the rate of decay of the ESR signal of cholestane; the  $t_{1/2}$  increasing from approximately 4 min to 12.6 min. Further increases in the amount of added cholesteryl palmitate, however, led to more rapid decay. For example, the addition of 19.8% cholesteryl palmitate again yielded a first half life of 4.9 min.

It is of significance that both the break in the order parameter, and the maximum for the  $t_{1/2}$  of reduction of the cholestane spin probe occur at approximately 4 mole% incorporated cholesteryl palmitate. As discussed above, it is probable that above this concentration, a separate ester phase may exist.

In order to investigate the effect on the observed rate of I being solubilized by a separate phase of excess ester, a sample containing 1 mole% cholestane was prepared in a manner analogous to the preparation of phospholipid multilayers, with the exception that no lecithin was present. In other words, cholestane was dispersed in a matrix of solid ester.

The resultant spectrum of the unhydrated sample exhibited one extremely broad resonance (approximately 15 gauss peak to peak). Since hydration did not produce the narrowing characteristic of the onset of rapid motion which has been reported upon the hydration of lecithin multilayers containing cholestane (54), it is concluded that the nitroxide is present in an inhomogeneous hydrophobic environment.

As stated previously, the presence of greater than 4-5 mole% cholesteryl palmitate in EYL multilayers results in more rapid permeation of ascorbate to the site of the cholestane nitroxide. If this were, in part, due to the partitioning of cholestane into a separate ester phase, rapid decay of the ESR signal would be expected for cholestane present in an ester milieu. However, the  $t_{1/2}$  for cholestane dispersed in cholesteryl palmitate was found to be on the order of 210 min, indicating that significant partitioning of cholestane into excess cholesteryl palmitate does not occur in EYL bilayers. This is in agreement with the low solubility of cholesterol in cholesteryl esters (186). Therefore, the dual nature of the effects of cholesteryl palmitate on the half life of cholestane are deemed not to be due to a phase partitioning of the label into excess ester, but instead reflect the influences of cholesteryl palmitate on ester incorporated into the phospholipid bilayer. It is clear also from the effect of added cholesterol on the ester labels. IV and V, that the interactions of cholesterol, cholesteryl esters, and lecithin are quite complex. Since large amounts of cholesterol and cholesteryl esters are present in atherosclerotic lesions, the importance of these interactions cannot be overstated. It has been shown that small amounts of cholesterol (<10 mole%) affect the architecture of the cholesteryl ester-lecithin mixed membrane, and that, conversely, less than 5 mole% cholesteryl palmitate profoundly perturbs the accessibility of the cholesterol steroid nucleus to ascorbate. The exact nature of these interactions awaits the results of future

magnetic resonance studies using specifically deuterated and perdeuterated cholesteryl esters as well as  $^{13}\text{C}$  enriched esters.

#### B. Incorporation of Cholesteryl Esters into EYL Vesicles

The early accumulation of small amounts of cholesteryl esters may be a contributing factor in the onset of atherosclerosis. For the sake of continuity, the effects of the incorporation of up to 5 mole% cholesteryl palmitate, or linoleate into EYL vesicles has already been discussed in Section 4H.

It was found that these esters in excess of 5 mole% could not be incorporated into EYL vesicles. This is in agreement with previous workers (184-186) who found that only 2-5 mole% of the unsaturated ester, cholesteryl linolenate, could be incorporated into a single lecithin-cholesteryl ester lamellar phase. Attempts to increase the solubility of cholesteryl palmitate in vesicle systems in the present study by the incorporation of cholesterol,  $\alpha$ -tocopherol, cardiolipin, or lysolecithin were unsuccessful.

In view of the small amounts of ester which appeared to be solubilized in the vesicles, experiments were performed in order to characterize these mixed vesicle systems.

One experiment involved the use of the C16 nitroxide labeled cholesteryl stearate, III, which was incorporated into EYL vesicles at a 200:1 mole ratio while unlabeled cholesteryl palmitate was added to increase the amount of ester present to 5 mole% of the total lipid. An ESR spectrum of this vesicle preparation was then determined, and the sample dialysed against 3 changes of 1000 ml H<sub>2</sub>O. Subsequent determination of ESR spectral intensity at identical spectrometer settings revealed that >90% of the labeled ester was still present.

A 1 ml aliquot of the vesicle sample was then diluted to 2 ml with the addition of 1 ml of  $2 \times 10^{-2} M$  sodium ascorbate, 0.3M NaCl. This results in ascorbate concentration of  $1 \times 10^{-2} M$ . Subsequent ESR spectra were recorded, and the rate of disappearance of the low field resonance was monitored as described in Section 2.B.2. The signal was found to decay with a first half life ( $t_{1/2}$ ) of 14.5 min. as would be expected for the nitroxide being embedded in the middle of the EYL bilayer. This rate of decay is inconsistent with the labeled ester being present in a separate ester phase. This possibility was further discounted because of the results of a study in which labeled ester was deposited in cholesteryl palmitate matrix via a procedure analogous to preparation of multilayers. It was found that the intensity of the low field resonance decayed extremely slowly ( $t_{1/2} > 100$  min) indicating that when the ester label is present in a phase of excess ester, the nitroxide is quite inaccessible to ascorbate i.e. the first half life of 14.5 min encountered for the

ester incorporated into vesicles is indicative that the label is incorporated into the bilayer membrane, and that a phase of excess ester is not present. The labeled ester would be expected to partition between the lecithin lamellar phase, and the excess ester phase, with a preference for the latter if the latter were present.

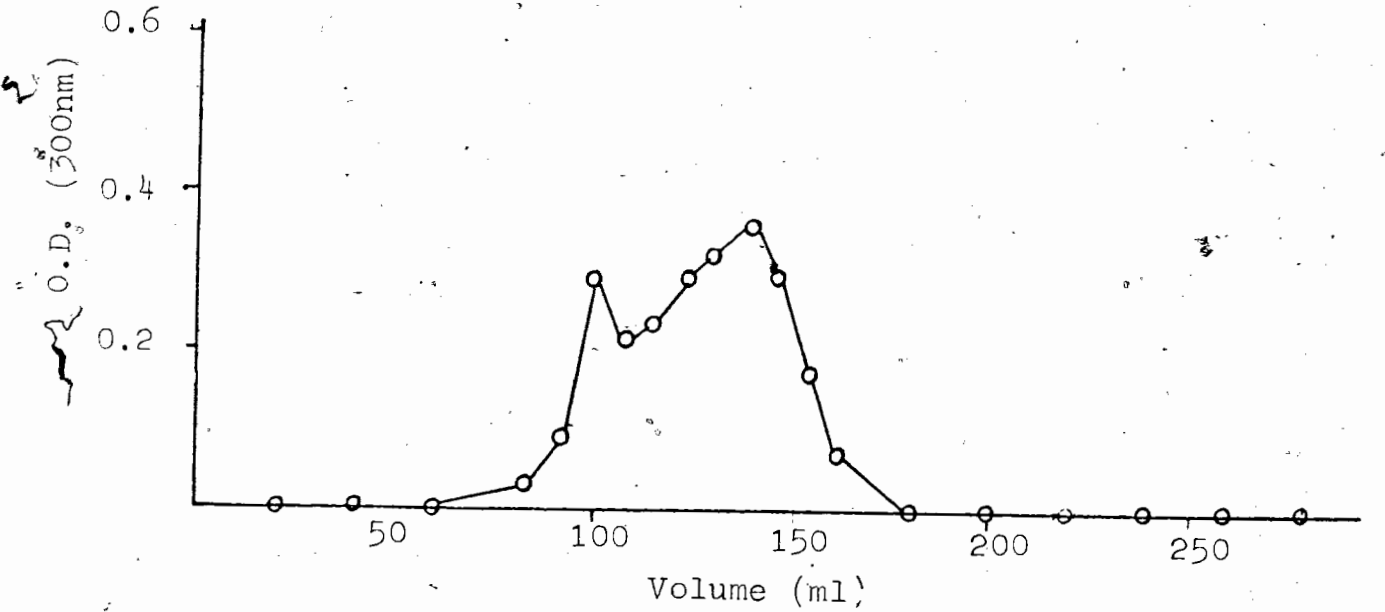
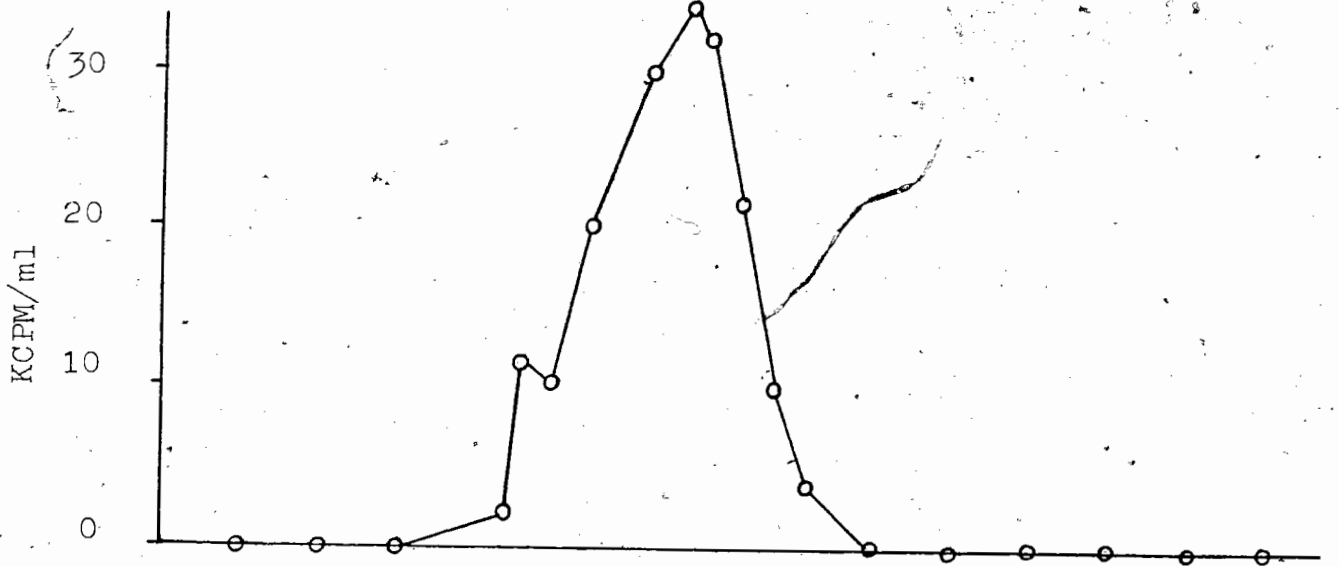
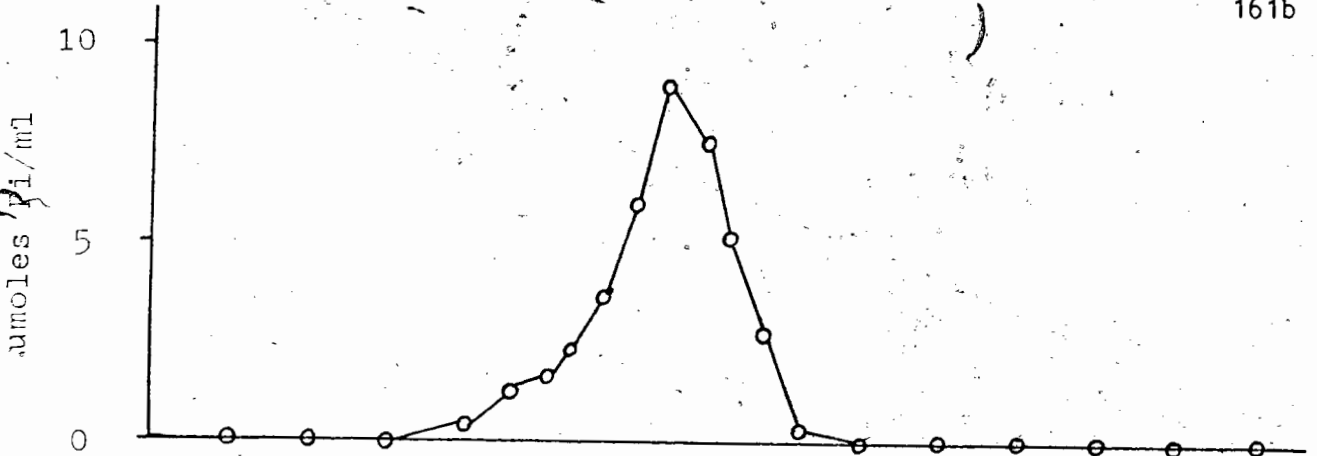
Gel filtration experiments were also performed using cholesteryl-1- $^{14}\text{C}$ -palmitate as a radioactive tracer. EYL vesicles were prepared with a total of 5 mole% co-added cholesteryl palmitate, applied to a 2.7x40 cm Sepharose 4B column, and eluted with 0.05M Tris pH=7.22, 0.05M KCl. The elution profile is shown in Figure 29. The bottom curve which depicts the optical density of the eluant at 300 nm is quite similar to that found by Sheetz and Chan (4), in that it shows a shoulder at lower eluant volume indicative of the presence of a small amount of larger vesicles (liposomes) in the preparation, while the larger peak attests to the preponderance of small vesicles. Electron microscopy of pure EYL vesicles and EYL vesicles containing 5 mole% cholesteryl palmitate also revealed the presence of small vesicles ( $\sim 300\text{\AA}$ ) in diameter as well as the presence of some larger liposomes. That the cholesteryl ester is incorporated in these EYL vesicles is evinced in the two upper curves in Fig.29. The top curve shows the amount of phosphorus present in the fractions, as determined by the method of Chen et al (188), while the middle curve shows the amount of labeled ester present in the various fractions. The overlap of these curves proves that the cholesteryl ester is indeed incorporated into the lecithin vesicles.

Figure 29. Gel filtration of 10% w/v egg yolk lecithin vesicles containing 5 mole% cholesteryl palmitate.

Bottom: O.D. at 300 nm vs. eluant volume

Middle: Counts per minute per ml vs. eluant volume

Top: umoles phosphate per ml vs. eluant volume.





### C. $^{13}\text{C}$ NMR of Lecithin-Cholesteryl Ester Dispersions

As discussed previously, 5 mole% appears to be the maximum amount to which cholesteryl esters may be incorporated into lecithin vesicles. Attempts to solubilize cholesteryl palmitate, or linoleate in an aqueous phase were not successful even above the melting point of the ester and with the aid of the detergents SDS or Tween-20.

It was found, however, that 25 mole% cholesteryl palmitate or linoleate could be suspended in 40% w/v EYL or DPL multilamellar liposomes prepared in  $\text{D}_2\text{O}$  for up to 12 hrs and in 0.3M sucrose for several days. These samples appeared macroscopically homogeneous. In light of previous work (184-186), it is probable that the excess ester, which is present as a separate phase, is either trapped between the "onion skin" layers of the EYL liposomes, or is present as patches within the hydrophobic region of the bilayers. Such a system of EYL and cholesteryl ester, it was thought, might mimic the fatty streaks which characterize primary sclerotic tissue since these streaks are known to be comprised of approximately 95% cholesteryl ester (189).

The  $^{13}\text{C}$  NMR spectra of EYL multilamellar liposomes, and liposomes with 25 mole% added cholesteryl palmitate at  $37^\circ\text{C}$  are shown in Figure 30. These spectra are very similar, as are the  $^{13}\text{C}$   $T_1$  relaxation times which are presented in Table XX. The difference spectrum (bottom) yields a "baseline" indicating that the cholesteryl palmitate contributes negligibly to the observed intensity.

Figure 30.  $^{13}\text{C}$  NMR spectra at 37 C of egg yolk lecithin and egg yolk lecithin-cholesteryl palmitate dispersions.

Top: 40% w/v EYL

Middle: 40% EYL containing 25 mole% cholesteryl palmitate

Bottom: Middle spectrum minus top spectrum. Sweep width = 5000 Hz. Field increases to the right.

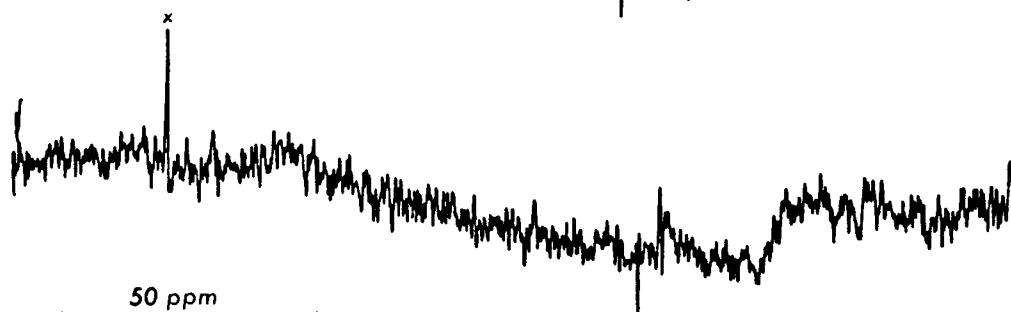
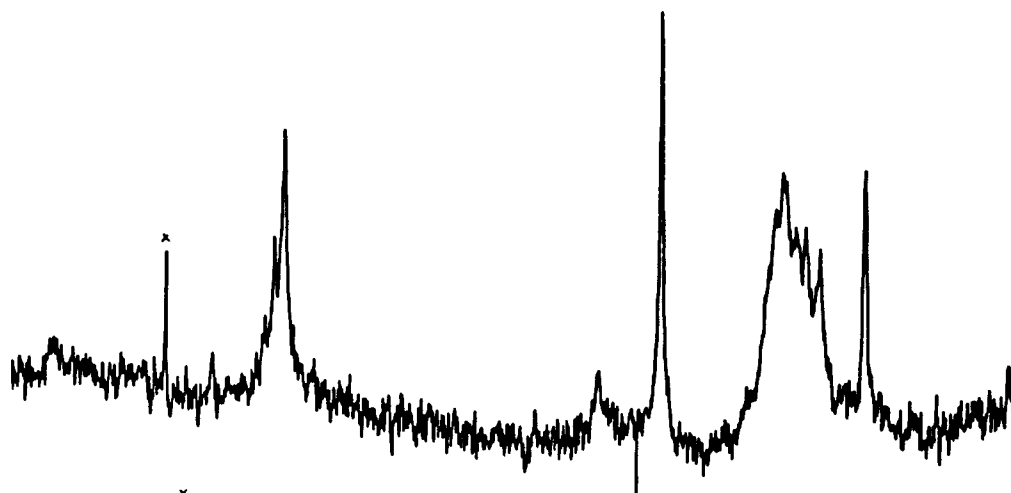
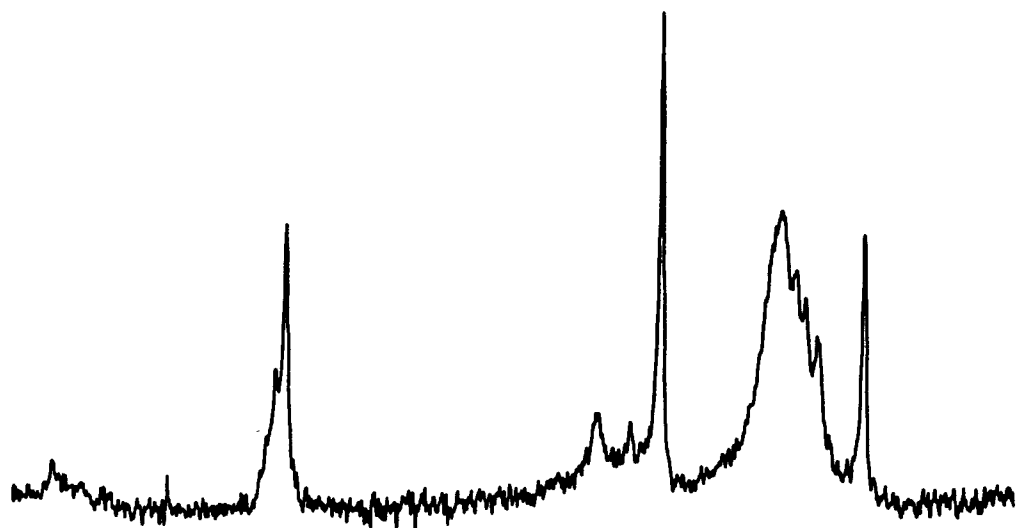
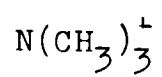


Table XX

$^{13}\text{C}$   $T_1$  relaxation times of lecithin carbons for 40% w/v EYL dispersions in 0.3 M sucrose, and for 40% w/v EYL dispersions containing 25 mole% cholesteryl palmitate.

$T_1$  (sec) at 37°C

Carbon	EYL	EYL + cholesteryl palmitate
$\text{N}^+(\text{Me})_3$	0.52	0.44
$(\text{CH}_2)_n$	0.48	0.46
$\text{CH}_2\text{CH}_2\text{CH}_3$	NR <sup>a</sup>	NR <sup>a</sup>
$\text{CH}_2\text{CH}_3$	1.06	1.10
$\text{CH}_3$	2.83	2.43
$\text{C}=\text{C}-\text{C}^*-\text{C}=\text{C}$	0.55	0.62
$\text{C}^*-\text{C}=\text{C}$	0.47	0.53
$\text{C}^*=\text{C}-\text{C}-\text{C}=\text{C}^*$	0.66	0.58
$\text{C}=\text{C}^*-\text{C}-\text{C}^*=\text{C}$	0.75	0.69

<sup>a</sup> NR = not resolved

On the other hand, the spectrum of EYL liposomes containing 25 mole% cholesteryl linoleate, which is shown in Figure 31, exhibits much sharper resonances. At 37°C, cholesteryl linoleate is in the isotropic liquid state ( $T_m=35.5^\circ\text{C}$ ), while the saturated ester, cholesteryl palmitate, is in its solid state. Unfortunately, the resonances of fatty acids esterified to cholesterol, and those esterified to lecithin overlap. The only peak which may be assigned to lecithin alone at this point is that of EYL- $\text{N}^+(\text{CH}_3)_3$  carbons.

In order to elucidate the origin of the sharp components of the spectrum of the EYL-cholesteryl linoleate mixed liposomes, further experiments were undertaken using the fully saturated phospholipid, dipalmitoyl lecithin. The spectrum of a DPL multilamellar dispersion in 0.3M sucrose at 37°C is shown in Figure 32. Note that the only resonance resolved due to DPL is that of the  $\text{N}^+(\text{CH}_3)_3$  carbons. Even this resonance is severely broadened (width at half height = 70 Hz) since the phospholipid is below its gel-liquid crystalline phase transition temperature ( $T_m=41^\circ\text{C}$ ). All of the sharp resonances downfield from the trimethylammonium resonance are due to sucrose.

This spectrum may be compared with that obtained for DPL liposomes containing 25 mole% cholesteryl linoleate under identical conditions (bottom trace, Figure 32). At 37°C, the cholesteryl linoleate is in the isotropic liquid state while DPL is in the gel state. While the lecithin trimethylammonium resonance is still

166a

Figure 31.  $^{13}\text{C}$  NMR spectrum of a 40% w/v dispersion of egg yolk lecithin in 0.3 M sucrose containing 25 mole% cholesteryl linoleate at  $37^\circ\text{C}$ . Sweep width = 5000 Hz. Field increases to the right.

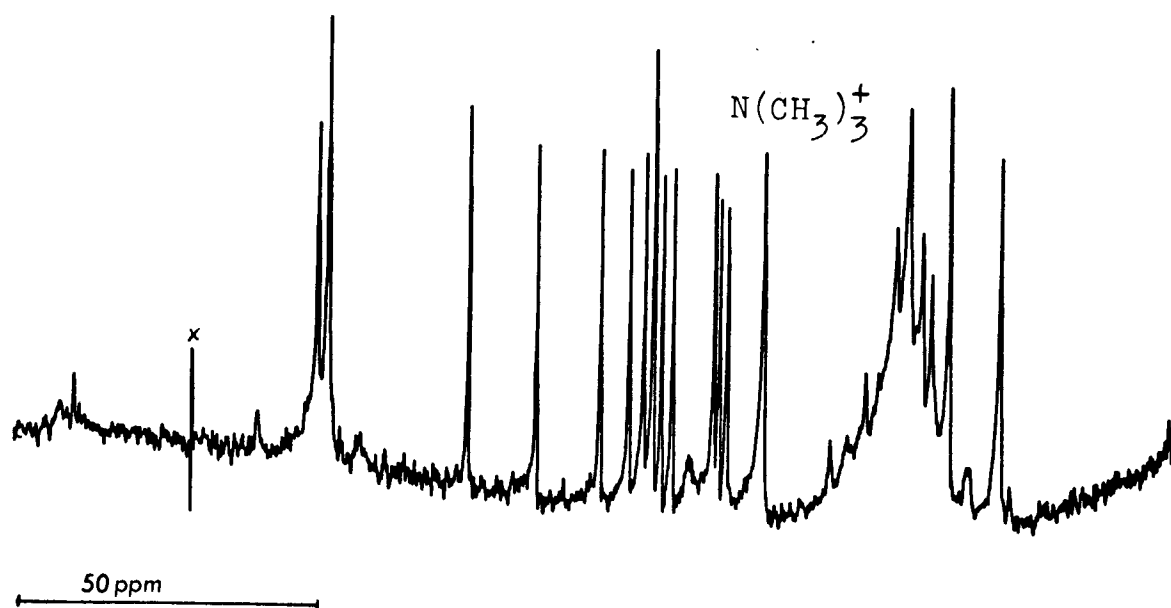


Figure 32.  $^{13}\text{C}$  NMR spectra at  $37^\circ\text{C}$  of dipalmitoyl lecithin and dipalmitoyl lecithin-cholesteryl linoleate dispersions. Top: 40% w/v DPL in 0.3 M sucrose  
Bottom: 40% w/v dispersion of DPL in 0.3 M sucrose containing 25 mole% cholesteryl linoleate.  
Sweep width = 5000 Hz. Field increases to the right



extremely broad, note the intensity and sharpness of the resonances in the olefinic region. The upfield and downfield olefinic resonances may be unequivocally assigned to the 10, 12 and 9,13 carbons,

respectively, of the linoleate moiety of the cholesteryl ester since DPL possesses two fully saturated fatty acid chains. Secondly, a family of sharp lines is present upfield in the region of the alkyl carbons. These resonances due to the cholesteryl ester are relatively narrow, suggesting the presence of pools of fluid sterol ester.

The top trace of Figure 33 shows the  $^{13}\text{C}$  spectrum of pure DPL liposomes at  $52^\circ\text{C}$ ,  $11^\circ$  above the gel-liquid crystalline transition temperature. In addition to the trimethylammonium resonance, three other very broad resonances are resolved, namely that due to carbons 4-13 of the palmitate chains, that due to the penultimate carbons (w-1) which appears as a high field shoulder, and that due to the terminal methyls (resonance at highest field), w. These resonances are severely broadened when compared to those of DPL vesicles at  $52^\circ\text{C}$  due to the much longer rotational reorientation times of the multilamellar liposomes. The spectrum of DPL-cholesteryl linoleate liposomes at  $52^\circ\text{C}$  is shown in the middle trace of Figure 33. It should be noted that in addition to sharp resonances due to the linoleate moiety, resonances are also resolved for carbons of the steroid nucleus, notably those of the unsaturated carbons C5 and C6 which flank the linoleate olefinic carbons. Assignments are given in Table XXI. The difference spectrum (DPL with cholesteryl linoleate

Figure 33.  $^{13}\text{C}$  NMR spectra at  $52^\circ\text{C}$  of dipalmitoyl lecithin and dipalmitoyl lecithin-cholesteryl linoleate dispersions in 0.3 M sucrose. Top: 40% w/v DPL. Middle: 40% w/v DPL dispersion containing 25 mole% cholesteryl linoleate. Bottom: Middle spectrum minus top spectrum. Sweep width = 5000 Hz. Field increases to the right.

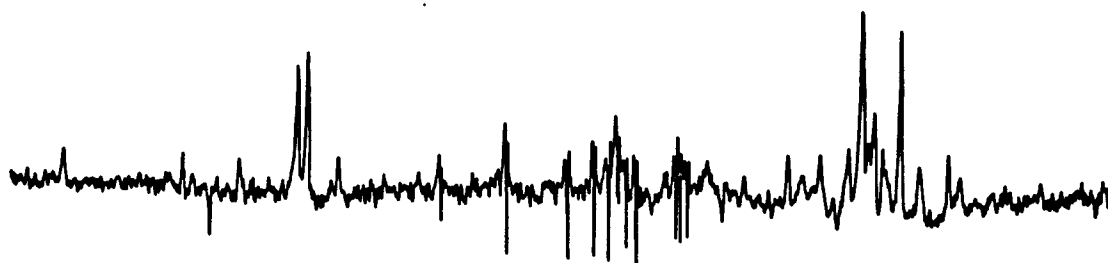
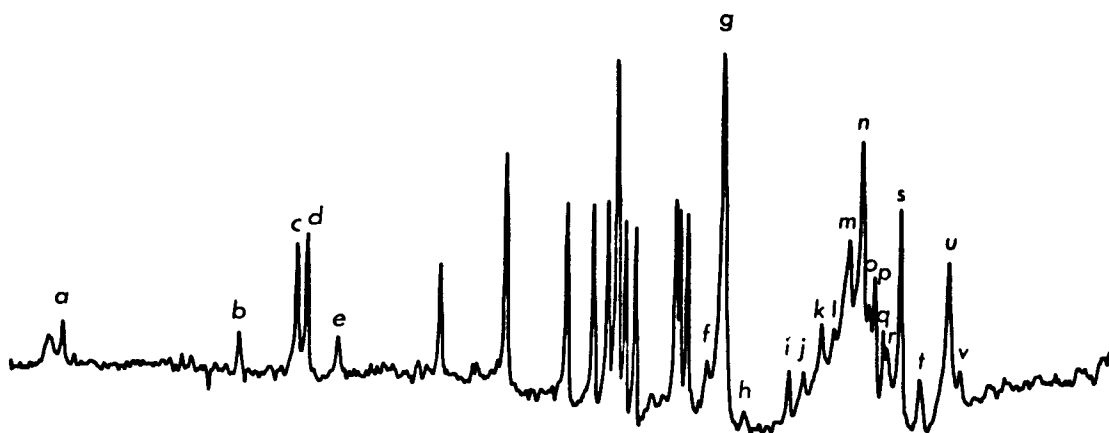
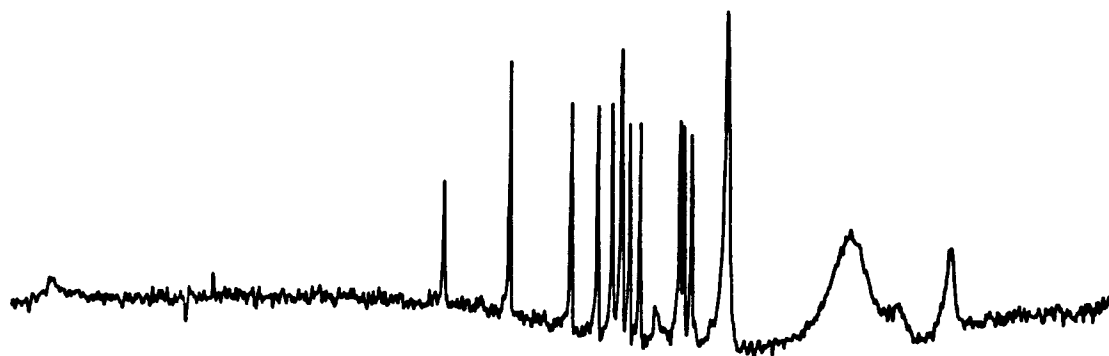


Table XXI

$^{13}\text{C}$  NMR assignments for cholesteryl linoleate carbons  
 in 40% w/v dispersions of DPL containing 25 mole%  
 cholesteryl linoleate at 52°C. Primes refer to carbons  
 of the linoleate chain.

Peak	Assignment
a	C1'
b	C5
c	C13', C9'
d	C10', C12'
e	C6
f	C4, C17
g	$\text{N}^+(\text{Me})_3$ of DPL
h	C9
i	C13
j	C12, C24
k	C1, C10, C20, C22
l	C2'
m	C16'
n	C4', C5', C7', C15'
o	C16, C25
p	C8', C14'
q	C11', C13
r	C15, C23
s	C17', C26, C27
t	C19, C21
u	C18'
v	C18

minus DPL) is shown in the bottom trace of Figure 33. Even above the  $T_m$  of DPL, the intensity of the sharp spectral lines is contributed to only by the ester, although certain of these peaks are superimposed on very broad phospholipid resonances.

One question remains. What is the state of the cholesteryl linoleate? From the work of Janiak et al (185), it may be reasonably assumed that less than 5% of the ester is present in a homogeneous phospholipid-ester lamellar phase, the excess ester being present as a separate phase.

This separate isotropic phase of cholesteryl linoleate may be either present as small liquid droplets captured in the aqueous phase between the lamellae of the liposomes, or perhaps as patches of ester in the hydrocarbon interior of the bilayers. Thus, such a system may parallel the mesomorphic droplets which characterize atherosclerotic lesions.

As previously mentioned, the  $^{13}\text{C}$   $T_1$  relaxation times for EYL alone, and the EYL-cholesteryl palmitate dispersion are very similar, since, in this case, the spectral intensity is due to the lecithin carbons. This indicates that the presence of patches of solid ester does not significantly perturb the average environment of the phospholipid molecules. Although up to 5 mole% of the ester may be present in a homogeneous lecithin-cholesteryl ester lamellar phase,

the  $^{13}\text{C}$   $T_1$ 's reflect an average value of those for phospholipid molecules which are adjacent to ester molecules, and those for phospholipid molecules which are not. Thus, little change would be expected in the observed relaxation times. Similarly, separate patches of ester will affect relatively few lecithin molecules resulting in little change in the experimentally determined  $T_1$ 's.

The  $^{13}\text{C}$   $T_1$  relaxation times for lecithin dispersions with incorporated cholesteryl linoleate on the other hand reflect the motional freedom of the ester since it is the ester carbons which contribute to the spectral intensity. These  $^{13}\text{C}$   $T_1$  relaxation times are given in Table XXII. The relaxation times are much shorter than those obtained previously for the lecithin carbons, while the lone resonance in this case which may be assigned to the phospholipid (the  $\text{N}^+(\text{CH}_3)_3$  carbons), yields a relatively unchanged relaxation time (0.52s vs 0.50s). This would seem to indicate that the droplets of excess ester are not associated with the lecithin headgroup region.

It is remarkable that the linoleate moiety of the cholesterol ester exhibits such low spin-lattice relaxation times. The  $T_1$ 's are approximately half those observed for lecithin fatty acid chains, although these values do increase as the chain terminus is approached. Times of 0.24, 0.51, 0.61 and 1.98 s are determined for the  $(\text{CH}_2)_n$ , w-2, w-1 and w carbons, respectively. Thus a fluidity

Table XXII

$^{13}\text{C}$   $T_1$  relaxation times for cholesteryl linoleate carbons  
in 40% w/v EYL dispersions containing 25 mole% cholesteryl  
linoleate

Carbon	$T_1$ (sec) at 37°C
$\text{N}^+(\text{Me})_3$	0.50
$(\text{CH}_2)_n$	0.24
$\text{CH}_2\text{CH}_2\text{CH}_3$	0.51
$\text{CH}_2\text{CH}_3$	0.61
$\text{CH}_3$	1.98
$\text{C}=\text{C}-\text{C}^*-\text{C}=\text{C}$	0.28
$\text{C}^*-\text{C}=\text{C}$	0.26
$\text{C}^*=\text{C}-\text{C}-\text{C}=\text{C}^*$	0.32
$\text{C}=\text{C}^*-\text{C}-\text{C}^*=\text{C}$	0.38

gradient exists along the cholesteryl ester chain. However, the lower values indicate more limited mobility than experienced by phospholipid fatty acid chains at the same temperature. This phenomenon has been previously noted for one of the linoleate carbons, C14, of enriched cholesteryl linoleate present in a turbid dispersion of lecithin, sphingomyelin, cholesterol and cholesterol linoleate (21,22). The value of 0.25 s determined for the  $^{13}\text{C}_{14}$  relaxation time in that investigation is in excellent agreement with the value of 0.26 s determined for the lecithin-cholesteryl linoleate dispersion.

Such low relaxation times for the linoleate resonances indicate a low rate and/or high order of motion of their acyl chains, indicating that excess ester may be tightly packed, even while in its liquid phase. However, the rotational correlation times of these droplets as a whole must be quite rapid in order to give rise to the motionally narrowed  $^{13}\text{C}$  resonance signals i.e. just as the rotation of phospholipid vesicles as a whole gives rise to high resolution  $^{13}\text{C}$  NMR signals, the ester droplets must be undergoing rapid reorientation in order to give rise to the resultant sharp resonances.

It has been reported (190) that extremely small quantities (0.1-0.5%) of cholesteryl esters may be suspended in aqueous solution above the melting point of the ester. Considering the large amounts of ester used in the present study, it is highly unlikely that the excess ester is suspended as droplets in the aqueous phase. Rather,



it is more probable that small ester droplets are associated with the hydrophobic region of the phospholipid bilayer. If, for example, the ester was present in a homogeneous lecithin-ester phase, the ester would be expected to experience the slow reorientation of the large lecithin liposomes, and consequently give rise to broad  $^{13}\text{C}$  NMR signals. However, a small droplet of ester above its transition temperature would be expected to undergo rotational reorientation at a faster rate than possible for large lecithin liposomes. Such a model could explain the motionally narrowed  $^{13}\text{C}$  spectra of cholesteryl linoleate at  $37^\circ\text{C}$ .

These lecithin-cholesteryl ester systems are extremely stable. No detectable amount of ester separated out over the course of several days. The ester is associated with the lecithin liposomes, solubilized by these liposomes, and thus, this system is a good model for the cholesteryl ester droplets and fatty streaks which characterize atherosclerotic tissue. In addition, the incorporation of large quantities of cholesterol into this system should more closely mimic the natural system, since cholesterol may be incorporated up to a 1:1 mole ratio of lecithin:cholesterol. Excess cholesterol above this amount should be expected to be solubilized to a certain extent by the ester droplets and thus the effects of cholesterol on the ester may be monitored.

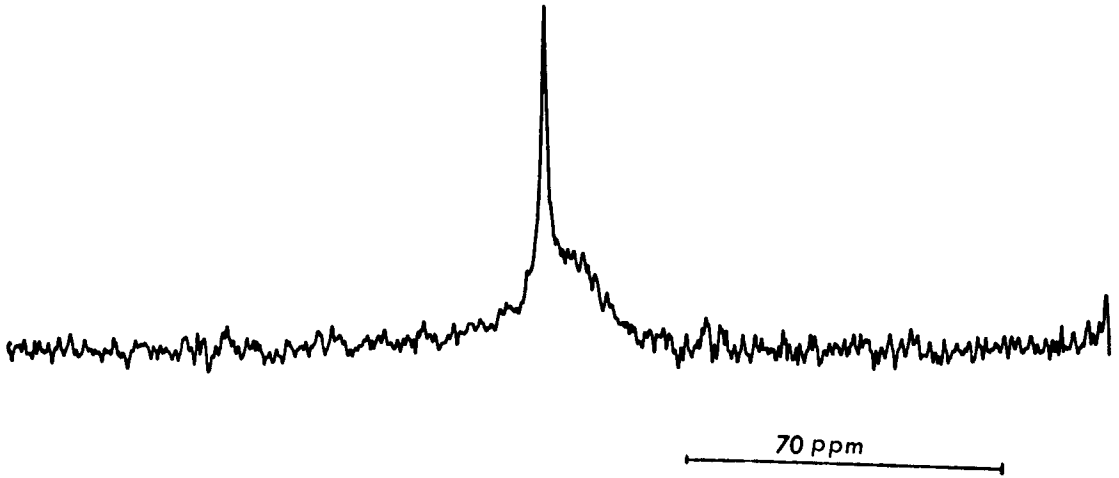
## D. Aorta Membrane

1.  $^{31}\text{P}$  NMR

The proton decoupled  $^{31}\text{P}$  NMR spectrum of the unsonicated aorta membrane prepared as described in Section 2.B.5 is shown in Figure 34. This spectrum, which represents the accumulation of 16,000 transients exhibits a solid state lineshape which is characteristic of chemical shift anisotropy of the phosphorus nuclei of the phospholipids (74-81). The sharp component has a chemical shift of 0.7 ppm upfield from external 85%  $\text{H}_3\text{PO}_4$ .

The phospholipids of class II aorta are known to be made up of 26.7% lecithin, 4.4% lysolecithin, 59.4% sphingomyelin and 9.5% cephalin (191). Since these lipids all have similar  $^{31}\text{P}$  chemical shifts (+2 ppm from  $\text{H}_3\text{PO}_4$  in  $\text{CHCl}_3$  solution) (192), the individual lipids would not be expected to be resolved in the coarse unsonicated dispersion. It should be noted that the residual chemical shift anisotropy  $\Delta\delta$ , which is the difference in chemical shift between the two extreme edges of the resonance, is approximately 30 ppm. This is contrasted by the rigid lattice values obtained from powder spectra of lecithin and cephalin which yielded anisotropies of 150-200 ppm (78,79). This collapse is indicative of averaging of the shielding tensor due to motion of the phosphate headgroups.

Figure 34.  $^{31}\text{P}$  NMR spectrum of unsonicated aorta membrane preparation,  $37^\circ\text{C}$ . Sweep width = 10,000 Hz. Field increases to the right.



Upon sonication of ~~the~~ coarse dispersion (liposomes), the  $^{31}\text{P}$  spectrum (Figure 35) consists of a single resonance with a halfwidth of 45 Hz, 0.8 ppm downfield from external 85%  $\text{H}_3\text{PO}_4$ . Sonication of the coarse suspension results in a substantial decrease in the viscosity of the sample from an almost solid-like to a liquid-like state, leading to a much more rapid tumbling of the smaller particles and consequent spectral narrowing.

The exact form of the particles is not known i.e. whether they are vesicular or micellar in nature. However, if vesicular structures are present, it may be possible to differentiate the inner and outer surfaces by the addition of paramagnetic shift reagent, if the rate of permeation of the lanthanide is sufficiently slow.

The addition of 150 ul of 0.1M  $\text{Pr}^{3+}$  to the sonicated dispersion results in a single broad resonance (halfwidth = 10 ppm) approximately 5 ppm downfield from the original resonance. This could be indicative either of rapid permeation of the lanthanide, or the absence of vesicular structures, although vesicular type membrane structures have been observed for aorta membranes prepared by differential centrifugation techniques (193).

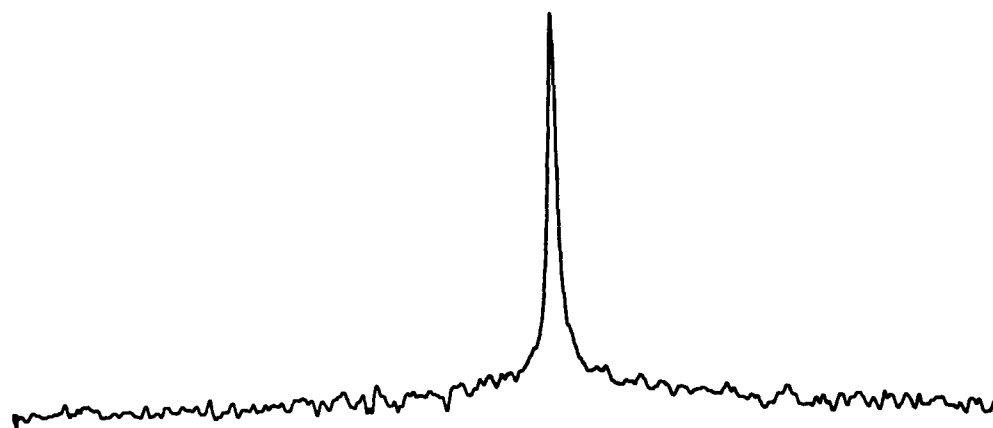
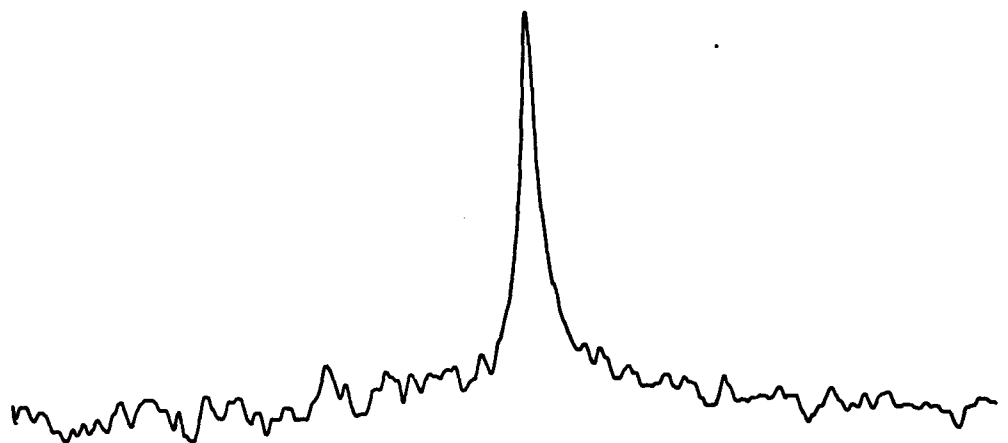
The addition of 300 ul of 0.2M EDTA results in the reappearance of a single narrow resonance 1.3 ppm upfield from external 85%  $\text{H}_3\text{PO}_4$  (Figure 35) with a halfwidth of 23 Hz. The further sharpening and the

Figure 35. High power proton noise decoupled

$^{31}\text{P}$  NMR spectrum of sonicated aorta membrane.  $37^\circ\text{C}$ .

Top: Before the addition of  $\text{Pr}^{3+}$ . Bottom: After  
the addition of  $\text{Pr}^{3+}$  and EDTA. Sweep width = 2000 Hz.

Field increases to the right.



15 ppm

upfield shift of approximately 0.5 ppm of this resonance from that which was obtained prior to  $\text{Pr}^{3+}$  addition indicates the presence of traces of polyvalent metal ions which are known to broaden and shift phosphorus resonance signals (194). Inorganic constituents of the aortic wall are known to include calcium, magnesium, and iron (195). The addition of EDTA removes these metal ions.

The spectrum shown in Figure 35 represents the co-addition of 4 blocks of 4,000 transients each. Once again, the sharpening of the resonance upon EDTA addition indicates either rapid permeation of EDTA through closed structures, or the exposure of the phospholipid binding sites for metal ions to the bulk solution.

This preliminary investigation has shown that membrane preparations of the human aorta do give rise to well resolved  $^{31}\text{P}$  NMR spectra, and therefore this technique holds promise for future investigations which should also include an investigation of the nature of the particles produced. It is clear, however, that even prior to sonication, the headgroups of the constituent phospholipids are rather mobile, as indicated by the linewidth prior to sonication.  $^{31}\text{P}$  NMR has the distinct advantage that the resonance observed is due to the phospholipids only, with no contribution due to nonphosphorus containing constituents (e.g. triglycerides, cholesterol, and cholesterol esters). It should be noted in this regard that in spite of the sharpness of the resonance signal of the sonicated



mixture, the time required for the determination of the spectrum is rather long. Whereas the spectrum shown in Figure 35 is the result of the accumulation of some 16,000 transients, spectra with a similar signal to noise ratio may be obtained from 10% w/v lecithin vesicles in approximately 200 scans. This is indicative of the relatively low concentration of phospholipid in aortic tissue. This fact will become clearer upon an examination of the  $^{13}\text{C}$  spectrum of the sonicated aorta preparation which is discussed in the following section (Section 5.D.2).

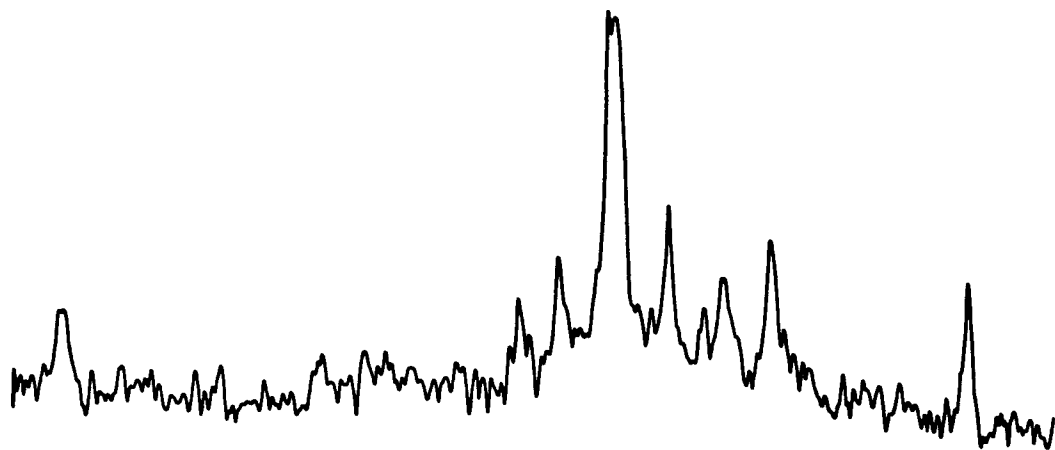
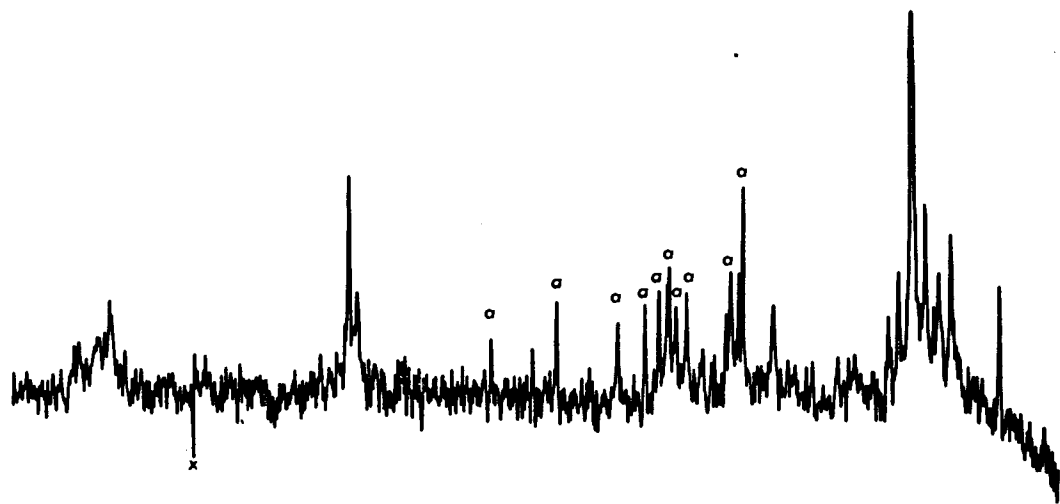
## 2. $^{13}\text{C}$ NMR

The aorta sample used for the determination of the  $^{31}\text{P}$  spectra was dialysed against distilled water as described in Section 2.B.5 to remove sucrose, and the inorganic ions added during the course of the  $^{31}\text{P}$  NMR experiments.

The  $^{13}\text{C}$  NMR spectrum of the sonicated aorta is shown in Figure 36 and represents some 120,000 transients accumulated with a  $55^\circ$  flip angle, and an interpulse time of 2 seconds. The resonances are narrow, indicative of lipids in a mobile environment, in spite of the probable presence of large amounts of cholesterol which is known to broaden the  $^{13}\text{C}$  spectra of lecithin vesicles (12). The resonances designated "a" are due to residual sucrose, either bound to the sample, or perhaps trapped within vesicular or multilamellar

Figure 36.  $^{13}\text{C}$  NMR spectrum of sonicated aorta,  $37^\circ\text{C}$ .

Top: Sweep width = 5000 Hz. Field increases to the right. Bottom: Expansion of the region 10.7 to 56.9 ppm downfield from TMS.



structures. It is unlikely however that these resonances are due to glycolipids, since these are known to make up only about 1% of the total lipid of aortic tissue (196).

The appearance of sucrose resonances in the  $^{13}\text{C}$  NMR spectrum is in itself, intriguing. The possibility of incomplete dialysis following the determination of the  $^{31}\text{P}$  spectra is improbable since resonances due to the Tris buffer, which should also have been resolved, were not present (8). The presence of sucrose after dialysis may arise from either its binding to some component of the aorta membrane, or from its being trapped inside vesicular structures formed upon sonication of the coarse dispersion. The latter case has been observed with vesicle preparations of rabbit muscle sarcoplasmic reticulum (10).

In order to account for the continued presence of sucrose, the following experiment was performed. A 1.05 gm aliquot of the previously sonicated aorta preparation was diluted with 3 ml  $\text{H}_2\text{O}$ , and divided into two aliquots. To the first was added only  $[^{14}\text{C}]$ -sucrose,  $3 \times 10^{-6}\text{M}$  (low sucrose sample), while to the other was added  $[^{14}\text{C}]$ -sucrose together with sufficient unlabeled sucrose to bring the total sucrose concentration up to 1.0M (high sucrose sample). The two aliquots were then resonicated under nitrogen at  $11^\circ\text{C}$  for approximately 10 minutes, and subsequently dialyzed separately against three changes of 2000 ml  $\text{H}_2\text{O}$  for a total time of 47 hours.

Assuming 99% equilibration for each dialysis step, this should lead to a dilution factor of approximately  $10^6$ , if no binding or trapping of sucrose occurs. However, a dilution of only approximately 80 times occurs for the low sucrose aliquot and of  $2.5 \times 10^3$  times for the high sucrose aliquot. The total amount retained for the low sucrose aliquot was 1.3% of that added ( $3.9 \times 10^{-4}$  umoles) while the total amount retained for the high sucrose aliquot was 0.4% of that added (39 umoles). Thus, while the total amount of sucrose retained is quite small, a higher percentage was retained for the low sucrose sample. This could result from a small amount of sucrose binding to some membrane component, for if sucrose was trapped inside vesicular structures, the same percentage retention of [ $^{14}\text{C}$ ]-sucrose should be expected for both high and low sucrose samples. Thus, the quantity of any vesicles which are impermeable to sucrose is rather low. It is also improbable that the more intense sharp resonances in the  $^{13}\text{C}$  NMR spectrum are due to fibrous elastin (197), but rather are assigned to the fatty acyl chains of triglycerides, cholesteryl esters, and phospholipids. Assignments are given in Table XXIII. The resonances for these membrane constituents are overlapping i.e. resonances for the  $\omega-1$  carbons of fatty acid chains occur at the same chemical shift, whether esterified to cholesterol, or glycerol. Therefore the  $^{13}\text{C}$  NMR spectrum bears a strong resemblance to that obtained for EYL vesicles. Of the fatty acids, a large number are unsaturated, with peaks being resolved for both singly and doubly unsaturated esters.

Table XXIII

$^{13}\text{C}$  Chemical shifts of sonicated aorta,  $37^\circ\text{C}$ .

The chemical shifts were measured relative to external

HMDS and corrected relative to TMS.

Carbon	Chemical Shift (ppm)
C1	171.9
C2	34.2
$(\text{CH}_2)_n$	30.2
$\text{CH}_3$	14.5
$\text{CH}_2\text{CH}_2$	23.2
$\text{CH}_2\text{CH}_2\text{CH}_3$	32.5
$\text{C}^*\text{H}_2-\text{CH}=\text{CH}$	27.7
$\text{CH}=\text{CH}-\text{C}^*\text{H}_2-\text{CH}=\text{CH}$	25.3
$\text{CH}=\text{C}^*\text{H}-\text{CH}_2-\text{C}^*\text{H}=\text{CH}$	128.3
$\text{CH}=\text{C}^*\text{H}-\text{CH}_2-\text{CH}_2$	129.9
$\text{N}^+(\text{Me})_3$	54.7

The major difference between the spectrum in Figure 36, and that of lecithin vesicles above the transition temperature is the very low relative intensity of the  $N^+(CH_3)_3$  resonance at 54.7 ppm. This reflects the low concentration of the phospholipids-lecithin, and sphingomyelin, which are present in the aorta sample. The major contributions to the intensity of this spectrum must therefore originate from nonphospholipid constituents, such as triglycerides, and cholesteryl esters. To give rise to such narrow linewidths, these molecules must be in a fluid environment, as was seen to be the case for cholesteryl linoleate in its isotropic liquid state when present in DPL dispersions.

Therefore aortic tissue contains sufficient amounts of unsaturated fatty acid esters to give rise to well resolved  $^{13}C$  NMR spectra. This fact may prove to be of importance in the investigation of the progressive development of atherosclerosis. Since apparent  $T_2^*$  measurements have been shown to be very sensitive to subtle changes in membrane structure (15), linewidth measurements of aorta membrane preparations for varying stages of the disease may be illuminating. Time requirements at present however make the determination of  $^{13}C$   $T_1$  relaxation times impractical.

## CHAPTER 6

## CONCLUSION

## A. Vitamin E, Phytol, and Phytanic Acid

The isoprenoids, Vitamin E, phytol, and phytanic acid have been successfully incorporated into lecithin vesicles up to a 1:1 mole ratio for the lecithin-phytol mixed vesicles, and up to a 3:1 mole ratio (lecithin:isoprenoid) for the lecithin-Vitamin E, and lecithin-phytanic acid systems.

The intercalation of phytol, Vitamin E, or phytanic acid has been shown to greatly increase the fluidity of the mixed membrane, as monitored by  $^{13}\text{C}$   $T_1$  relaxation times. The disruptive effect was found to increase in the order phytol < Vitamin E < phytanic acid. For example, the incorporation of 25 mole% Vitamin E increases the  $^{13}\text{C}$   $T_1$  relaxation times for the lecithin fatty acid carbons by 50-100%, while the largest increases, which were found upon the incorporation of 25 mole% phytanic acid, were on the order of 150-200%. However, little change in lecithin  $T_1$ 's was noted upon the incorporation of 25 mole% of the unbranched acid, palmitic acid.

The perturbations caused by the incorporation of phytol, Vitamin E, and phytanic acid as monitored by the  $^{13}\text{C}$   $T_1$ 's have been found



to correlate with permeability increases of mixed phospholipid-phytyl compound vesicles to the  $\text{Pr}^{3+}$  cation using  $^{31}\text{P}$  NMR spectroscopy.

At  $33^\circ\text{C}$ , the permeability of egg yolk lecithin vesicles was increased by approximately 8 times upon the incorporation of 25 mole% phytol, by approximately 48 times upon the incorporation of 25 mole% Vitamin E, and by approximately 2900 times upon the incorporation of 25 mole% phytanic acid. In other words, the permeability of the two component (lecithin:phytyl) vesicles increases in the order phytol < Vitamin E < phytanic acid. This is the same order in which the  $^{13}\text{C}$   $T_1$  relaxation times increase. Incorporation of a smaller amount of Vitamin E which approaches physiological concentrations (3 mole%) still results in a permeability increase to 300% of the rate for pure egg yolk lecithin vesicles. As seen above with  $^{13}\text{C}$  spin lattice relaxation effects, no change in the rate of  $\text{Pr}^{3+}$  permeation was observed upon the incorporation of 25 mole% of the unbranched acid, palmitic acid.

It is known that phytol, Vitamin E, and phytanic acid form expanded monolayers when spread at an air-water interface (46). In addition, Vitamin E, unlike cholesterol or palmitic acid, is not able to fit into cavities between adjacent phospholipid molecules in lecithin-Vitamin E mixed monolayers, but rather displaces its full area requirement. Thus, the disruptive effects of phytol, Vitamin E and phytanic acid have been explained in terms of the difficulty in accommodating these branched chain compounds in an ordered bilayer

arrangement, and decreased lipid-lipid packing density. Concomitant decreases in the Van der Waals attractive forces between adjacent lipids would result in a destabilization of the mixed bilayer.

Therefore, it is possible that certain physiological effects of the branched chain compounds, Vitamin E, phytol and phytanic acid, may be structural in origin. For example, Refsum's disease is characterized by the presence of large amounts of phytanate in the nerve tissue (up to 24% of the fatty acids of the choline glycerophosphatides) (96). Patients afflicted with this disorder cannot  $\alpha$ -oxidize and decarboxylate phytanic acid, and consequently, this branched chain fatty acid accumulates. The result is a severe degeneration of the nervous system, neurological defects, and eventual death. It would appear that the severe demyelination characteristic of Refsum's disease may be caused by the destabilization of the myelin sheath by phytanic acid.

Also, several investigations (198-201) have shown that a correlation exists between the function of membrane bound cooperative enzymes such as  $(Mg^{2+}, Ca^{2+})$ -ATPase and membrane fluidity. While a certain degree of membrane fluidity is necessary for the enzyme activity, the overaccumulation of branched chain compounds may lead to too great an amount of free movement with disastrous consequences which may include a failure of compartmentalization. Thus, the incorporation of branched chain compounds into model membranes results

in a destabilization, increased fluidity, and increased permeability. These effects which have been shown to be structural in origin may have important physiological consequences.

The position occupied by the branched chain compound, phytol, in the lecithin-phytol bilayer has been determined by means of an intermolecular linear electric field effect upon the  $^{13}\text{C}$  chemical shifts of the phytol olefinic carbons C2 and C3. The incorporation of phytol into phospholipid bilayers exposes the phytol C2-C3 olefinic pair to an electric field originating in the lecithin hydrophilic region at the membrane surface. The result for phytol incorporated into egg yolk lecithin vesicles at  $52^\circ\text{C}$  is an upfield shift of 0.46 ppm for C2, and a downfield shift of 0.51 ppm for C3. This characteristic upfield-downfield chemical shift is caused by an electric field which originates at the membrane surface inducing a polarization of the phytol olefinic bond such that the carbon nearer the surface, C2, experiences an increased electron density and its  $^{13}\text{C}$  resonance is consequently shifted upfield. The carbon further from the membrane surface experiences a decreased electron density and its  $^{13}\text{C}$  resonance signal is shifted downfield by an approximately equal amount. Not only are these shifts in the correct direction for an orientation of phytol such that the phytol double bond is approximately  $4.7\text{\AA}$  below the plane of the lecithin headgroup, but also, changes in the magnitude of the field effect through variation of the electric field by a change in phospholipid, or by the addition

of ions, are in close agreement with theoretical predictions. Very recently, molecular orbital calculations of the effect on  $^{13}\text{C}$  chemical shifts for hydrocarbon frameworks caused by the presence of an electric dipole have also been interpreted in terms of a simple bond polarization model (128). Electric field effects on  $^{13}\text{C}$  chemical shifts have been reported previously (124,202,203). However, these field effects are intramolecular in origin. Thus, the incorporation of phytol into phospholipid vesicles is a rare example of an intermolecular linear electric field effect.

#### B. Cholesteryl Esters

The accumulation of cholesteryl esters in the intimal layer of the aorta has been associated with the progressive development of atherosclerosis, but little attention has been paid to the effects of the initial buildup at a molecular level. As the disease progresses, the absolute amount of free cholesterol and cholesteryl esters both increase substantially, eventually forming up to 70% of the total lipid present. The buildup of cholesterol ester is most dramatic. The cholesterol ester/free cholesterol ratio for disease free Type 0 tissue is 5.6/8.0, while for more advanced Type III tissue it rises to 33.8/19.3 (102,204), a 2.5-fold increase from a ratio of 0.7 (Type 0) to 1.75 (Type III). It is possible that changes in the aorta during the initial stages of atherosclerosis are dependent upon the amount of cholesteryl ester which is present.

The results which have been presented here give insight into the structure and properties of membranes containing cholesteryl esters, and the mutual interactions of phospholipids, cholesterol and cholesterol esters, thereby offering insight into the molecular interactions which occur in atherosclerotic tissue. The main conclusions of this study are summarized below:

1. Small amounts of cholesteryl ester, up to 5 mole% may be incorporated into phospholipid vesicles. The incorporation has been demonstrated with the use of a radioactive tracer technique, as well as ESR experiments employing spin labeled cholesteryl esters.

2. The effect of the incorporation of 5 mole% cholesteryl palmitate, which is in its solid state at 33°C (the temperature of the NMR experiments), into lecithin vesicles is to increase the permeability of the mixed membrane to  $\text{Pr}^{3+}$  cations by approximately 10-fold and to EDTA anions by > 1000-fold. This effect is opposite to that caused by the intercalation of cholesterol (99). Thus, the permeability properties of the aortic membrane should depend upon the relative ratio of free to esterified cholesterol which is present, a ratio which changes as atherosclerosis progresses.

3. The incorporation of 5 mole% cholesteryl linoleate into lecithin vesicles at 33°C, has been shown to have no effect upon the permeability of the mixed membrane to the  $\text{Pr}^{3+}$  cation. The unsaturated ester, at this temperature, is in a more fluid liquid crystalline form i.e. above  $T_m$ . Therefore, the properties of the membranes containing cholesteryl esters depend not only on the relative amounts of free and esterified cholesterol, but also on the relative amounts of saturated and unsaturated cholesteryl esters.

4. Larger quantities of cholesteryl esters, 25 mole% of the total lipid present, have been dispersed in macroscopically homogeneous egg yolk lecithin multilamellar liposomes. At 37°C, the presence of the saturated ester, cholesteryl palmitate, while in its solid phase, has little effect on the fluidity of the lecithin fatty acyl chains as evidenced by  $^{13}\text{C}$   $T_1$  relaxation times. No resonances due to the saturated ester are resolved. However, at 37°C, it is possible to resolve sharp natural abundance  $^{13}\text{C}$  resonance signals for both the cholesterol and fatty acid chain moieties of the unsaturated ester, cholesteryl linoleate, which is in an isotropic liquid phase. This system therefore holds promise in the investigation of the nature of the fatty streaks and mesomorphic droplets which characterize sclerotic tissue. These lesions are known to be made up of approximately 95% cholesteryl esters.

5. Electron spin resonance studies based on the rate of ascorbate permeation to the site of nitroxide spin labeled cholesteryl esters incorporated in dipalmitoyl lecithin multilayers have shown that cholesteryl esters are incorporated into the model membranes in a "horseshoe" type of configuration with the ester linkage near the aqueous interface, and both the cholesterol and fatty acid moieties deeply embedded in the hydrophobic region.

6. Low amounts (< 10 mole%) of incorporated cholesterol increase the rate of ascorbate permeation to the site of the two nitroxide labeled cholesteryl esters, cholesteryl-5-doxylpalmitate (IV) and cholesteryl -16-doxylstearate (V) by 200-300%. Higher levels of added cholesterol have little effect on the rate of ascorbate reduction of the 5-labeled species, while increasing concentrations of cholesterol (up to 50 mole%) decreased the rate for the 16-labeled species back to its original level. Thus, low amounts of cholesterol (less than 10 mole%) introduce large changes in the properties of multilayer model membranes containing cholesteryl esters.

7. The incorporation of 4 mole% cholesteryl palmitate decreases the rate of ascorbate reduction of the 3-doxylcholestane spin probe. (I), by approximately 300%; however, higher concentrations (up to 18 mole%) of incorporated cholesteryl palmitate gradually increase this rate back to its original value. Thus cholesteryl

palmitate produces concentration dependent effects on the rate of ascorbate permeation to the site of the spin labeled cholesterol analogue, 3-doxylcholestane. In addition, these effects are deemed not to be due to the solubilization of the labeled molecule in a separate phase of excess ester since cholesteryl ester phases are known to solubilize less than 8 wt % cholesterol whereas cholesterol may be incorporated into lecithin model membranes up to a 1:1 mole ratio (205). Thus, the effects upon the rate of ascorbate permeation to the site of the cholesterol analogue are due to the mutual interactions of phospholipid, cholesterol, and cholesteryl ester.

8. It has been shown possible to study the properties of unsonicated aortic membranes by means of  $^{31}\text{P}$  NMR. Such a technique eliminates the possibility of resonances of triglycerides or cholesteryl esters interfering with those of phospholipid. Sonication of the membrane produces extremely narrow resonances (width at half height = 23Hz). Such a system should be amenable to permeability studies using the lanthanide shift technique.



9. High resolution  $^{13}\text{C}$  NMR spectra of a sonicated aortic membrane have been obtained for the first time. The signal intensity is contributed to mostly by triglycerides and cholesteryl esters. Therefore, the avenue is open for further  $^{13}\text{C}$  NMR studies employing samples at various stages of atherosclerosis which may assist in the elucidation of changes occurring in membrane structure and fluidity during the progression of the disease.

## CHAPTER 7

## FUTURE DIRECTIONS

One consequence of the destabilizing effect of the intercalation of phytol, phytanic acid, or Vitamin E into membranes would be expected to be a pushing apart of adjacent membrane constituents. It may therefore be possible that the decrease in the strength of lipid-lipid interactions and decreased packing density should be manifested in an increase in the rate of lateral and/or transverse diffusion of membrane components. Such changes, which may be found to correlate with membrane permeability, could be monitored by standard magnetic resonance techniques developed by McConnell and co-workers (65,66) or by Cullis (36).

Since the proposal has been made (98) that even before morphological changes occur, the permeability of the aortic intima increases, the application of the  $^{31}\text{P}$  permeability technique using presclerotic aorta membranes and/or lower temperatures to slow the rate to a measurable level may be illuminating. Alternatively, since the time required for the determination of a  $^{31}\text{P}$  spectrum is on the order of two hours, the use of ESR to monitor the rate of reduction by permeating ascorbate of an encapsulated water soluble spin probe such as tempocholine chloride may prove to be a superior method. The rate

of tempocholine efflux could be determined by prior incubation experiments whereby lecithin vesicles are added to an aqueous solution of the water soluble spin label. Aliquots could be removed after various time intervals, and treated with ascorbate at 0°C. Since pure EYL vesicles are very impermeable to cold ascorbate, immediately after the ascorbate addition, the residual ESR signal would result from that tempocholine which had crossed the bilayer to the enclosed volume of the vesicles during the specified incubation period. Thus, the rate of tempocholine permeation at any desired temperature may be determined. Subtraction of this rate from the rate of reduction of ESR signal intensity following addition of ascorbate to the outside bulk solution for vesicles containing encapsulated tempocholine will result in a measurement of the permeation of ascorbate. Thus, the rate of ascorbate permeation through the membrane, and not just to the site of an intercalated nitroxide label could be measured. Such a technique could be applied to increasingly heterogeneous reconstituted aortic membranes in order to study the properties of more physiological systems.

## BIBLIOGRAPHY

1. J.P. Reeves, and R.M. Dowben, *J. Cell Physiol.* 73. 49 (1969)
2. A.D. Bangham, and R.W. Horne, *J. Mol. Biol.* 8. 660 (1964).
3. C. Huang, *Biochemistry* 8. 344-(1969).
4. M.P. Sheetz, and S.I. Chan, *Biochemistry* 11, 4573 (1972).
5. E.G. Finer, *J. Magn. Reson.* 13, 76 (1974).
6. M. Bloom, E.E. Burnell, M.I. Valic, and G. Weeks, *Chem. Phys. Lipids* 14. 107 (1975).
7. Y.K. Levine, N.J.M. Birdsall, A.G. Lee, and J.C. Metcalfe, *Biochemistry* 11, 1416 (1972).
8. J.C. Metcalfe, N.J.M. Birdsall, J. Feeney, A.G. Lee, Y.K. Levine, and P. Partington, *Nature* 233, 199 (1971).
9. J.C. Metcalfe, N.J.M. Birdsall, and A.G. Lee, in "Proceedings of the 8th meeting of the Federation of European Biochemistry Societies. Vol. 28. Mitochondria and Biomembranes." North Holland, Amsterdam 1972. pp. 197-217.
10. J.C. Metcalfe, *Chem. Phys. Lipids* 8. 333 (1972).
11. J.C. Metcalfe, N.J.M. Birdsall, and A.G. Lee. *Ann. N.Y. Acad. Sci.* 222, 460 (1973).
12. K.M. Keough, E. Oldfield, D. Chapman, and P. Beynon, *Chem. Phys. Lipids* 10, 37 (1973).
13. J.G. Batchelor, J.H. Prestegard, R.J. Cushley, and S.R. Lipsky, *Biochem. Biophys. Res. Commun.* 48. 70 (1972).
14. B. Sears, W.C. Hutton, and T.E. Thompson, *Biochem. Biophys. Res. Commun.* 60, 1141 (1974).
15. B. Sears, *J. Membrane Biol.* 20. 59 (1975).
16. B. Sears, W.C. Hutton, and T.E. Thompson, *Biochemistry* 15, 1635 (1976).
17. P.E. Godici, and F.R. Landsberger, *Biochemistry* 13, 362 (1974).
18. P.E. Godici, and F.R. Landsberger, *Biochemistry* 14, 3927 (1975).

19. J. Urbina, and J.S. Waugh. Proc. Nat. Acad. Sci. USA 71. 5062 (1974).
20. S.J. Opella, J.P. Yesinowski, and J.S. Waugh. Proc. Nat. Acad. Sci. USA 73. 3812 (1976).
21. W. Stoffel, B.D. Tunggal, O. Zierenberg, E. Schreiber, and E. Binczek. Hoppe-Seyler's Z. Physiol. Chem. 355. 1367 (1974).
22. W. Stoffel, O. Zierenberg, B.D. Tunggal, and E. Schreiber, Hoppe-Seyler's Z. Physiol. Chem. 355. 1381 (1974).
23. Yu. E. Shapiro, A.V. Viktorov, V.I. Volkova, L.I. Barsukov, V.F. Bystrov, and L.D. Bergelson. Chem. Phys. Lipids 14. 227 (1975).
24. P.L. Yeagle, W.C. Hutton, and R.B. Martin. Biochim. Biophys. Acta 465. 173 (1977).
25. B. DeKruyff, A.M.H.P. VanDenBesselaar, and L.L.M. VanDeenen. Biochim. Biophys. Acta 465. 443 (1977).
26. V.F. Bystrov, Yu.E. Shapiro, A.V. Viktorov, L.I. Barsukov, and L.D. Bergelson. FEBS Lett. 25. 337 (1972).
27. L.I. Barsukov, Yu.E. Shapiro, A.V. Viktorov, V.I. Volkova, V.F. Bystrov, and L.D. Bergelson. Chem. Phys. Lipids 14, 211 (1975).
28. J.A. Berden, R.W. Barker, and G.K. Radda. Biochim. Biophys. Acta 375. 186 (1975).
29. B. DeKruyff, P.R. Cullis, and G.K. Radda. Biochim. Biophys. Acta 406. 6 (1975).
30. A.F. Horwitz, and M.P. Klein, J. Supramol. Structure 1. 19. (1972).
31. R.W. Barker, J.D. Bell, G.K. Radda, and R.E. Richards. Biochim. Biophys. Acta 260. 161 (1972).
32. D.G. Davis, and G. Inesi, Biochim. Biophys. Acta 241. 1 (1971).
33. D.G. Davis, and G. Inesi, Biochim. Biophys. Acta 282. 180 (1972).
34. M.C. Uhing. Chem. Phys. Lipids 14, 303 (1975).

35. P.L. Yeagle, W.C. Hutton, C. Huang, and R.B. Martin  
Proc. Nat. Acad. Sci. USA 72. 3477 (1975).
36. P.R. Cullis. FEBS Lett. 70. 223 (1976).
37. G. Torosian, and A.P. Lemberger. J. Pharm. Sci. 57,  
17 (1968).
38. G.L. Gaines, Jr., J. Colloid. Interface Sci. 28. 334 (1968).
39. R.A. Demel. L.L.M. VanDeenen, and B.A. Pethica. Biochim.  
Biophys. Acta 135, 11 (1967).
40. D.O. Shah, and J.H. Schulman, J. Lipid Res. 6. 341 (1965).
41. D.O. Shah, and J.H. Schulman. Biochim. Biophys.  
Acta 135, 184 (1967).
42. D.O. Shah, and J.H. Schulman. J. Lipid Res. 8,  
215 (1967).
43. D.O. Shah, and J.H. Schulman. J. Lipid Res, 8.  
227 (1967).
44. D.O. Shah, and J.H. Schulman. In "Molecular  
association in biological and related systems."  
Advances in chemistry series. Vol. 84. Edited  
by R.F. Gould, American Chemical Society Publications,  
Washington, D.C. 1968.
45. M. Cereijido. F. Villalonga, M. Fernández, and  
C.A. Rotunno. In "The molecular basis of membrane  
function." Edited by D.C. Tosteson. Prentice  
Hall, Englewood Cliffs, N.J. 1969.
46. G.L. Gaines Jr. In "Insoluble monolayers at liquid-gas  
interfaces." Interscience monographs on physical  
chemistry. Vol. 1. Edited by I. Prigogine. Interscience,  
New York. 1966.
47. R.A. Demel, W.S.M. GeurtsVanKessel, and L.L.M. VanDeenen.  
Biochim. Biophys. Acta 226. 26 (1972).
48. B. DeKruyff, R.A. Demel, A.J. Slotboom. L.L.M. VanDeenen,  
and A.F. Rosenthal, Biochim. Biophys. Acta 307, 1 (1973).
49. B. DeKruyff, R.A. Demel, and L.L.M. VanDeenen. Biochim.  
Biophys. Acta 255. 331 (1972).

50. B. Maggio, A.T. Diplock, and J.A. Lucy. *Biochem. J.* 161, 111 (1977).
51. W.L. Hubbell, and H.M. McConnell, *J. Amer. Chem. Soc.* 93, 314 (1971).
52. B.G. McFarland, and H.M. McConnell. *Proc. Nat. Acad. Sci. USA* 68, 1274 (1971)
53. K.W. Butler, I.C.P. Smith, and H. Schneider. *Biochim. Biophys. Acta* 219, 514 (1970).
54. J. Hsia, H. Schneider, and I.C.P. Smith. *Can. J. Biochem.* 49, 614 (1971).
55. S.J. Paterson, K.W. Butler, P. Huang, J. Labelle, I.C.P. Smith, and H. Schneider. *Biochim. Biophys. Acta* 266, 603 (1972).
56. D. Marsh, and I.C.P. Smith. *Biochim. Biophys. Acta* 298, 133 (1973).
57. S. Schreier-Muccillo, K.W. Butler, and I.C.P. Smith. *Arch. Biochem. Biophys.* 159, 297 (1973).
58. H. Schindler, and J. Seelig. *J. Chem. Phys.* 59, 1841 (1973).
59. H. Schindler, and J. Seelig. *J. Chem. Phys.* 61, 2946 (1974)..
60. J. Seelig, *J. Amer. Chem. Soc.* 92, 3881 (1970).
61. O.H. Griffith, P.J. Dellinger, and S.P. Van. *J. Membrane Biol.* 15, 159 (1974).
62. G.B. Birrell, and O.H. Griffith. *Arch. Biochem. Biophys.* 172, 455 (1976).
63. M.A. Hemminga, *J. Magn. Reson.* 25, 25 (1977).
64. S.R. Van, and O.H. Griffith. *J. Membrane Biol.* 20, 155. (1975).
65. R.D. Kornberg, and H.M. McConnell, *Biochemistry* 10, 1111 (1971).
66. P. Devaux, and H.M. McConnell. *J. Amer. Chem. Soc.* 94, 4475 (1972).
67. C.J. Scandella, P. Devaux, and H.M. McConnell, *Proc. Nat. Acad. Sci. USA* 69, 2056 (1972).

68. P. Devaux, and H.M. McConnell, *Ann. N.Y. Acad. Sci.* 222, 489 (1973).
69. M.G. McNamee, and H.M. McConnell, *Biochemistry* 12, 2951 (1973).
70. H. Trauble, and E. Sackman, *J. Amer. Chem. Soc.* 94, 4499 (1971).
71. A. Rousselet, C. Guthmann, J. Matricon, A. Bienvenue, and P.F. Devaux, *Biochim. Biophys. Acta* 426, 372 (1976).
72. A. Rousselet, A. Colbeau, P.M. Vignais, and P.F. Devaux, *Biochim. Biophys. Acta* 426, 372 (1976).
73. S. Schreier-Muccillo, D. Marsh, and I.C.P. Smith, *Arch. Biochem. Biophys.* 172, 1 (1976).
74. D.G. Davis, *Biochem. Biophys. Res. Commun.* 49, 1492 (1972).
75. J.A. Berden, P.R. Cullis, D.I. Hoult, A.C. McLaughlin, G.K. Radda, and R.E. Richards, *FEBS Lett.* 46, 55 (1974).
76. A.C. McLaughlin, P.R. Cullis, J.A. Berden, and R.E. Richards, *J. Magn. Reson.* 20, 146 (1975).
77. P.R. Cullis, B. DeKruyff, and R.E. Richards, *Biochim. Biophys. Acta* 426, 433 (1976).
78. S.J. Kohler, and M.P. Klein, *Biochemistry* 15, 967 (1976).
79. S.J. Kohler, and M.P. Klein, *Biochemistry* 16, 519 (1977).
80. J. Seelig, and H. Gally, *Biochemistry* 15, 5199 (1976).
81. W. Niederberger, and J. Seelig, *J. Amer. Chem. Soc.* 98, 3704 (1976).
82. E. Oldfield, D. Chapman, and W. Derbyshire, *FEBS Lett.* 16, 102 (1971).
83. J. Seelig, and A. Seelig, *Biochem. Biophys. Res. Commun.* 57, 406 (1974).
84. A. Seelig, and J. Seelig, *Biochemistry* 13, 4839 (1974).
85. G.W. Stockton, C.F. Polnaszek, L.C. Leitch, A.P. Tulloch, and I.C.P. Smith, *Biochem. Biophys. Res. Commun.* 60, 844 (1974).
86. G.W. Stockton, C.F. Polnaszek, A.P. Tulloch, F. Hasan, and I.C.P. Smith, *Biochemistry* 15, 954 (1976).



87. A.L. Tappel, *Vitamins Hormones* 20. 493 (1962).
88. S.R. Fahrenholtz, F.H. Doleiden, A.M. Trozzolo, and A.A. Lamola, *Photochem. Photobiol.* 20, 505 (1974).
89. C.S. Foote, T. Ching, and G.G. Geller. *Photochem. Photobiol.* 20, 511 (1974).
90. B. Stevens, R.D. Small, Jr., and S.R. Perez, *Photochem. Photobiol.* 20, 515 (1974).
91. M. Iwakami, Nagoya *J. Med. Sci.* 28. 50 (1965).
92. J. Baraud, P. Courbin, and A. Maurice, *Arch. Sci. Physiol.* 23. 437 (1969).
93. J.A. Lucy, and J.T. Dingle, *Nature* 204. 156 (1964).
94. F. Weber, U. Gloor, and O. Wiss, *Helv. Chim. Acta* 41, 1038 (1958).
95. G.J. Cardinale, T.J. Carty, and R.H. Abeles. *J. Biol. Chem.* 245, 3771 (1970).
96. M.C. MacBrinn, and J.S. O'Brien, *J. Lipid Res.* 9. 552 (1968).
97. I. Molenaar, J. Vos, and F.A. Hommes, *Vitamins-Hormones* 30, 45 (1972).
98. C. Pries, and F.B. Klynstra. *Lancet* i, 750 (1971).
99. D. Papahadjopoulos, S. Nir, and S. Ohki, *Biochim. Biophys. Acta* 266, 561 (1972).
100. J.E. Kirk, and T.J.S. Laursen, *J. Gerontol.* 10, 288 (1955).
101. J.E. Kirk in "Blood vessels and lymphatics." Edited by D.I. Abramson, Academic Press, New York. 1962. p. 587.
102. C.J.F. Bottcher, F.P. Woodford, C.Ch. TerHaar Romeny-Wachter, E. Boelsma-VanHoute, and C.M. VanGent. *Lancet* i, 1378 (1960).
103. R.W. St.Clair, H.B. Lofland, and T.B. Clarkson. *J. Atheroscler. Res.* 10, 193 (1969).
104. W.S. Singleton, M.S. Gray, M.L. Brown, and J.L. White. *J. Am. Oil Chem. Soc.* 42, 53 (1965).

105. W.F. Boss, C.J. Kelley, and F.R. Landsberger. Analytical Biochem. 64.289 (1975).
106. R.L. Vold, J.S. Waugh, M.P. Klein, and D.E. Phelps. J. Chem. Phys. 48, 3381 (1968).
107. G.G. McDonald, and J.S. Leigh, Jr., J. Magn. Reson. 9. 358 (1973).
108. A. Abragam, In "The principles of nuclear magnetism. The international series of monographs on physics." Edited by N.F. Mott, E.C. Bullard, and D.H. Wilkinson. Oxford University Press, London. 1961.
109. C.P. Slichter, In "Principles of magnetic resonance." Edited by F. Seitz. Harper and Row. New York. 1963.
110. A.G. Lee, N.J.M. Birdsall, and J.C. Metcalfe. Meth. Membrane Biol. 2. 1 (1974).
111. L.J. Berliner, Ed., "Spin labeling. Theory and applications." Molecular biology international series of monographs and textbooks. Academic Press. New York. 1976.
112. F. Bloch, Phys. Rev. 70, 460 (1946).
113. F. Bloch, W.W. Hansen, and M. Packard. Phys. Rev. 70. 474 (1946).
114. J.W. Emsley, J. Feeney, and L.H. Sutcliffe, In "High resolution NMR spectroscopy." Volume 1. Pergamon Press, Oxford. 1965. pp. 10-58.
115. T.C. Farrar, and E.D. Becker, In "Pulse and Fourier transform NMR. Introduction to theory and methods." Academic Press, New York. 1971.
116. A. Carrington, and A.D. McLachlan, In "Introduction to magnetic resonance." Edited by S.A. Rice. Harper and Row, New York. 1967.
117. J.R. Lyerla, D.M. Grant, and R.K. Harris. J. Chem. Phys. 55, 585 (1971).
118. A. Allerhand, D. Doddrell, and R. Komoroski. J. Chem. Phys. 55. 189 (1971).
119. K.F. Kuhlmann, D.M. Grant, and R.K. Harris, J. Chem. Phys. 52. 3439 (1969).

120. N. Bloembergen, E.M. Purcell, and R.V. Pound. Phys. Rev. 73. 679 (1948).
121. I. Solomon. Phys. Rev. 99. 559 (1955).
122. D.E. Woessner, J. Chem. Phys. 36. 1 (1962).
123. R.F. Zürcher, Prog. NMR Spectry. 2. 205 (1967).
124. J.G. Batchelor, J.H. Prestegard, R.J. Cushley, and S.R. Lipsky, J. Amer. Chem. Soc. 95. 6358 (1973).
125. A.D. Buckingham. Can. J. Chem. 38. 300 (1960).
126. W.J. Horsley, and H. Sternlicht, J. Amer. Chem. Soc. 90. 3738 (1968).
127. J.G. Batchelor, R.J. Cushley, and J.H. Prestegard, J. Org. Chem. 39. 1698 (1974).
128. K. Seidman, and G.E. Maciel, J. Amer. Chem. Soc. 99. 3254 (1977).
129. R.J.W. LeFevre, Advan. Phys. Org. Chem. 3. 1 (1965).
130. P.J. Nordio, In "Spin labeling. Theory and applications." Edited by L.J. Berliner; Academic Press. New York. Chapter 2. 1976.
131. J. Seelig, In "Spin labeling. Theory and applications." Edited by L.J. Berliner. Academic Press, New York. Chapter 10. 1976.
132. W.L. Hubbell, and H.M. McConnell, Proc. Nat. Acad. Sci. USA 63. 16 (1969).
133. I.C.P. Smith and K.W. Butler, In "Spin labeling. Theory and applications." Edited by L.J. Berliner. Academic Press, New York. Chapter 11. 1976.
134. A. Saupe, G. Englert, and A. Povh. In "Ordered fluids and liquid crystals." Advances in chemistry series. Volume 63. Edited by R.F. Gould, American Chemical Society Publications. Washington. 1967.
135. S. Schreier-Muccillo, D. Marsh, H. Dugas, H. Schneider, and I.C.P. Smith. Chem. Phys. Lipids 10. 11 (1973).
136. N.H. Tattrie, J.R. Bennett, and R. Cyr, Can. J. Biochem. 46, 819 (1968).

137. T.C. Farrar, S.J. Druck, R.R. Shoup, and E.D. Becker. J. Amer. Chem. Soc. 94, 699 (1972).
138. A. Abe, R.L. Jernigan, and P.J. Flory, J. Amer. Chem. Soc. 88, 631 (1966).
139. R.A. Goodman, E. Oldfield, and A. Allerhand, J. Amer. Chem. Soc. 95, 7553 (1973).
140. G. Stokes, Trans. Cambridge Phil. Soc. 9, 5 (1856).
141. A. Einstein, Z. Elektrochem. 14, 235 (1908).
142. D.M. Grant, and B.V. Cheney, J. Amer. Chem. Soc. 89, 5315 (1967).
143. B.V. Cheney, and D.M. Grant, J. Amer. Chem. Soc. 89, 5319, (1967)
144. J.L. Lippert, and W.L. Peticolas, Proc. Nat. Acad. Sci. USA 68, 1572 (1971).
145. J.L. Lippert, and W.L. Peticolas, Biochim. Biophys. Acta 255, 43 (1972).
146. A.F. Horwitz, and M.P. Klein, J. Supramol. Structure 2, 281 (1973).
147. B.D. Ladbrooke, R.M. Williams, and D. Chapman, Biochim. Biophys. Acta 150, 333 (1968).
148. A. Gillis, and R.J. Cushley, unpublished observations.
149. J.H. Noggle, and R.E. Schirmer, In "The nuclear Overhauser effect." Academic Press, New York, 1971.
150. R. Freeman, H. Hill, and R. Kaptein, J. Magn. Reson. 7, 327 (1972).
151. T. Hanai, D.A. Haydon, and J. Taylor, J. Theor. Biol. 9, 278 (1965).
152. M.H.F. Wilkins, Ann. N.Y. Acad. Sci. 195, 291 (1972).
153. P.B. Hitchcock, R. Mason, K.K. Thomas, and G.G. Shipley, Proc. Nat. Acad. Sci. USA 71, 3036 (1974).
154. M. Sundaralingam, and L.H. Jensen, Science 150, 1035 (1965).
155. J.H. Dumbleton, and T.R. Lomer, Acta Cryst. 19, 301 (1965).

156. R.C. Weast, Ed., "Handbook of chemistry and physics." 53rd Edition, The Chemical Rubber Co., Cleveland. 1972.
157. G.L. Nelson, G.C. Levy, and J.D. Cargioli, J. Amer. Chem. Soc. 94. 3089 (1972).
158. N.P. Franks, J. Mol. Biol. 100. 345 (1976).
159. D.L. Worcester, and N.P. Franks, J. Mol. Biol. 100. 359 (1976).
160. J.B. Stothers, ~~In~~ "Carbon-13 NMR spectroscopy." Academic Press, New York. 1972.
161. G.W. Stockton, and I.C.P. Smith, Chem. Phys. Lipids 17. 251 (1976).
162. J. deGier, J.G. Mandersloot, and L.L.M. VanDeenen. Biochim. Biophys. Acta 173. 143 (1969).
163. L. Salem, Can. J. Biochem. Physiol. 40. 1287 (1962).
164. V.F. Bystrov, N.I. Dubrovina, L.I. Barsukov, and L.D. Bergelson, Chem. Phys. Lipids 6. 343 (1971).
165. L.I. Barsukov, A.M. Parfen'eva, A.V. Viktorov, Yu. Ye. Shapiro, V.F. Bystrov, and L.D. Bergelson. Biofizika 19, 456 (1974).
166. M.S. Fernández, H. Celis, and M. Montal, Biochim. Biophys. Acta 323. 600 (1973).
167. J. Reuben, Naturwissenschaften 62, 172 (1975).
168. Y.K. Levine, A.G. Lee, N.J.M. Birdsall, J.C. Metcalfe and J.D. Robinson. Biochim. Biophys. Acta 291, 592 (1973).
169. R.A. Demel, K.K. Bruckdorfer, and L.L.M. VanDeenen. Biochim. Biophys. Acta 255. 311 (1972).
170. R.A. Demel, K.R. Bruckdorfer, and L.L.M. VanDeenen. Biochim. Biophys. Acta 255. 321 (1972).
171. E.C. McCormick, and R.H. McCluer, Circulation 22, 651 (1969).
172. T. Ito, Jap. Circulation J. 33, 25 (1969).

173. R.M.C. Matthews, and G.W. Wade, *J. Magn. Reson.* 19, 166 (1975).
174. L.Y. Abrogast, G.H. Rothblat, M.H. Leslie, and R.A. Cooper, *Proc. Nat. Acad. Sci. USA* 73, 3680 (1976).
175. C. Taupin, and H.M. McConnell, In "Proceedings of the 8th meeting of the Federation of European Biochemistry Societies. Volume 28. Mitochondria and biomembranes." North Holland, Amsterdam, 1972. p. 219.
176. R.D. Kornberg, M.G. McNamee, and H.M. McConnell, *Proc. Nat. Acad. Sci. USA* 69, 1508 (1972).
177. S.I. Chan, M.P. Sheetz, C.H.A. Seiter, G.W. Feigenson, M. Hsu, A. Lau, and A. Yau, *Ann. N.Y. Acad. Sci.* 222, 499 (1973).
178. R. Pagano, and T.E. Thompson, *J. Mol. Biol.* 38, 41 (1968).
179. D.W. Deamer, and D. Branton, *Science* 158, 665 (1967).
180. R.C. Macdonald, *Biochim. Biophys. Acta* 448, 193 (1976).
181. R.D. Lapper, S.J. Paterson, and I.C.P. Smith, *Can. J. Biochem.* 50, 969 (1972).
182. J. Seelig, H. Limacher, and P. Bader, *J. Amer. Chem. Soc.* 94, 6364 (1972).
183. A.K. Grover, and R.J. Cushley, unpublished observations
184. C.R. Loomis, M.J. Janiak, D.M. Small, and G.G. Shipley, *J. Mol. Biol.* 86, 309 (1974).
185. M.J. Janiak, C.R. Loomis, G.G. Shipley, and D.M. Small, *J. Mol. Biol.* 86, 325 (1974).
186. D.M. Small, and G.G. Shipley, *Science* 185, 222 (1974).
187. H. Trauble, *J. Membrane Biol.* 4, 193 (1971).
188. P.S. Chen, Jr., T.Y. Yoribara, and H. Warner, *Analyt. Chem.* 28, 1756 (1956).
189. P.D. Lang, and W. Insull, Jr., *J. Clin. Invest.* 49, 1479 (1970).
190. B. Lundberg, *Chem. Phys. Lipids* 14, 309 (1975).

191. C.J.F. Böttcher, and C.M. VanGent, *J. Atheroscler. Res.* 1, 36 (1961).
192. T.O. Henderson, T. Glonek, and T.C. Myers, *Biochemistry* 13, 623, (1974).
193. V. Krupa, R.J. Boegman, and G.S. Marks, *Biochim. Biophys. Acta* 304, 260 (1973).
194. M. Lunde, M. Mudgett, and T.C. Myers, *Arch. Biochem. Biophys.* 142, 508 (1971).
195. J.E. Kirk, In "Blood vessels and lymphatics." Edited by D.I. Abramson. Academic Press, New York. 1962. p. 83.
196. J.L. Foote, and E. Coles, *J. Lipid Res.* 9, 482 (1968).
197. D.W. Urry, and L.W. Mitchell, *Biochem. Biophys. Res. Commun.* 68, 1153 (1976).
198. B. Bloj, R.D. Morero, R.N. Farias, and R.E. Trucco, *Biochim. Biophys. Acta* 311, 67 (1973).
199. B. Bloj, R.D. Morero, and R.N. Farias, *FEBS Lett.* 38, 101 (1973).
200. F. Sineriz, B. Bloj, R.N. Farias, and R.E. Trucco, *J. Bacteriol.* 115, 723 (1973).
201. R.N. Farias, B. Bloj, R.D. Morero, F. Sineriz, and R.E. Trucco, *Biochim. Biophys. Acta* 415, 231 (1975).
202. T. Yonemoto, *J. Magn. Reson.* 12, 93 (1973).
203. T. Yonemoto, *J. Magn. Reson.* 13, 153 (1974).
204. D.G. Cornwell, J.C. Geer, and R.V. Panganamala, In "International encyclopedia of pharmacology and therapeutics. Section 24. Pharmacology of lipid transport and atherosclerotic processes." Edited by E.J. Masaro. Pergamon Press, Oxford (1975).
205. D. Chapman, and S.A. Penkett, *Nature* 211, 1304 (1966).
206. L. Stryer, In "Biochemistry", W.H. Freeman & Co., San Francisco. 1975.